

Radioisotope Dating of Meteorites: III. The Eucrites (Basaltic Achondrites)

Andrew A. Snelling, Answers in Genesis, PO Box 510, Hebron, Kentucky 41048.

Abstract

Meteorites date the earth with a 4.55 ± 0.07 Ga Pb-Pb isochron called the geochron. They appear to consistently yield 4.55–4.57 Ga radioisotope ages, adding to the uniformitarians' confidence in the radioisotope dating methods. Achondrites, meteorites not containing chondrules, account for about 8% of meteorites overall. About 3% of the witnessed falls of all meteorite types are the achondrites known as eucrites, which makes them the fourth most common meteorite to fall. Eucrites are similar to basalts and are believed to be space debris from the crust of main belt asteroid 4-Vesta. Many radioisotope dating studies in the last 45 years have used the K-Ar, Ar-Ar, Rb-Sr, Sm-Nd, U-Th-Pb, Lu-Hf, Mn-Cr, Hf-W, Al-Mg, I-Xe, and Pu-Xe methods to yield an abundance of isochron and model ages for these basaltic achondrites from whole-rock samples, and mineral and other fractions. Such age data for 12 eucrites were tabulated and plotted on frequency versus age histogram diagrams. They strongly cluster in many of these eucrites at 4.55–4.57 Ga, dominated by Pb-Pb and U-Pb isochron and model ages, testimony to that technique's supremacy as the uniformitarians' ultimate dating tool, which they consider very reliable. These ages are confirmed by Rb-Sr, Lu-Hf, and Sm-Nd isochron ages, but agreement could be due to calibration with the Pb-Pb system. There is also scatter of the U-Pb, Pb-Pb, Th-Pb, Rb-Sr, K-Ar, and Ar-Ar model ages, in most cases likely due to thermal disturbances resulting from metamorphism or impact cratering of the parent asteroid. No pattern was found in these meteorites' isochron ages similar to the systematic patterns of isochron ages found in Precambrian rock units during the RATE project, so there is no evidence of past accelerated radioisotope decay having occurred in these eucrites, and therefore on their parent asteroid. This is not as expected, yet it is the same for all meteorites so far studied. Thus it is argued that accelerated radioisotope decay must have only occurred on the earth, and only the 500–600 million years' worth we have physical evidence for during the Flood. Otherwise, due to their 4.55–4.57 Ga "ages" these eucrites and their parent asteroid are regarded as originally representing "primordial material" that God made on Day One of the Creation Week, from which He made the non-earth portion of the solar system on Day Four, which is compatible with the Hebrew text of Genesis. Thus today's measured radioisotope compositions of these eucrites could reflect a geochemical signature of that "primordial material," which included atoms of all elemental isotopes. So if most of the measured daughter isotopes were already in these basaltic achondrites when they were formed on their parent asteroid, then their 4.55–4.57 Ga "ages" obtained by Pb-Pb and U-Pb isochron and model age dating are likely not their true real-time ages, which according to the biblical paradigm is only about 6000 real-time years. Further investigation of radioisotope ages data for meteorites in remaining groups of achondrites, for lunar rocks, and for rocks from every level in the earth's geologic record, should enable the interim ideas presented here to be confirmed or modified.

Keywords: meteorites, classification, achondrites, eucrites, asteroids, 4-Vesta, radioisotope dating, Bereba, Cachari, Caldera, Camel Donga, Ibitira, Juvinas, Moama, Moore County, Pasamonte, Serra de Magé, Stannern, Yamato 75011, K-Ar, Ar-Ar, Rb-Sr, Sm-Nd, U-Th-Pb, Lu-Hf, Mn-Cr, Hf-W, Al-Mg, I-Xe, Pu-Xe, isochron ages, model ages, discordant radioisotope ages, accelerated radioactive decay, thermal disturbance, resetting, "primordial material," geochemical signature, mixing, inheritance

Introduction

In 1956 Claire Patterson at the California Institute of Technology in Pasadena reported a Pb-Pb isochron age of 4.55 ± 0.07 Ga for three stony and two iron meteorites, which since then has been declared the age of the earth (Patterson 1956). Adding weight to that claim is the fact that many meteorites appear to consistently date to around the same "age" (Dalrymple 1991, 2004), thus bolstering the evolutionary community's confidence that they have successfully dated the age of the earth and

the solar system at around 4.56 Ga. These apparent successes have also strengthened their case for the supposed reliability of the increasingly sophisticated radioisotope dating methods.

Creationists have commented little on the radioisotope dating of meteorites, apart from acknowledging the use of Patterson's geochron to establish the age of the earth, and that many meteorites give a similar old age. Morris (2007) did focus on the Allende carbonaceous chondrite as an example of a well-studied meteorite analyzed by many

radioisotope dating methods, but he only discussed the radioisotope dating results from one, older paper (Tatsumoto, Unruh, and Desborough 1976).

In order to rectify this lack of engagement by the creationist community with the meteorite radioisotope dating data, Snelling (2014a) obtained as much radioisotope dating data as possible for the Allende CV3 carbonaceous chondrite meteorite (due to its claimed status as the most studied meteorite), displayed the data, and attempted to analyze them. He found that both isochron and model ages for the total rock, separated components, or combinations of these strongly clustered around a Pb-Pb age of 4.56–4.57 Ga, the earliest (Tatsumoto, Unruh, and Desborough 1976) and the latest (Amelin et al. 2010) determined Pb-Pb isochron ages at 4.553 ± 0.004 Ga and 4.56718 ± 0.0002 Ga respectively being essentially the same. Apart from scatter of the U-Pb, Th-Pb, Rb-Sr, and Ar-Ar ages, no systematic pattern was found in the Allende isochron and model ages similar to the systematic pattern of isochron ages found in Precambrian rock units during the RATE project that was interpreted as produced by an episode of past accelerated radioisotope decay (Snelling 2005c; Vardiman, Snelling, and Chaffin 2005).

Snelling (2014b) subsequently gathered together all the radioisotope ages obtained for 10 ordinary (H, L, and LL) and five enstatite (E) chondrites and similarly displayed the data. They generally clustered, strongly in the Richardton (H5), St. Marguerite (H4), Bardwell (L5), Bjurböle (L4), and St. Séverin (LL6) ordinary chondrite meteorites, at 4.55–4.57 Ga, dominated by Pb-Pb and U-Pb isochron and model ages, but confirmed by Ar-Ar, Rb-Sr, Re-Os, and Sm-Nd isochron ages. There was also scatter of the U-Pb, Th-Pb, Rb-Sr, and Ar-Ar model ages, in some cases possibly due to thermal disturbance. Again, no pattern was found in these meteorites' isochron ages indicative of past accelerated radioisotope decay.

Snelling (2014a, b) then sought to discuss the possible significance of this clustering in terms of various potential creationist models for the history of radioisotopes and their decay. He favored the idea that asteroids and the meteorites derived from them

are “primordial material” left over from the formation of the solar system, which is compatible with the Hebrew text of Genesis that could suggest God made “primordial material” on Day One of the Creation Week, from which He made the non-earth portion of the solar system on Day Four. Thus he argued that today’s measured radioisotope compositions of all these chondrites may reflect a geochemical signature of that “primordial material,” which included atoms of all elemental isotopes. So if some of the daughter isotopes were already in these chondrites when they were formed, then the 4.55–4.57 Ga “ages” for them obtained by Pb-Pb and U-Pb isochron and model age dating are likely not their true real-time ages, which according to the biblical paradigm is only about 6000 real-time years.

However, Snelling (2014a, b) admitted that drawing firm conclusions from the radioisotope dating data for just these 16 chondrite meteorites was premature, and recommended further studies of more meteorites. This present contribution is therefore designed to further document the radioisotope dating data for more meteorites, the basaltic achondrites or eucrites, so as to continue the discussion of the potential significance of these data.

The Classification of Achondrite Meteorites

The most recent classification scheme for the meteorites is that of Weisberg, McCoy, and Krot (2006), which is reproduced in Fig. 1. Based on their bulk compositions and textures, Krot et al. (2005) divided meteorites into two major categories, chondrites (meteorites containing chondrules) and achondrites (meteorites not containing chondrules or non-chondritic meteorites). They further subdivided the achondrites into primitive achondrites and igneously differentiated achondrites. However, Weisberg, McCoy and Krot (2006) simply subdivided all meteorites into three categories—chondrites, primitive achondrites and achondrites (fig. 1).

The non-chondritic meteorites contain virtually none of the components found in chondrites. It is conventionally claimed that they were derived from chondritic materials by planetary melting, and that

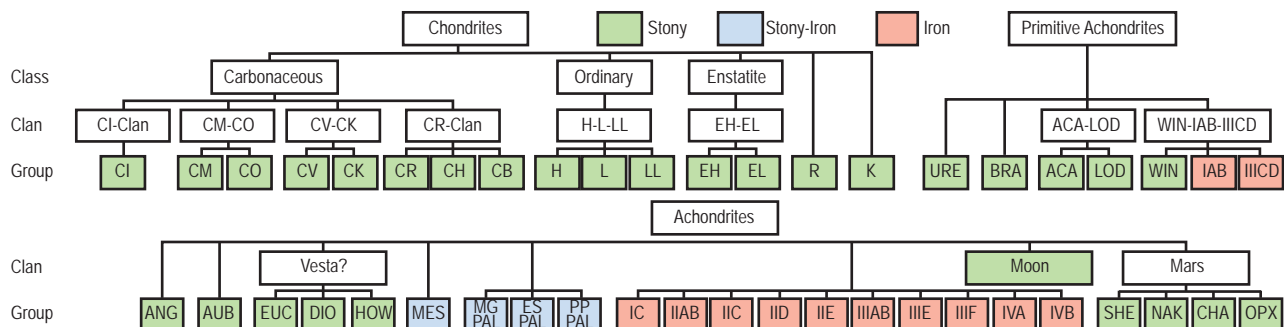


Fig. 1. The classification system for meteorites (after Weisberg, McCoy, and Krot 2006).

fractionation caused their bulk compositions to deviate to various degrees from chondritic materials (Krot et al. 2005). The degrees of melting that these rocks experienced are highly variable, and thus, these meteorites have been divided into the two major categories—primitive and differentiated. However, there is no clear-cut boundary between these categories.

The differentiated non-chondritic meteorites, or achondrites (fig. 1), are conventionally regarded as having been derived from parent bodies that experienced large-scale partial melting, isotopic homogenization (ureilites are the only exception), and subsequent differentiation. Based on abundance of FeNi-metal, these meteorites are commonly divided into three types—achondrites, stony-irons, and irons. Each of these types contains several meteorite groups and ungrouped members (fig. 1). Several groups of achondrites and iron meteorites are likely to be genetically related and were possibly derived from single asteroids or planetary bodies.

The achondrites account for about 8% of meteorites overall, and the majority of them (about two-thirds) are HED meteorites (howardites, eucrites, and diogenites), believed to have originated from the crust of asteroid 4-Vesta (Norton 2002) (fig. 1). Other types include martian, lunar, and several types thought to originate from as-yet unidentified asteroids. These groups have been determined on the basis of, for example, their bulk Fe/Mn and $^{17}\text{O}/^{18}\text{O}$ ratios, which are thought to be characteristic “fingerprints” for each parent body (Mittlefehldt et al. 1998).

The achondrites represent the products of classical igneous processes acting on the silicate-oxide system of asteroidal bodies—partial to complete melting, differentiation, and magmatic crystallization (Mittlefehldt 2005). Iron meteorites represent the complimentary metal-sulfide system products of this process. Thus the achondrites consist of materials similar to terrestrial basalts and plutonic rocks, so they exhibit igneous textures, or igneous textures modified by impact and/or thermal metamorphism, and distinctive mineralogies indicative of igneous processes.

The HED meteorites are sometimes grouped with the angrites and aubrites (fig. 1) and termed the asteroidal achondrites, because of all having been differentiated on parent asteroidal bodies. The howardite-eucrite-diogenite (HED) meteorites have been traditionally classified into the one clan, because there is strong evidence they originated on the same parent body, the asteroid 4-Vesta (Binzel and Xu 1993; Consolmagno and Drake 1977; Drake 2001; Mandler and Elkins-Tanton 2013; McCord, Adams, and Johnson 1970; McSween et al. 2011; McSween et al. 2013, 2014; Righter and Drake 1997). This

was one of the first links made between meteorites and an asteroid (Cloutis, Binzel, and Gaffey 2014; McCord, Adams, and Johnson 1970). Initially their spectroscopic similarity, which suggested the HED achondrites are impact ejecta off 4-Vesta, was deemed dynamically dubious owing to the apparent lack of a plausible pathway from Vesta to the earth. The discovery of the Vesta family of asteroids or “Vestoids” (Binzel and Xu 1993) extending from Vesta to resonance delivery zones solidified the link. This link has stood the test of time and has been confirmed by the in situ results provided by the Dawn mission to this asteroid (McSween et al. 2014). Thus the HED clan allows the confident association of specific types of igneous processes with an asteroid body of known size.

The HED clan is the most extensive suite of differentiated crustal rocks from an asteroid (Mittlefehldt 2005). Evidence that these achondrites belong in the same clan includes their identical oxygen isotopic compositions (Clayton and Mayeda 1996), similarities in Fe/Mn ratios in pyroxenes, the occurrence of polymict breccias consisting of materials of eucritic and diogenitic parentage (for example, the howardites), and the existence of rocks intermediate between diogenites and cumulate eucrites (Krot et al. 2005). The suite of meteorites comprising the HED clan is composed of mafic and ultramafic igneous rocks, most of which are breccias. The parent lithologies were mostly metamorphosed, which has obscured original igneous zoning in most cases (Mittlefehldt 2005). The suite contains four main igneous lithologies—basalt and cumulate gabbro (eucrites), and orthopyroxenite and harzburgite (diogenites). When both eucrite and diogenite clasts are present in a meteorite that is a polymict breccia, then it is a howardite. These lithologies are consistent with a postulated layered crust model for the HED parent body, 4-Vesta (Mandler and Elkins-Tanton 2013; McSween et al. 2013, 2014; Righter and Drake 1997; Takeda 1997).

The Eucrites

The eucrites are the most common of the achondrites. About 3% of the witnessed falls of all meteorite types are eucrites, which makes them the fourth most common meteorite to fall (Norton 2002). Of the HED meteorites, eucrites are by far the most common, about 52%. Until the meteorite finds in Antarctica became available with their large cache of eucrites, eucrites were defined as monomict breccias. However, the large number of eucrites recovered that show a wide variation of lithic fragments, unlike the fragments in howardites, has prompted the acceptance of eucrites as either monomict or polymict.

The most obvious external characteristic of a freshly fallen eucrite is its very black and lustrous fusion crust compared to the dull black crust of a chondrite, due to the intense heating of the outer surface during passage through the earth's atmosphere (Norton 2002). Eucrites are Ca-rich and this combined with the usually present small amount of Fe gives these meteorites a "wet" look (fig. 2). Fusion crusts form in the final second or two of the ablation process as meteorites pass rapidly through the earth's atmosphere during the fireball stage. The fusion crusts then rapidly cool, so contraction cracks often form, leaving the outer surface of the meteorites looking much like the crazing on pottery (figs. 2 and 3).



Fig. 2. The shiny black crust on this eucrite from Camel Donga, Western Australia, is typical of calcium-rich eucrites. Note the contraction cracks through the crust. The specimen measures 5 cm (about 2 in) in its longest dimension (after Norton 2002).



Fig. 3. Contraction cracks in the crust of the Pasamonte eucrite. The specimen is about 6.2 cm (about 2.5 in) long (after Norton 2002).

The similarities of eucrites chemically and petrographically to terrestrial basalts is frequently noted, but a broken face of a eucrite exposes a light gray interior, which is unlike the dark gray to black interiors of terrestrial basalts. Eucrite textures are also fine-grained, and often glomeroporphyritic due to clumps of phenocrysts set in the groundmass. This

is typical of terrestrial volcanic rocks that have cooled more slowly, producing glomerocrysts of interlocking plagioclase and pyroxene crystals. If basaltic lava contains dissolved gases when it suddenly erupts onto the earth's surface, the sudden reduction in pressure releases the gases which quickly form bubbles that make their way to the top of the flow. The eucrite, Ibitira, one of the few unbrecciated eucrites known, shows a remarkable vesicular texture (fig. 4), similar to that seen in a terrestrial basalt lava flow as that just described. Microscopically, the resemblance of most eucrites to terrestrial basalts is also most striking (fig. 5a and b).



Fig. 4. This unbrecciated eucrite called Ibitira fell in the village of that name near Martinho Campos, Minas Gerais, Brazil, in 1957. It is the only eucrite known to have a vesicular texture. The millimeter-sized gas holes cover 5–7 vol. % of the rock. The scale rule is in cm so the specimen is about 10 cm (about 4 in) wide (after Norton 2002).

Mineralogically, the eucrites are quite simple. They consist almost entirely of plagioclase (30–50%) and clinopyroxene (40–60%), the clinopyroxene usually dominating by 10–20%. The plagioclase in eucrites is calcic, being primarily anorthite with some bytownite, that is, within the range An_{75-95} , and igneous zoning is commonly preserved. The clinopyroxene is low-Ca pigeonite, with a composition that varies widely from specimen to specimen, and even within a given specimen. A typical pyroxene composition (wollastonite-enstatite-ferrosilite) in mole percent might be $Wo_{1-25} En_{42-48} Fs_{43-52}$. Minor minerals include chromite ($FeCr_2O_4$), Fe-Ni metal, ilmenite ($FeTiO_3$) and troilite (FeS) as opaque minerals, orthopyroxene, and polymorphs of silica—quartz, tridymite, and cristobalite.

Eucrites are subdivided into three major subclasses—the noncumulate eucrites (basaltic eucrites), the cumulate eucrites (cumulate gabbros),

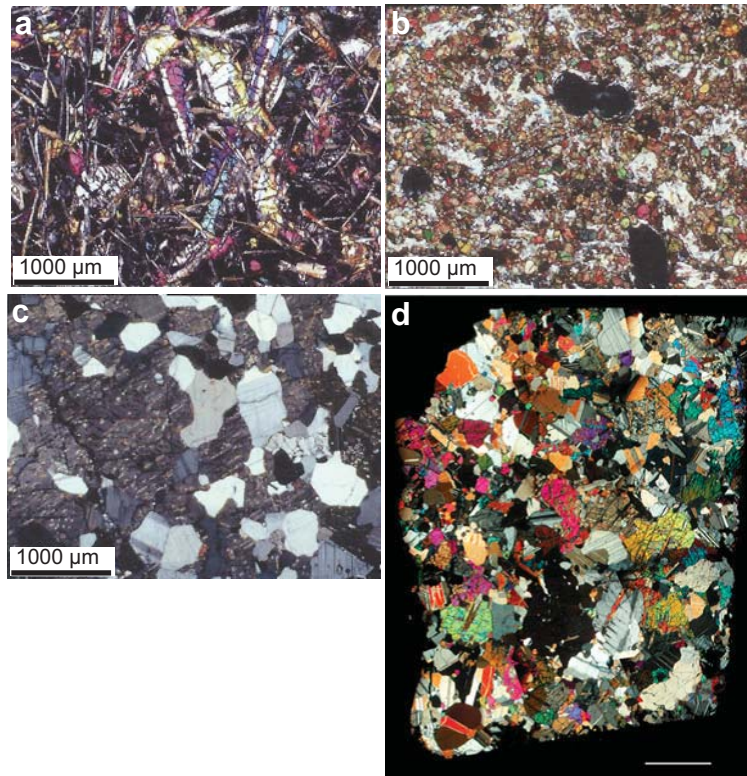


Fig. 5. Thin section photomicrographs in transmitted light under crossed polars of four typical eucrites (basaltic achondrites) (after Krot et al. 2005; McSween et al. 2011). (a) The unequilibrated noncumulate eucrite Pasamonte, showing the typical basaltic texture of plagioclase (light) and pyroxene (colored). (b) The metamorphosed (equilibrated) noncumulate eucrite Ibitira, showing a recrystallized texture with plagioclase (white) and pyroxene (colored), with the round, dark areas in the center, bottom, and left being vesicles. (c) The cumulate eucrite Serra de Magé, consisting of large crystals of plagioclase (lighter material with straight twin lamellae) and mostly orthopyroxene with complex augite exsolution lamellae (darker material with irregular, sometimes worm-like exsolution lamellae). (d) The cumulate eucrite Moore County, consisting of large crystals of plagioclase (lighter material with straight twin lamellae) and colorful abundant orthopyroxene (with occasional exsolution lamellae) (scale bar is 2.5 mm [0.09 in]).

and the polymict eucrites (polymict breccias of basaltic and cumulate eucrites) (Krot et al. 2005; Mittlefehldt 2005).

Noncumulate (basaltic) eucrites are mostly fragmental breccias of fine to medium grained, subophitic to ophitic basalts that are postulated to have formed originally as quickly cooled surface lava flows. They are known as unequilibrated, unmetamorphosed or least-metamorphosed, noncumulate eucrites (such as Pasamonte—see fig. 5a), and are composed of pigeonite and plagioclase, with minor silica, ilmenite, and chromite, and accessory phosphates, troilite, Fe-Ni metal, fayalitic olivine, zircon, and baddeleyite. As a result of their apparent fast cooling their pyroxenes (pigeonite of Mg# ~70–20) are zoned, and exsolution lamellae are only visible by TEM. However, most noncumulate eucrites appear to have been subsequently metamorphosed, and are thus known as metamorphosed or equilibrated noncumulate eucrites (such as Juvinas, Stannern, and Ibitira—see fig. 5b). They are highly abundant and so are also collectively referred to as the ordinary eucrites. They are unbrecciated or

monomict-brecciated, metamorphosed basalts and contain homogeneous low-Ca pigeonite (Mg# ~42–30) with fine exsolution lamellae of high-Ca pyroxene. The pyroxenes were originally ferroan pigeonite ($\sim\text{Wo}_{7-15} \text{En}_{29-43} \text{Fs}_{48-58}$) which exsolved augite during metamorphism. In most eucrites, pyroxene Fe/Mg is uniform as a result of metamorphism, but original igneous zoning is preserved in very few. Plagioclase is calcic, with most in the range An_{75-93} , and igneous zoning is commonly preserved.

Cumulate eucrites are coarse-grained gabbros, many unbrecciated (such as Serra de Magé—see fig. 5c, and Moore County—see fig. 5d), composed of pigeonite, plagioclase, and minor chromite with silica, ilmenite, Fe-Ni metal, troilite, and phosphate as trace accessory phases. The original igneous pyroxene was pigeonite ($\sim\text{Wo}_{7-16} \text{En}_{38-61} \text{Fs}_{32-46}$) which exsolved augite and, in some, inverted to orthopyroxene. They contain orthopyroxene inverted from low-Ca clinopyroxene (Mg# ~67–58) and orthopyroxene inverted from pigeonite (Mg# ~57–45). Plagioclase is generally more calcic than that typical for basaltic eucrites, with most in the range An_{91-95} .

Polymict eucrites are polymict breccias consisting of fragmental and melt-matrix breccias mostly of eucritic material, but they also contain <10 vol.% of diogenitic component in the form of orthopyroxenite.

The Radioisotope Dating of the Eucrites

To thoroughly investigate the radioisotope dating of the eucrite achondrites all the relevant literature was searched. The objective was to find eucrite achondrites that have been dated by more than one radioisotope method, and a convenient place to start was Dalrymple (1991, 2004), who compiled lists of such data. The 12 eucrite achondrite meteorites that were found to have been dated multiple times by more than one radioisotope method—Bereba, Cachari, Caldera, Camel Donga (fig. 2), Ibitira (figs. 4 and 5b), Juvinas, Moama, Moore County (fig. 5d), Pasamonte (figs. 3 and 5a), Serra de Magé (fig. 5c), Stannern, and Yamato 75011—thus became the focus of this study. When papers containing radioisotope dating results for these eucrites were found, the reference lists were also scanned to find further relevant papers. In this way a comprehensive set of papers, articles and abstracts on radioisotope dating of these basaltic achondrite meteorites was collected. While it cannot be claimed that all the papers, articles and abstracts which have ever been published containing radioisotope dating results for these eucrites have thus been obtained, the cross-checking undertaken between these publications does indicate the data set obtained is very comprehensive.

All the radioisotope dating results of these 12 eucrites were then compiled and tabulated. For ease of viewing and comparing the radioisotope dating data, the isochron and model ages for some or all components of each of these 12 eucrites were tabulated separately—the isochron ages in Table 1 and the model ages in Table 2. The data in these tables were then plotted on frequency versus age histogram diagrams, with the same color coding being used to show the ages obtained by the different radioisotope dating methods—the isochron ages for whole-rock samples and some or all components of each of these 12 eucrites (fig. 6), and the model ages for whole-rock samples and components of each of these 12 eucrites (fig. 7).

Discussion

In contrast to the Allende CV3 carbonaceous chondrite meteorite (Snelling 2014a), there have been fewer radioisotope ages obtained for these eucrites (basaltic achondrites), even though all the radioisotope dating methods have been used on some of them, and a few of the methods on others. Yet the outcome is similar to that found for the ordinary and enstatite chondrites (Snelling 2014b).

Isochron ages

A 4.55–4.57 Ga isochron age for Bereba, Ibitira, Juvinas, Pasamonte, Serra de Magé, and Yamato 75011 is clearly defined by a strong clustering of their isochron radioisotope data, via the Pb-Pb, U-Pb, Sm-Nd, Rb-Sr, and Lu-Hf methods, though not all these methods cluster for each of these eucrites (fig. 6). As expected, the Mn-Cr, Hf-W, Al-Mg, and I-Xe methods also yield isochron ages that coincide with the Pb-Pb and/or U-Pb isochron ages, simply because the Mn-Cr method is calibrated against the Pb-Pb isochron age of the Lewis Cliff 86010 angrite achondrite (Lugmair and Galer 1992; Lugmair and Shukolyukov 1998), the Hf-W method is calibrated against the Hf-W and Mn-Cr isochron ages of the St. Marguerite H4 chondrite anchored to the weighted average of its U-Pb whole-rock ages (Göpel, Manhès, and Allègre 1994; Kleine et al. 2002, 2004, 2005; Polnau and Lugmair 2001), the Al-Mg method is calibrated against the Pb-Pb isochron age of the CAIs in the CR chondrite Acfer 059 (Amelin et al. 2002; Amelin, Wadhwa and Lugmair 2006; Wadhwa et al. 2004), and the I-Xe method is calibrated against the I-Xe isochron age of the Shallowater aubrite achondrite (Claydon, Crowther, and Gilmour 2013), which is calibrated against the I-Xe isochron and Pb-Pb model ages of phosphate grains from the Acapulco primitive achondrite (Brazzle et al. 1999; Göpel, Manhès, and Allègre 1992, 1994; Nichols et al. 1994).

There is also considerable scattering of the isochron radioisotope age data for these and the other eucrites studied (fig. 6). Many Rb-Sr isochron ages are younger than the 4.55–4.57 Ga clustering (for Bereba, Juvinas, Moore County, Pasamonte, Stannern, and Yamato 75011), though some are older (for Juvinas and Yamato 75011). Similarly many Sm-Nd isochron ages are younger than the 4.55–4.57 Ga clustering (for Bereba, Cachari, Ibitira, Juvinas, Moama, Moore County, Serra de Magé, and Stannern), while a few are older (for Bereba, Ibitira, and Moore County). Somewhat surprisingly, all the Pb-Pb isochron ages for Bereba, Cachari, Moama, Moore County, Serra de Magé, and Stannern, and one for Juvinas, are younger than the 4.55–4.57 Ga clustering, much younger in the case of Stannern. In contrast, the U-Pb isochron (concordia) ages are always in or close to that clustering.

No consistent pattern is evident of Rb-Sr and Sm-Nd isochron ages always being younger than the Lu-Hf and U-Th-Pb isochron ages respectively in the order of the parents' atomic weights or their decay rates (half-lives), according to their β and α decay mode respectively. Such a pattern would be potentially indicative of a past episode of accelerated radioisotope decay, as suggested by Snelling (2005c) and Vardiman, Snelling, and Chaffin (2005) from their radioisotope investigations of earth rocks and minerals.

Table 1. Isochron ages for whole-rock samples and some or all components of 12 eucrite achondrites, with the details and literature sources.

Sample	Method	Date	Error +/-	Note	Source	Type
Bereba						
eight fractions (whole rock and mineral)	Rb-Sr	4.17	0.26		Birck and Allègre 1978	isochron age
	Rb-Sr	4.08	0.26		Basaltic Volcanism Study Project 1981	isochron age
one whole-rock sample plotted with 12 other samples	Rb-Sr	4.55	0.19	ten other meteorites plus three plagioclase samples	Hans, Kleine, and Bourdon 2013	isochron age
one sample plotted with 14 other meteorites	Lu-Hf	4.604	0.039		Blichort-Toft et al. 2002	isochron age
whole rock and plagioclase samples	Pb-Pb	4.522	0.004		Carlson, Tera, and Boctor 1988	isochron age
plagioclase and whole rock + leachate	Pb-Pb	4.52			Tera, Carlson, and Boctor 1997	isochron age
three zircon grains intercept concordia	U-Pb	4.538	0.026		Lee et al. 2009	isochron age
three point analyses of one apatite grain	U-Pb	4.196	0.013		Zhou et al. 2011	isochron age
five point analyses of three zircon grains	U-Pb	4.552	0.021		Zhou et al. 2013	isochron age
whole rock + mineral separates	Sm-Nd	4.79			Carlson, Tera, and Boctor 1988	isochron age
one sample plotted with 17 other meteorites	Sm-Nd	4.464	0.075		Blichort-Toft et al. 2002	isochron age
one sample plotted with seven other meteorites	Hf-W	4.5632	0.0014		Kleine et al. 2004	isochron age
	Hf-W	4.55	0.0041		Kleine et al. 2005	isochron age
Cacheri						
one sample plotted with 17 other meteorites	Lu-Hf	4.604	0.039		Blichort-Toft et al. 2002	isochron age
mean of three isochrons	Pb-Pb	4.453	0.015		Tera, Carlson, and Boctor 1997	isochron age
six fractions	²⁰⁶ Pb- ²⁰⁴ Pb	4.453	0.015		Tera, Carlson, and Boctor 1997	isochron age
eight fractions	²⁰⁷ Pb- ²⁰⁶ Pb	4.451	0.015		Tera, Carlson, and Boctor 1997	isochron age
eight fractions	²⁰⁷ Pb- ²⁰⁴ Pb	4.455	0.016		Tera, Carlson, and Boctor 1997	isochron age
sixteen analyses of six zircon grains	²⁰⁷ Pb- ²⁰⁴ Pb	4.558	0.025		Zhou et al. 2013	isochron age
three analyses of one zircon grain	U-Pb	4.546	0.01		Zhou et al. 2011	isochron age
three analyses of one zircon grain	U-Pb	4.548	0.024		Zhou et al. 2013	isochron age
six fractions	Sm-Nd	3.99	0.21		Tera, Carlson, and Boctor 1997	isochron age
one sample plotted with 17 other meteorites	Sm-Nd	4.464	0.075		Blichort-Toft et al. 2002	isochron age
Caldera						
one whole-rock sample plotted with 14 other meteorites	Lu-Hf	4.604	0.039		Blichort-Toft et al. 2002	isochron age
pyroxene and plagioclase fractions	Pb-Pb	4.5161	0.0028		Galer and Lugmair 1996	isochron age
four points on one zircon grain	U-Pb	4.563	0.18		Zhou et al. 2013	isochron age
two whole rocks, plagioclase, and pyroxene fractions	Sm-Nd	4.544	0.019		Wadhwa and Lugmair 1996	isochron age
four fractions	Mn-Cr	4.545			Lugmair and Shukolyukov 1998	isochron age
Camel Donga						
matrix samples with pyroxenes, inverse	Ar-Ar	3.706	0.097		Kennedy et al. 2013	isochron age

Sample	Method	Date	Error +/-	Note	Source	Type
matrix samples with pyroxenes, inverse	Ar-Ar	3.685	0.085		Kennedy et al. 2013	isochron age
mean of two, inverse	Ar-Ar	3.703	0.059		Kennedy et al. 2013	isochron age
thirty-five point analyses of 14 zircon grains	U-Pb	4.512	0.011		Zhou et al. 2013	isochron age
	Hf-W	4.546	0.005		Kleine et al. 2005	isochron age
	Hf-W	4.545	0.0035		Kleine et al. 2005	isochron age
Ibitira						
whole rock plus four mineral separates	Rb-Sr	4.52	0.25		Birck and Allègre 1978	isochron age
Ibitira samples plotted with Juvinas samples, plus whole-rock samples of eight other meteorites	Rb-Sr	4.57	0.13		Birck and Allègre 1978	isochron age
one sample plotted with 14 other meteorites	Lu-Hf	4.604	0.039		Blichert-Toft et al. 2002	isochron age
three whole-rock samples	²⁰⁷ Pb- ²⁰⁶ Pb	4.556			Chen and Wasserburg 1985	isochron age
nine samples (pyroxenes)—external normalization (EN)	²⁰⁷ Pb- ²⁰⁶ Pb	4.55703	0.00082		Amelin, Wadhwa, and Lugmair 2006	isochron age
nine samples (pyroxenes)—EN and double spike (DS)	²⁰⁷ Pb- ²⁰⁶ Pb	4.55744	0.00055		Amelin, Wadhwa, and Lugmair 2006	isochron age
pyroxene leachates and residues	Pb-Pb	4.5561	0.0023		Iizuka et al. 2013	isochron age
residues of eight pyroxene-rich and two whole-rock fractions and washes of two pyroxene-rich and one plagioclase-rich fractions (13-point isochron)	Pb-Pb	4.5565	0.0013		Iizuka et al. 2014	isochron age
residues of one whole-rock and six pyroxene-rich fractions (7-point isochron)	Pb-Pb	4.55675	0.00057		Iizuka et al. 2014	isochron age
residues of eight pyroxene-rich and two whole-rock fractions and washes of two pyroxene-rich and one plagioclase-rich fractions (13-point chord)	U-Pb	4.5569	0.0014		Iizuka et al. 2014	isochron age (concordia)
residues of one whole-rock and six pyroxene-rich fractions (7-point chord)	U-Pb	4.556	0.0052		Iizuka et al. 2014	isochron age (concordia)
whole rock plus five mineral separates	Sm-Nd	4.46	0.02		Prinzhofer, Papanastassiou, and Wasserburg 1992	isochron age
two whole-rock samples plus multiple plagioclase, pyroxene and phosphate separates	Sm-Nd	4.57	0.09		Nyquist et al. 1999	isochron age
two whole-rock samples plus phosphate and pyroxene separates	Sm-Nd	4.6	0.05		Nyquist et al. 1999	isochron age
two whole-rock samples plus pyroxene and plagioclase separates	Sm-Nd	4.41	0.07		Nyquist et al. 1999	isochron age
one sample plotted with 17 other meteorites	Sm-Nd	4.464	0.075		Blichert-Toft et al. 2002	isochron age
three fractions	Hf-W	4.549	0.012		Kleine et al. 2005	isochron age
three fractions	Mn-Cr	4.557	0.003		Lugmair and Shukolyukov 1998	isochron age
after Lugmair and Shukolyukov (1998) using Pb-Pb age of D'Orbigny	Mn-Cr	4.5574	0.0025		Iizuka et al. 2014	isochron age
after Yin, Amelin, and Jacobsen (2009) using the Pb-Pb age of D'Orbigny	Mn-Cr	4.5559	0.0032		Iizuka et al. 2014	isochron age

Sample	Method	Date	Error +/-	Note	Source	Type
whole rock, pyroxene (2) and plagioclase (2) fractions	Al-Mg	4.5614			Wadhwa et al. 2004	isochron age
whole rock, pyroxene (2) and plagioclase (2) fractions	Al-Mg	4.5607			Amelin, Wadhwa, and Lugmair 2006	isochron age
relative to Shallowater	I-Xe	4.555	0.001		Claydon, Crowther, and Gilmour 2013	isochron age
Juvinas						
one whole-rock sample plotted with six other meteorites	Rb-Sr	4.39	0.26		Papanastassiou and Wasserburg 1969	isochron age
four mineral separates plus whole rock	Rb-Sr	4.6	0.07		Allègre et al. 1975	isochron age
earlier data plotted with Ibitira	Rb-Sr	4.58	0.14		Birck and Allègre 1978	isochron age
revised Allègre et al. (1975) age	Rb-Sr	4.5	0.07		Quitte, Birck, and Allègre 2000	isochron age
whole-rock and plagioclase samples plotted with eleven other samples	Rb-Sr	4.55	0.19	ten other meteorites and two plagioclase samples	Hans, Kleine, and Bourdon 2013	isochron age
one sample plotted with nine other meteorites	Lu-Hf	4.55		adjusted to agree with other methods	Patchett and Tatsumoto 1980	isochron age
one sample plotted with 14 other meteorites	Lu-Hf	4.604	0.039		Blichert-Toft et al. 2002	isochron age
pyroxene and plagioclase fractions	Pb-Pb	4.3209	0.017		Galer and Lugmair 1996	isochron age
	²⁰⁷ Pb- ²⁰⁶ Pb	4.556	0.012	eight samples	Tatsumoto and Unruh 1975	isochron age
	²⁰⁷ Pb- ²⁰⁶ Pb	4.54	0.0007	nine samples	Manhes, Allègre, and Provost 1984	isochron age
	²⁰⁶ Pb- ²³⁸ U	4.531	0.003	upper intercept	Manhes, Allègre, and Provost 1984	isochron age
	²⁰⁶ Pb- ²³⁸ U	4.539	0.004	upper intercept	Manhes, Allègre, and Provost 1984	isochron age
	²⁰⁶ Pb- ²³⁸ U	4.545	0.0012	seven samples	Manhes, Allègre, and Provost 1984	isochron age
	²⁰⁷ Pb- ²³⁵ U	4.543	0.003	eight samples	Manhes, Allègre, and Provost 1984	isochron age
	²³² Th- ²⁰⁸ Pb	4.47	0.03	nine samples	Manhes, Allègre, and Provost 1984	isochron age
twenty analyses of seven zircon grains	U-Pb	4.53	0.033		Zhou et al. 2013	isochron age
whole rock (2), plagioclase, and pyroxene fractions	Sm-Nd	4.56	0.08		Lugmair 1974; Lugmair, Scheinin, and Marti 1975	isochron age
one sample plotted with 17 other meteorites	Sm-Nd	4.464	0.075		Blichert-Toft et al. 2002	isochron age
five samples plotted with seven other meteorites	Hf-W	4.5632	0.0014		Kleine et al. 2004	isochron age
	Hf-W	4.5457	0.0036	five fractions	Kleine et al. 2005	isochron age
five fractions	Mn-Cr	4.5625	0.001		Lugmair and Shukloyukov 1998	isochron age
	Mn-Cr	4.5642	0.0012		Schiller, Baker, and Bizzarro 2010	isochron age
whole rock, pyroxene (3), and plagioclase (3) fractions	Al-Mg	4.561			Wadhwa et al. 2004	isochron age
Moama						
whole-rock sample plotted with 12 other samples	Rb-Sr	4.55	0.19	ten other meteorites and three plagioclase samples	Hans, Kleine, and Bourdon 2013	isochron age
one sample plotted with nine other meteorites	Lu-Hf	4.55			Patchett and Tatsumoto 1980	isochron age
one sample plotted with 14 other meteorites	Lu-Hf	4.604	0.039		Blichert-Toft et al. 2002	isochron age
whole rock, WR leachate, and plagioclase and pyroxene separates	²⁰⁷ Pb- ²⁰⁶ Pb	4.439	0.097		Tera, Carlson, and Boctor 1997	isochron age

Sample	Method	Date	Error +/-	Note	Source	Type
whole rock, WR leachate, and plagioclase and pyroxene separates	^{207}Pb - ^{204}Pb	4.416	0.092		Tera, Carlson, and Boctor 1997	isochron age
whole rock, WR leachate, and plagioclase and pyroxene separates	^{206}Pb - ^{204}Pb	4.423	0.094		Tera, Carlson, and Boctor 1997	isochron age
mean of the Pb-Pb isochron ages	mean Pb-Pb	4.426	0.094		Tera, Carlson, and Boctor 1997	isochron age
	Sm-Nd	4.52	0.05		Hamet et al. 1978	isochron age
whole rock, plus two pyroxene and plagioclase separates	Sm-Nd	4.46	0.03		Jacobsen and Wasserburg 1984	isochron age
whole rock, pyroxene and plagioclase fractions	Sm-Nd	4.594	0.079	plus Hamet et al. 1978 and Jacobsen and Wasserburg 1984 data	Boyet, Carlson, and Horan 2010	isochron age
Moore County						
one sample plotted with eight other meteorites	Rb-Sr	4.557	0.253		Cumming 1969	isochron age
one whole-rock sample plotted with six other meteorites	Rb-Sr	4.39	0.26		Papanastassiou and Wasserburg 1969	isochron age
plagioclase sample plotted with 12 other samples	Rb-Sr	4.55	0.19	ten other meteorites and two plagioclase samples	Hans, Kleine, and Bourdon 2013	isochron age
one sample plotted with nine other meteorites and adjusted to agree with other methods	Lu-Hf	4.55			Patchett and Tatsumoto 1980	isochron age
one sample plotted with 14 other meteorites	Lu-Hf	4.604	0.039		Blichert-Toft et al. 2002	isochron age
whole rock (3), pyroxene (2) and plagioclase (2) fractions and leachates	^{207}Pb - ^{204}Pb	4.477	0.022		Tera, Carlson, and Boctor 1997	isochron age
	^{207}Pb - ^{206}Pb	4.494	0.017			isochron age
	^{206}Pb - ^{204}Pb	4.481	0.02			isochron age
	mean Pb-Pb	4.484	0.019			isochron age
internal	Sm-Nd	4.6	0.04		Unruh, Nakamura, and Tatsumoto 1977	isochron age
whole rock, pyroxene plagioclase (2) fractions	Sm-Nd	4.456	0.025		Tera, Carlson, and Boctor 1997	isochron age
	Sm-Nd	4.457	0.025		Tera, Carlson, and Boctor 1997	isochron age
one sample plotted with 17 other meteorites	Sm-Nd	4.464	0.075		Blichert-Toft et al. 2002	isochron age
whole rock, pyroxene and plagioclase fractions	Sm-Nd	4.542	0.085	plus Tera, Carlson, and Boctor 1997 and Blichert-Toft et al. 2002 data	Boyet, Carlson, and Horan 2010	isochron age
two fractions	Mn-Cr	4.549			Lugmair and Shukolyukov 1998	isochron age
Pasamonte						
one sample plotted with five other meteorites	Rb-Sr	4.411	0.088		Shields, Pinson, and Hurley 1965	isochron age
one sample plotted with eight other meteorites	Rb-Sr	4.557	0.253		Cumming 1969	isochron age
one whole-rock sample plotted with six other meteorites	Rb-Sr	4.39	0.26		Papanastassiou and Wasserburg 1969	isochron age
two whole-rock samples plotted with nine other meteorites	Rb-Sr	4.33	0.49		Birck and Allègre 1978	isochron age
whole-rock sample plotted with 12 other samples	Rb-Sr	4.55	0.19	ten other meteorites and three plagioclase samples	Hans, Kleine, and Bourdon 2013	isochron age
one sample plotted with nine other meteorites and adjusted to agree with other methods	Lu-Hf	4.55			Patchett and Tatsumoto 1980	isochron age

Sample	Method	Date	Error +/-	Note	Source	Type
one sample plotted with 14 other meteorites	Lu-Hf	4.604	0.039		Blichert-Toft et al. 2002	isochron age
revised Unruh, Nakamura, and M. Tatsumoto 1977 age	Pb-Pb	4.573	0.011		Quitté, Birck, and Allègre 2000	isochron age
whole rock and 13 mineral separates	²⁰⁷ Pb- ²⁰⁶ Pb	4.53	0.03		Unruh, Nakamura, and Tatsumoto 1977	isochron age
six sample points (whole rock, plag, and density fractions)	Sm-Nd	4.58	0.12		Unruh, Nakamura, and Tatsumoto 1977	isochron age
two samples plotted with seven other meteorites	Hf-W	4.5632	0.0014		Kleine et al. 2004	isochron age
Serra De Magé						
whole-rock sample plotted with 12 other samples	Rb-Sr	4.55	0.19	ten other meteorites and three plagioclase samples	Hans, Kleine, and Bourdon 2013	isochron age
one sample plotted with nine other meteorites and adjusted to agree with other methods	Lu-Hf	4.55			Patchett and Tatsumoto 1980	isochron age
one sample plotted with 14 other meteorites	Lu-Hf	4.604	0.039		Blichert-Toft et al. 2002	isochron age
whole rock, two whole rock leachates, and pyroxene and plagioclase fractions	²⁰⁷ Pb- ²⁰⁴ Pb	4.406	0.045		Tera, Carlson, and Boctor 1997	isochron age
	²⁰⁷ Pb- ²⁰⁶ Pb	4.39	0.016		Tera, Carlson, and Boctor 1997	isochron age
	²⁰⁶ Pb- ²⁰⁴ Pb	4.4	0.037		Tera, Carlson, and Boctor 1997	isochron age
	mean Pb-Pb	4.399	0.035		Tera, Carlson, and Boctor 1997	isochron age
	Sm-Nd	4.41	0.02		Lugmair, Scheinin, and Carlson 1977	isochron age
one sample plotted with 17 other meteorites	Sm-Nd	4.464	0.075		Blichert-Toft et al. 2002	isochron age
one sample plotted with seven other meteorites	Hf-W	4.5632	0.0014		Kleine et al. 2004	isochron age
three fractions	Mn-Cr	4.553	0.003		Lugmair and Shukolyukov 1998	isochron age
Stannern						
one whole-rock sample plotted with six other meteorites	Rb-Sr	4.39	0.26		Papanastassiou and Wasserburg 1969	isochron age
eight fractions (whole rock, three plagioclase, pyroxene, plus three others)	Rb-Sr	3.3	0.5		Birck and Allègre 1978	isochron age
whole-rock sample plotted with 12 other samples	Rb-Sr	4.55	0.19	ten other meteorites and three plagioclase samples	Hans, Kleine, and Bourdon 2013	isochron age
two samples plotted with nine other meteorites	Lu-Hf	4.55	0.019		Patchett and Tatsumoto 1980	isochron age
one sample plotted with 14 other meteorites	Lu-Hf	4.604	0.039		Blichert-Toft et al. 2002	isochron age
three-point isochron based on whole rock, pyroxene, and plagioclase fractions	²⁰⁷ Pb- ²⁰⁴ Pb	4.131	0.012		Tera, Carlson, and Boctor 1997	isochron age
	²⁰⁷ Pb- ²⁰⁶ Pb	4.124	0.023			isochron age
	²⁰⁶ Pb- ²⁰⁴ Pb	4.13	0.012			isochron age
	mean Pb-Pb	4.128	0.016			isochron age
	Sm-Nd	4.48	0.07		Lugmair and Scheinin 1975	isochron age
one sample plotted with 17 other meteorites	Sm-Nd	4.464	0.075		Blichert-Toft et al. 2002	isochron age
whole rock, magnetic, and two non-magnetic fractions	Hf-W	4.564	0.002		Kleine et al. 2005	isochron age
Yamato 75011						
whole rock and density fractions 73 matrix	Rb-Sr	4.52	0.11	(decay constant 0.0139)	Bansal, Shih, and Wiesmann 1985	isochron age

Sample	Method	Date	Error +/-	Note	Source	Type
whole rock and density fractions 73 matrix	Rb-Sr	4.42	0.11	(decay constant 0.0142)	Bansal, Shih, and Wiesmann 1985	isochron age
whole rock and density fractions 84B clast	Rb-Sr	4.56	0.11	(decay constant 0.0139)	Bansal, Shih, and Wiesmann 1985	isochron age
whole rock and density fractions 84B clast	Rb-Sr	4.46	0.1	(decay constant 0.0142)	Bansal, Shih, and Wiesmann 1985	isochron age
73 matrix, five data points, old decay constant	Rb-Sr	4.56	0.06		Nyquist et al. 1986	isochron age
73 matrix, five data points, new decay constant	Rb-Sr	4.46	0.06		Nyquist et al. 1986	isochron age
73 matrix, nine data points, old decay constant	Rb-Sr	4.6	0.05		Nyquist et al. 1986	isochron age
73 matrix, nine data points, new decay constant	Rb-Sr	4.5	0.05		Nyquist et al. 1986	isochron age
five data points	U-Pb	4.552	0.017		Misawa et al. 2005	isochron age
73 matrix, 84B clast, 10 data points	Sm-Nd	4.55	0.14		Nyquist et al. 1986	isochron age
84B clast, seven data points	Sm-Nd	4.54	0.21		Nyquist et al. 1986	isochron age

However, it also has to be taken into account that there is still disagreement over the values of the decay constants and half-lives of, for example, ^{87}Rb and ^{176}Lu (Snelling 2014c, d), because of there being discrepancies between determinations based on comparisons of the Rb-Sr and Lu-Hf ages of meteorites (primarily eucrites), lunar rocks, and earth minerals and rocks with their U-Pb, K-Ar, and Ar-Ar ages. Indeed, the comparisons of ages involving meteorites (primarily eucrites) and lunar rocks yield a slightly higher decay constant and a slightly faster decay rate (half-life) for both ^{87}Rb and ^{176}Lu than for age comparisons involving earth rocks and minerals.

Thus if the different decay constants are used in calculating the Rb-Sr and Lu-Hf ages of eucrites, then the affect would be only small (0.6–4.0%) and would still result in Rb-Sr ages that are apparently too young and Lu-Hf ages that are apparently too old. This would not change the conclusion that there are no systematic isochron age differences based on the different atomic weights of the parent radioisotopes that would be due to a past accelerated decay event. Since in most instances the old decay constants have been used for calculating the isochron Rb-Sr ages but the meteorite decay constant has been used for calculating the isochron Lu-Hf ages, recalculating the isochron Rb-Sr ages using the meteorite decay constant would only bring them closer to agreement with the isochron Lu-Hf ages. This only serves to reinforce the lack of any consistent pattern in the isochron ages obtained by the different radioisotope systems, and thus there is no evidence of a past accelerated decay event.

Model ages

In contrast to the isochron ages for these eucrites (basaltic achondrites), there are many

more model ages for them (fig. 7). A 4.55–4.57 Ga model age for Bereba, Cacheri, Camel Donga, Ibitira, and Juvinas is very clearly defined by a strong clustering of Pb-Pb and U-Pb model ages, and for Yamato 75011 supported by Sm-Nd and Rb-Sr model ages. As again expected, the Pu-Xe, Al-Mg, and Mn-Cr model ages always plot in, or closely adjacent to, the strong clustering of Pb-Pb and U-Pb model ages. This is because the Pu-Xe model ages are calibrated against the Pb-Pb isochron age of the Angra dos Reis (ADOR) angrite achondrite (Lugmair and Galer 1992; Lugmair and Marti 1977; Miura et al. 1998; Shukolyukov and Begemann 1996a, b), the Al-Mg model ages are calibrated against the Pb-Pb isochron age of the CAIs in the Allende CV3 chondrite (Jacobsen et al. 2008; Schiller, Baker, and Bizzarro 2010), and the Mn-Cr model age for Caldera is calibrated against its Sm-Nd and Pb-Pb isochron ages (Galer and Lugmair 1996; Wadhwa and Lugmair 1996).

Scattering of the model ages is prolific, with K-Ar and Ar-Ar model ages generally being younger than the 4.55–4.57 Ga clustering for all these eucrite meteorites, except for a few that are older for Ibitira, Moore County, Pasamonte, Serra de Magé, and Stannern (fig. 7). Similarly the U-Pb model ages are either younger or older than the clustering, or in most instances both, whereas for Camel Donga they are usually younger, but for Juvinas and Yamato 75011 they are invariably older. Some of the Pb-Pb model ages for Bereba, Cacheri, Camel Donga, Ibitira, Juvinas, and Stannern are younger than the 4.55–4.57 Ga clustering, sometimes much younger, and a few for Ibitira, Juvinas, and Pasamonte are much older. For Yamato 75011 the Rb-Sr model ages are scattered either side of the strong clustering. Where available for Ibitira and Pasamonte, the Th-Pb model ages are nearly all older.

Table 2. Model ages for whole-rock samples and some or all components of 12 eucrite achondrites, with the details and literature sources.

Sample	Method	Date	Error +/-	Note	Source	Type
Bereba						
whole rock samples	K-Ar	2.8			Heymann, Mazor, and Anders 1968	model age
pyroxene	K-Ar	3			Hampel et al. 1980	model age
plagioclase	K-Ar	3.3			Hampel et al. 1980	model age
	K-Ar	3.31			Shukolyukov and Begemann 1996b	model age
whole rock	Pb-Pb	4.44			Manhès et al. 1975	model age
whole rock sample	Pb-Pb	4.44			Manhès et al. 1975	model age
	Pb-Pb	4.415			Manhès et al. 1975	model age
whole rock samples	Pb-Pb	4.536			Carlson Tera, and Boctor 1988	model age
whole rock, single stage model	Pb-Pb	4.536			Tera, Carlson, and Boctor 1997	model age
mean of all Pb isotope combinations on all samples	Pb-Pb	4.521	0.0004		Tera, Carlson, and Boctor 1997	model age
zircons	²⁰⁷ Pb- ²⁰⁶ Pb	4.534	0.016		Bukovanska and Ireland 1993	model age
weighted average of five analyses of three zircon grains	²⁰⁷ Pb- ²⁰⁶ Pb	4.552	0.02		Zhou et al. 2013	model age
Spot 1-1	²⁰⁷ Pb- ²⁰⁶ Pb	4.515	0.025		Zhou et al. 2013	model age
Spot 1-2	²⁰⁷ Pb- ²⁰⁶ Pb	4.569	0.02		Zhou et al. 2013	model age
Spot 2	²⁰⁷ Pb- ²⁰⁶ Pb	4.574	0.026		Zhou et al. 2013	model age
Spot 3-1	²⁰⁷ Pb- ²⁰⁶ Pb	4.549	0.019		Zhou et al. 2013	model age
Spot 3-2	²⁰⁷ Pb- ²⁰⁶ Pb	4.545	0.024		Zhou et al. 2013	model age
Spot 1-1	²⁰⁷ Pb- ²³⁵ U	4.425	0.034		Zhou et al. 2013	model age
Spot 1-2	²⁰⁷ Pb- ²³⁵ U	4.572	0.03		Zhou et al. 2013	model age
Spot 2	²⁰⁷ Pb- ²³⁵ U	4.563	0.032		Zhou et al. 2013	model age
Spot 3-1	²⁰⁷ Pb- ²³⁵ U	4.637	0.037		Zhou et al. 2013	model age
Spot 3-2	²⁰⁷ Pb- ²³⁵ U	4.49	0.031		Zhou et al. 2013	model age
Spot 1-1	²⁰⁶ Pb- ²³⁸ U	4.229	0.089		Zhou et al. 2013	model age
Spot 1-2	²⁰⁶ Pb- ²³⁸ U	4.579	0.085		Zhou et al. 2013	model age
Spot 2	²⁰⁶ Pb- ²³⁸ U	4.539	0.084		Zhou et al. 2013	model age
Spot 3-1	²⁰⁶ Pb- ²³⁸ U	4.841	0.114		Zhou et al. 2013	model age
Spot 3-2	²⁰⁶ Pb- ²³⁸ U	4.369	0.083		Zhou et al. 2013	model age
	Pu-Xe	4.498	0.016		Shukolyukov and Begemann 1996a	model age
whole rock sample relative to ADOR	Pu-Xe	4.512	0.018		Miura et al. 1998	model age
Cachari						
whole rock sample	Ar-Ar	3.04	0.7		Bogard et al. 1985	model age
whole rock sample	Ar-Ar	3.47	0.4		Bogard et al. 1985	model age
whole rock sample	Pb-Pb	4.13			Tera, Carlson, and Boctor 1987	model age
three analyses of one zircon grain	²⁰⁷ Pb- ²⁰⁶ Pb	4.549	0.013	weighted average	Zhou et al. 2011	model age
sixteen analyses of six zircon grains	²⁰⁷ Pb- ²⁰⁶ Pb	4.551	0.014	weighted mean	Zhou et al. 2013	model age
Grain 1-1	²⁰⁷ Pb- ²⁰⁶ Pb	4.539	0.017	ages using Canyon Diablo troilite Pb	Zhou et al. 2013	model age

Sample	Method	Date	Error +/-	Note	Source	Type
Grain 1-2	^{207}Pb - ^{206}Pb	4.533	0.017	ages using Canyon Diablo troilite Pb	Zhou et al. 2013	model age
Grain 1-3	^{207}Pb - ^{206}Pb	4.556	0.017	ages using Canyon Diablo troilite Pb	Zhou et al. 2013	model age
Grain 2-1	^{207}Pb - ^{206}Pb	4.535	0.019	ages using Canyon Diablo troilite Pb	Zhou et al. 2013	model age
Grain 3-1	^{207}Pb - ^{206}Pb	4.579	0.016	ages using Canyon Diablo troilite Pb	Zhou et al. 2013	model age
Grain 3-2	^{207}Pb - ^{206}Pb	4.587	0.016	ages using Canyon Diablo troilite Pb	Zhou et al. 2013	model age
Grain 3-3	^{207}Pb - ^{206}Pb	4.596	0.016	ages using Canyon Diablo troilite Pb	Zhou et al. 2013	model age
Grain 4-1	^{207}Pb - ^{206}Pb	4.565	0.019	ages using Canyon Diablo troilite Pb	Zhou et al. 2013	model age
Grain 4-2	^{207}Pb - ^{206}Pb	4.546	0.021	ages using Canyon Diablo troilite Pb	Zhou et al. 2013	model age
Grain 5-1	^{207}Pb - ^{206}Pb	4.51	0.019	ages using Canyon Diablo troilite Pb	Zhou et al. 2013	model age
Grain 5-2	^{207}Pb - ^{206}Pb	4.516	0.019	ages using Canyon Diablo troilite Pb	Zhou et al. 2013	model age
Grain 5-3	^{207}Pb - ^{206}Pb	4.524	0.018	ages using Canyon Diablo troilite Pb	Zhou et al. 2013	model age
Grain 5-4	^{207}Pb - ^{206}Pb	4.563	0.018	ages using Canyon Diablo troilite Pb	Zhou et al. 2013	model age
Grain 5-5	^{207}Pb - ^{206}Pb	4.54	0.019	ages using Canyon Diablo troilite Pb	Zhou et al. 2013	model age
Grain 6-1	^{207}Pb - ^{206}Pb	4.558	0.019	ages using Canyon Diablo troilite Pb	Zhou et al. 2013	model age
Grain 6-2	^{207}Pb - ^{206}Pb	4.515	0.019	ages using Canyon Diablo troilite Pb	Zhou et al. 2013	model age
Grain 6-3	^{207}Pb - ^{206}Pb	4.564	0.02	ages using Canyon Diablo troilite Pb	Zhou et al. 2013	model age
Grain 1-1	^{207}Pb - ^{206}Pb	4.539	0.018	ages using terrestrial common Pb	Zhou et al. 2013	model age
Grain 1-2	^{207}Pb - ^{206}Pb	4.533	0.018	ages using terrestrial common Pb	Zhou et al. 2013	model age
Grain 1-3	^{207}Pb - ^{206}Pb	4.557	0.016	ages using terrestrial common Pb	Zhou et al. 2013	model age
Grain 2-1	^{207}Pb - ^{206}Pb	4.536	0.019	ages using terrestrial common Pb	Zhou et al. 2013	model age
Grain 3-1	^{207}Pb - ^{206}Pb	4.58	0.016	ages using terrestrial common Pb	Zhou et al. 2013	model age

Sample	Method	Date	Error +/-	Note	Source	Type
Grain 3-2	^{207}Pb - ^{206}Pb	4.588	0.016	ages using terrestrial common Pb	Zhou et al. 2013	model age
Grain 3-3	^{207}Pb - ^{206}Pb	4.596	0.016	ages using terrestrial common Pb	Zhou et al. 2013	model age
Grain 4-1	^{207}Pb - ^{206}Pb	4.566	0.019	ages using terrestrial common Pb	Zhou et al. 2013	model age
Grain 4-2	^{207}Pb - ^{206}Pb	4.547	0.021	ages using terrestrial common Pb	Zhou et al. 2013	model age
Grain 5-1	^{207}Pb - ^{206}Pb	4.51	0.019	ages using terrestrial common Pb	Zhou et al. 2013	model age
Grain 5-2	^{207}Pb - ^{206}Pb	4.516	0.019	ages using terrestrial common Pb	Zhou et al. 2013	model age
Grain 5-3	^{207}Pb - ^{206}Pb	4.524	0.018	ages using terrestrial common Pb	Zhou et al. 2013	model age
Grain 5-4	^{207}Pb - ^{206}Pb	4.563	0.018	ages using terrestrial common Pb	Zhou et al. 2013	model age
Grain 5-5	^{207}Pb - ^{206}Pb	4.54	0.019	ages using terrestrial common Pb	Zhou et al. 2013	model age
Grain 6-1	^{207}Pb - ^{206}Pb	4.559	0.019	ages using terrestrial common Pb	Zhou et al. 2013	model age
Grain 6-2	^{207}Pb - ^{206}Pb	4.515	0.017	ages using terrestrial common Pb	Zhou et al. 2013	model age
Grain 6-3	^{207}Pb - ^{206}Pb	4.565	0.02	ages using terrestrial common Pb	Zhou et al. 2013	model age
weighted averages of three analyses of one zircon grain	^{207}Pb - ^{206}Pb	4.55	0.039		Zhou et al. 2013	model age
Spot 7-1	^{207}Pb - ^{206}Pb	4.529	0.013		Zhou et al. 2013	model age
Spot 7-2	^{207}Pb - ^{206}Pb	4.549	0.032		Zhou et al. 2013	model age
Spot 7-3	^{207}Pb - ^{206}Pb	4.596	0.093		Zhou et al. 2013	model age
weighted averages of three analyses of one zircon grain	^{207}Pb - ^{235}U	4.568	0.033		Zhou et al. 2013	model age
Spot 7-1	^{207}Pb - ^{235}U	4.561	0.013		Zhou et al. 2013	model age
Spot 7-2	^{207}Pb - ^{235}U	4.562	0.029		Zhou et al. 2013	model age
Spot 7-3	^{207}Pb - ^{235}U	4.565	0.081		Zhou et al. 2013	model age
weighted averages of three analyses of one zircon grain	^{206}Pb - ^{238}U	4.608	0.096		Zhou et al. 2013	model age
Spot 7-1	^{206}Pb - ^{238}U	4.555	0.01		Zhou et al. 2013	model age
Spot 7-2	^{206}Pb - ^{238}U	4.586	0.027		Zhou et al. 2013	model age
Spot 7-3	^{206}Pb - ^{238}U	4.659	0.081		Zhou et al. 2013	model age
whole rock sample relative to ADOR	Pu-Xe	4.498			Shukolyukov and Begemann 1996a	model age

Sample	Method	Date	Error +/-	Note	Source	Type
glass sample relative to ADOR	Pu-Xe	4.517			Shukolyukov and Begemann 1996b	model age
Caldera						
whole rock sample	K-Ar	4.19			Shukolyukov and Begemann 1996b	model age
pyroxene fraction	Pb-Pb	4.525	0.0019		Galer and Lugmair 1996	model age
weighted mean of four points on one zircon grain	Pb-Pb	4.542	0.08		Zhou et al. 2013	model age
Spot 1-1	²⁰⁷ Pb- ²⁰⁶ Pb	4.591	0.034		Zhou et al. 2013	model age
Spot 1-2	²⁰⁷ Pb- ²⁰⁶ Pb	4.502	0.045		Zhou et al. 2013	model age
Spot 1-3	²⁰⁷ Pb- ²⁰⁶ Pb	4.49	0.03		Zhou et al. 2013	model age
Spot 1-4	²⁰⁷ Pb- ²⁰⁶ Pb	4.573	0.029		Zhou et al. 2013	model age
Spot 1-1	²⁰⁷ Pb- ²³⁵ U	4.575	0.069		Zhou et al. 2013	model age
Spot 1-2	²⁰⁷ Pb- ²³⁵ U	4.491	0.074		Zhou et al. 2013	model age
Spot 1-3	²⁰⁶ Pb- ²³⁸ U	5.131	0.156		Zhou et al. 2013	model age
Spot 1-4	²⁰⁶ Pb- ²³⁸ U	5.048	0.133		Zhou et al. 2013	model age
Spot 1-1	²⁰⁶ Pb- ²³⁸ U	4.54	0.204		Zhou et al. 2013	model age
Spot 1-2	²⁰⁶ Pb- ²³⁸ U	4.467	0.207		Zhou et al. 2013	model age
Spot 1-3	²⁰⁷ Pb- ²³⁵ U	4.68	0.05		Zhou et al. 2013	model age
Spot 1-4	²⁰⁷ Pb- ²³⁵ U	4.714	0.044		Zhou et al. 2013	model age
anchored to other meteorite dates	Mn-Cr	4.537	0.012		Wadhwa and Lugmair 1996	model age
	Pu-Xe	4.513			Shukolyukov and Begemann 1996a	model age
Camel Donga						
matrix samples with pyroxenes, weighted	Ar-Ar	3.704	0.079		Kennedy et al. 2013	plateau age
matrix samples with pyroxenes, weighted	Ar-Ar	3.67	0.08		Kennedy et al. 2013	plateau age
weight mean of two	Ar-Ar	3.693	0.051		Kennedy et al. 2013	plateau age
pyroxene fraction	Pb-Pb	4.5109	0.001		Iizuka et al. 2013	model age
thirty-five point analyses of 14 zircon grains	²⁰⁷ Pb- ²⁰⁶ Pb	4.531	0.01	weighted average	Zhou et al. 2013	model age
Spot 1-1	²⁰⁷ Pb- ²⁰⁶ Pb	4.525	0.014		Zhou et al. 2013	model age
Spot 1-2	²⁰⁷ Pb- ²⁰⁶ Pb	4.579	0.012		Zhou et al. 2013	model age
Spot 2-1	²⁰⁷ Pb- ²⁰⁶ Pb	4.551	0.023		Zhou et al. 2013	model age
Spot 2-2	²⁰⁷ Pb- ²⁰⁶ Pb	4.547	0.017		Zhou et al. 2013	model age
Spot 3	²⁰⁷ Pb- ²⁰⁶ Pb	4.552	0.051		Zhou et al. 2013	model age
Spot 4	²⁰⁷ Pb- ²⁰⁶ Pb	4.512	0.02		Zhou et al. 2013	model age
Spot 5-1	²⁰⁷ Pb- ²⁰⁶ Pb	4.572	0.033		Zhou et al. 2013	model age
Spot 5-2	²⁰⁷ Pb- ²⁰⁶ Pb	4.516	0.032		Zhou et al. 2013	model age
Spot 5-3	²⁰⁷ Pb- ²⁰⁶ Pb	4.531	0.02		Zhou et al. 2013	model age
Spot 6	²⁰⁷ Pb- ²⁰⁶ Pb	4.479	0.034		Zhou et al. 2013	model age
Spot 7-1	²⁰⁷ Pb- ²⁰⁶ Pb	4.546	0.014		Zhou et al. 2013	model age
Spot 7-2	²⁰⁷ Pb- ²⁰⁶ Pb	4.517	0.02		Zhou et al. 2013	model age
Spot 7-3	²⁰⁷ Pb- ²⁰⁶ Pb	4.557	0.013		Zhou et al. 2013	model age
Spot 7-4	²⁰⁷ Pb- ²⁰⁶ Pb	4.53	0.021		Zhou et al. 2013	model age
Spot 8	²⁰⁷ Pb- ²⁰⁶ Pb	4.484	0.022		Zhou et al. 2013	model age
Spot 9-1	²⁰⁷ Pb- ²⁰⁶ Pb	4.546	0.019		Zhou et al. 2013	model age
Spot 9-2	²⁰⁷ Pb- ²⁰⁶ Pb	4.542	0.023		Zhou et al. 2013	model age
Spot 9-3	²⁰⁷ Pb- ²⁰⁶ Pb	4.536	0.018		Zhou et al. 2013	model age
Spot 9-4	²⁰⁷ Pb- ²⁰⁶ Pb	4.471	0.03		Zhou et al. 2013	model age

Sample	Method	Date	Error +/-	Note	Source	Type
Spot 9-5	^{207}Pb - ^{206}Pb	4.507	0.032		Zhou et al. 2013	model age
Spot 9-6	^{207}Pb - ^{206}Pb	4.514	0.025		Zhou et al. 2013	model age
Spot 9-7	^{207}Pb - ^{206}Pb	4.535	0.037		Zhou et al. 2013	model age
Spot 10-1	^{207}Pb - ^{206}Pb	4.519	0.022		Zhou et al. 2013	model age
Spot 10-2	^{207}Pb - ^{206}Pb	4.481	0.022		Zhou et al. 2013	model age
Spot 10-3	^{207}Pb - ^{206}Pb	4.525	0.019		Zhou et al. 2013	model age
Spot 11	^{207}Pb - ^{206}Pb	4.534	0.046		Zhou et al. 2013	model age
Spot 12-1	^{207}Pb - ^{206}Pb	4.566	0.019		Zhou et al. 2013	model age
Spot 12-2	^{207}Pb - ^{206}Pb	4.537	0.017		Zhou et al. 2013	model age
Spot 12-3	^{207}Pb - ^{206}Pb	4.536	0.018		Zhou et al. 2013	model age
Spot 12-4	^{207}Pb - ^{206}Pb	4.57	0.015		Zhou et al. 2013	model age
Spot 12-5	^{207}Pb - ^{206}Pb	4.551	0.026		Zhou et al. 2013	model age
Spot 13	^{207}Pb - ^{206}Pb	4.511	0.022		Zhou et al. 2013	model age
Spot 14-1	^{207}Pb - ^{206}Pb	4.478	0.013		Zhou et al. 2013	model age
Spot 14-2	^{207}Pb - ^{206}Pb	4.479	0.016		Zhou et al. 2013	model age
Spot 14-3	^{207}Pb - ^{206}Pb	4.52	0.014		Zhou et al. 2013	model age
thirty-five point analyses of 14 zircon grains	^{207}Pb - ^{235}U	4.492	0.023	weighted average	Zhou et al. 2013	model age
Spot 1-1	^{207}Pb - ^{235}U	4.461	0.034		Zhou et al. 2013	model age
Spot 1-2	^{207}Pb - ^{235}U	4.419	0.033		Zhou et al. 2013	model age
Spot 2-1	^{207}Pb - ^{235}U	4.466	0.042		Zhou et al. 2013	model age
Spot 2-2	^{207}Pb - ^{235}U	4.513	0.035		Zhou et al. 2013	model age
Spot 3	^{207}Pb - ^{235}U	4.561	0.064		Zhou et al. 2013	model age
Spot 4	^{207}Pb - ^{235}U	4.405	0.036		Zhou et al. 2013	model age
Spot 5-1	^{207}Pb - ^{235}U	4.531	0.043		Zhou et al. 2013	model age
Spot 5-2	^{207}Pb - ^{235}U	4.48	0.042		Zhou et al. 2013	model age
Spot 5-3	^{207}Pb - ^{235}U	4.493	0.036		Zhou et al. 2013	model age
Spot 6	^{207}Pb - ^{235}U	4.691	0.042		Zhou et al. 2013	model age
Spot 7-1	^{207}Pb - ^{235}U	4.469	0.034		Zhou et al. 2013	model age
Spot 7-2	^{207}Pb - ^{235}U	4.486	0.035		Zhou et al. 2013	model age
Spot 7-3	^{207}Pb - ^{235}U	4.433	0.034		Zhou et al. 2013	model age
Spot 7-4	^{207}Pb - ^{235}U	4.513	0.035		Zhou et al. 2013	model age
Spot 8	^{207}Pb - ^{235}U	4.597	0.037		Zhou et al. 2013	model age
Spot 9-1	^{207}Pb - ^{235}U	4.53	0.035		Zhou et al. 2013	model age
Spot 9-2	^{207}Pb - ^{235}U	4.657	0.037		Zhou et al. 2013	model age
Spot 9-3	^{207}Pb - ^{235}U	4.451	0.035		Zhou et al. 2013	model age
Spot 9-4	^{207}Pb - ^{235}U	4.586	0.038		Zhou et al. 2013	model age
Spot 9-5	^{207}Pb - ^{235}U	4.374	0.041		Zhou et al. 2013	model age
Spot 9-6	^{207}Pb - ^{235}U	4.545	0.039		Zhou et al. 2013	model age
Spot 9-7	^{207}Pb - ^{235}U	4.498	0.045		Zhou et al. 2013	model age
Spot 10-1	^{207}Pb - ^{235}U	4.539	0.036		Zhou et al. 2013	model age
Spot 10-2	^{207}Pb - ^{235}U	4.451	0.035		Zhou et al. 2013	model age
Spot 10-3	^{207}Pb - ^{235}U	4.497	0.035		Zhou et al. 2013	model age
Spot 11	^{207}Pb - ^{235}U	4.52	0.05		Zhou et al. 2013	model age
Spot 12-1	^{207}Pb - ^{235}U	4.473	0.035		Zhou et al. 2013	model age
Spot 12-2	^{207}Pb - ^{235}U	4.476	0.035		Zhou et al. 2013	model age
Spot 12-3	^{207}Pb - ^{235}U	4.431	0.035		Zhou et al. 2013	model age
Spot 12-4	^{207}Pb - ^{235}U	4.496	0.035		Zhou et al. 2013	model age
Spot 12-5	^{207}Pb - ^{235}U	4.568	0.039		Zhou et al. 2013	model age
Spot 13	^{207}Pb - ^{235}U	4.523	0.036		Zhou et al. 2013	model age
Spot 14-1	^{207}Pb - ^{235}U	4.437	0.033		Zhou et al. 2013	model age
Spot 14-2	^{207}Pb - ^{235}U	4.405	0.034		Zhou et al. 2013	model age
Spot 14-3	^{207}Pb - ^{235}U	4.447	0.034		Zhou et al. 2013	model age
thirty-five point analyses of 14 zircon grains	^{206}Pb - ^{238}U	4.417	0.079	weighted average	Zhou et al. 2013	model age
Spot 1-1	^{206}Pb - ^{238}U	4.32	0.101		Zhou et al. 2013	model age

Sample	Method	Date	Error +/-	Note	Source	Type
Spot 1-2	²⁰⁶ Pb- ²³⁸ U	4.077	0.096		Zhou et al. 2013	model age
Spot 2-1	²⁰⁶ Pb- ²³⁸ U	4.279	0.12		Zhou et al. 2013	model age
Spot 2-2	²⁰⁶ Pb- ²³⁸ U	4.438	0.104		Zhou et al. 2013	model age
Spot 3	²⁰⁶ Pb- ²³⁸ U	4.582	0.167		Zhou et al. 2013	model age
Spot 4	²⁰⁶ Pb- ²³⁸ U	4.174	0.101		Zhou et al. 2013	model age
Spot 5-1	²⁰⁶ Pb- ²³⁸ U	4.439	0.112		Zhou et al. 2013	model age
Spot 5-2	²⁰⁶ Pb- ²³⁸ U	4.4	0.111		Zhou et al. 2013	model age
Spot 5-3	²⁰⁶ Pb- ²³⁸ U	4.41	0.104		Zhou et al. 2013	model age
Spot 6	²⁰⁶ Pb- ²³⁸ U	5.196	0.119		Zhou et al. 2013	model age
Spot 7-1	²⁰⁶ Pb- ²³⁸ U	4.301	0.101		Zhou et al. 2013	model age
Spot 7-2	²⁰⁶ Pb- ²³⁸ U	4.417	0.1		Zhou et al. 2013	model age
Spot 7-3	²⁰⁶ Pb- ²³⁸ U	4.165	0.1		Zhou et al. 2013	model age
Spot 7-4	²⁰⁶ Pb- ²³⁸ U	4.476	0.101		Zhou et al. 2013	model age
Spot 8	²⁰⁶ Pb- ²³⁸ U	4.857	0.112		Zhou et al. 2013	model age
Spot 9-1	²⁰⁶ Pb- ²³⁸ U	4.495	0.105		Zhou et al. 2013	model age
Spot 9-2	²⁰⁶ Pb- ²³⁸ U	4.923	0.114		Zhou et al. 2013	model age
Spot 9-3	²⁰⁶ Pb- ²³⁸ U	4.267	0.101		Zhou et al. 2013	model age
Spot 9-4	²⁰⁶ Pb- ²³⁸ U	4.852	0.108		Zhou et al. 2013	model age
Spot 9-5	²⁰⁶ Pb- ²³⁸ U	4.091	0.102		Zhou et al. 2013	model age
Spot 9-6	²⁰⁶ Pb- ²³⁸ U	4.616	0.112		Zhou et al. 2013	model age
Spot 9-7	²⁰⁶ Pb- ²³⁸ U	4.415	0.115		Zhou et al. 2013	model age
Spot 10-1	²⁰⁶ Pb- ²³⁸ U	4.584	0.105		Zhou et al. 2013	model age
Spot 10-2	²⁰⁶ Pb- ²³⁸ U	4.385	0.1		Zhou et al. 2013	model age
Spot 10-3	²⁰⁶ Pb- ²³⁸ U	4.435	0.103		Zhou et al. 2013	model age
Spot 11	²⁰⁶ Pb- ²³⁸ U	4.489	0.118		Zhou et al. 2013	model age
Spot 12-1	²⁰⁶ Pb- ²³⁸ U	4.271	0.099		Zhou et al. 2013	model age
Spot 12-2	²⁰⁶ Pb- ²³⁸ U	4.343	0.103		Zhou et al. 2013	model age
Spot 12-3	²⁰⁶ Pb- ²³⁸ U	4.206	0.101		Zhou et al. 2013	model age
Spot 12-4	²⁰⁶ Pb- ²³⁸ U	4.334	0.103		Zhou et al. 2013	model age
Spot 12-5	²⁰⁶ Pb- ²³⁸ U	4.607	0.11		Zhou et al. 2013	model age
Spot 13	²⁰⁶ Pb- ²³⁸ U	4.549	0.106		Zhou et al. 2013	model age
Spot 14-1	²⁰⁶ Pb- ²³⁸ U	4.346	0.1		Zhou et al. 2013	model age
Spot 14-2	²⁰⁶ Pb- ²³⁸ U	4.246	0.1		Zhou et al. 2013	model age
Spot 14-3	²⁰⁶ Pb- ²³⁸ U	4.288	0.1		Zhou et al. 2013	model age
	Al-Mg	4.5647	0.0004		Schiller, Baker, and Bizzarro 2010	model age
relative to ADOR	Pu-Xe	4.521	0.02		Shukolyukov and Begemann 1996a	model age
average of seven samples relative to ADOR	Pu-Xe	4.507	0.016		Miura et al. 1998	model age
Ibitira						
whole-rock samples	K-Ar	3.2			Heymann, Mazor, and Anders 1968	model age
	Ar-Ar	4.49			Garrison and Bogard 1995	model age
using 15 stepwise temperature extractions	Ar-Ar	4.495	0.015		Bogard and Garrison 1995	plateau age
Sample at 400°C	Ar-Ar	3.354	0.048		Bogard and Garrison 1995	extraction age
Sample at 500°C	Ar-Ar	3.205	0.051		Bogard and Garrison 1995	extraction age
Sample at 600°C	Ar-Ar	3.525	0.023		Bogard and Garrison 1995	extraction age
Sample at 700°C	Ar-Ar	3.874	0.008		Bogard and Garrison 1995	extraction age
Sample at 775°C	Ar-Ar	4.361	0.009		Bogard and Garrison 1995	extraction age
Sample at 825°C	Ar-Ar	4.469	0.01		Bogard and Garrison 1995	extraction age
Sample at 875°C	Ar-Ar	4.502	0.009		Bogard and Garrison 1995	extraction age
Sample at 930°C	Ar-Ar	4.493	0.009		Bogard and Garrison 1995	extraction age
Sample at 975°C	Ar-Ar	4.491	0.009		Bogard and Garrison 1995	extraction age
Sample at 1025°C	Ar-Ar	4.509	0.008		Bogard and Garrison 1995	extraction age

Sample	Method	Date	Error +/-	Note	Source	Type
Sample at 1100°C	Ar-Ar	4.452	0.029		Bogard and Garrison 1995	extraction age
Sample at 1200°C	Ar-Ar	4.491	0.098		Bogard and Garrison 1995	extraction age
Sample at 1300°C	Ar-Ar	4.588	0.036		Bogard and Garrison 1995	extraction age
Sample at 1400°C	Ar-Ar	4.48	0.103		Bogard and Garrison 1995	extraction age
Sample at 1550°C	Ar-Ar	7.998	0.425		Bogard and Garrison 1995	extraction age
after Bogard and Garrison (1995)	Ar-Ar	4.487	0.015		Yamaguchi et al. 2001	plateau (model) age
five extractions releasing 89% of Ar	Ar-Ar	4.487	0.016		Bogard and Garrison 2003	plateau age
after Bogard and Garrison (1995)	Ar-Ar	4.4858	0.015		Claydon, Crowther, and Gilmour 2012	plateau (model) age
	^{207}Pb - ^{206}Pb	4.55	0.01		Wasserburg et al. 1977	model age
Ibitira WR-1	^{207}Pb - ^{206}Pb	4.554	0.008		Chen and Wasserburg 1985	model age
Ibitira WR-2	^{207}Pb - ^{206}Pb	4.556	0.006		Chen and Wasserburg 1985	model age
	^{207}Pb - ^{206}Pb	4.56	0.003		Manhès, Göpel, and Allègre 1987	model age
pyroxene fraction	Pb-Pb	4.5558	0.0005		lizuka et al. 2013	model age
whole rock fraction A017_7 residue	Pb-Pb	4.5564	0.0011		lizuka et al. 2014	model age
whole rock fraction A017_7 wash-1	Pb-Pb	4.5543	0.0022		lizuka et al. 2014	model age
whole rock fraction A017_7 wash-2	Pb-Pb	4.584	0.0022		lizuka et al. 2014	model age
whole rock fraction A039_5 residue	Pb-Pb	4.556	0.0008		lizuka et al. 2014	model age
whole rock fraction A039_5 wash-1	Pb-Pb	4.5894	0.0022		lizuka et al. 2014	model age
whole rock fraction A039_5 wash-2	Pb-Pb	4.5881	0.0036		lizuka et al. 2014	model age
whole rock fraction A047_3 residue	Pb-Pb	4.5572	0.0013		lizuka et al. 2014	model age
whole rock fraction A047_3 wash-1	Pb-Pb	4.608	0.0024		lizuka et al. 2014	model age
whole rock fraction A047_3 wash-2	Pb-Pb	4.6043	0.0054		lizuka et al. 2014	model age
pyroxene-rich fraction GSC030_HF1 residue	Pb-Pb	4.5558	0.0007		lizuka et al. 2014	model age
pyroxene-rich fraction GSC030_HF1 wash-1	Pb-Pb	4.5533	0.0002		lizuka et al. 2014	model age

Sample	Method	Date	Error +/-	Note	Source	Type
pyroxene-rich fraction GSC030_HF1 wash-2	Pb-Pb	4.556	0.0021		lizuka et al. 2014	model age
pyroxene-rich fraction GSC030_HF2 residue	Pb-Pb	4.5559	0.0007		lizuka et al. 2014	model age
pyroxene-rich fraction GSC030_HF2 wash-1	Pb-Pb	4.553	0.0002		lizuka et al. 2014	model age
pyroxene-rich fraction GSC030_HF2 wash-2	Pb-Pb	4.558	0.0024		lizuka et al. 2014	model age
pyroxene-rich fraction A015_4 residue	Pb-Pb	4.5558	0.0009		lizuka et al. 2014	model age
pyroxene-rich fraction A015_4 wash-1	Pb-Pb	4.5361	0.002		lizuka et al. 2014	model age
pyroxene-rich fraction A015_4 wash-2	Pb-Pb	4.6139	0.0549		lizuka et al. 2014	model age
pyroxene-rich fraction A015_5 residue	Pb-Pb	4.5506	0.0075		lizuka et al. 2014	model age
pyroxene-rich fraction A015_5 wash-1	Pb-Pb	4.5141	0.0021		lizuka et al. 2014	model age
pyroxene-rich fraction A015_5 wash-2	Pb-Pb	4.5709	0.0201		lizuka et al. 2014	model age
pyroxene-rich fraction A015_6 residue	Pb-Pb	4.552	0.001		lizuka et al. 2014	model age
pyroxene-rich fraction A015_6 wash-1	Pb-Pb	4.5211	0.001		lizuka et al. 2014	model age
pyroxene-rich fraction A015_6 wash-2	Pb-Pb	4.5329	0.0242		lizuka et al. 2014	model age
pyroxene-rich fraction A017_5 residue	Pb-Pb	4.5581	0.0013		lizuka et al. 2014	model age
pyroxene-rich fraction A017_5 wash-2	Pb-Pb	4.5727	0.0025		lizuka et al. 2014	model age
pyroxene-rich fraction A017_6 residue	Pb-Pb	4.5546	0.0009		lizuka et al. 2014	model age
pyroxene-rich fraction A017_6 wash-1	Pb-Pb	4.552	0.001		lizuka et al. 2014	model age
pyroxene-rich fraction A017_6 wash-2	Pb-Pb	4.5265	0.0065		lizuka et al. 2014	model age
pyroxene-rich fraction A039_2 residue	Pb-Pb	4.5563	0.0007		lizuka et al. 2014	model age
pyroxene-rich fraction A039_2 wash-1	Pb-Pb	4.5634	0.0016		lizuka et al. 2014	model age

Sample	Method	Date	Error +/-	Note	Source	Type
pyroxene-rich fraction A039_2 wash-2	Pb-Pb	4.539	0.0038		lizuka et al. 2014	model age
pyroxene-rich fraction A039_3 residue	Pb-Pb	4.5562	0.0008		lizuka et al. 2014	model age
pyroxene-rich fraction A039_3 wash-1	Pb-Pb	4.5822	0.0024		lizuka et al. 2014	model age
pyroxene-rich fraction A039_3 wash-2	Pb-Pb	4.5594	0.0045		lizuka et al. 2014	model age
pyroxene-rich fraction A047_1 residue	Pb-Pb	4.5565	0.0006		lizuka et al. 2014	model age
pyroxene-rich fraction A047_1 wash-1	Pb-Pb	4.5583	0.0014		lizuka et al. 2014	model age
pyroxene-rich fraction A047_1 wash-2	Pb-Pb	4.5815	0.0125		lizuka et al. 2014	model age
pyroxene-rich fraction A047_2 residue	Pb-Pb	4.5567	0.0007		lizuka et al. 2014	model age
pyroxene-rich fraction A047_2 wash-1	Pb-Pb	4.5632	0.002		lizuka et al. 2014	model age
pyroxene-rich fraction A047_2 wash-2	Pb-Pb	4.5843	0.0159		lizuka et al. 2014	model age
plagioclase-rich fraction A015_7 residue	Pb-Pb	4.5381	0.0052		lizuka et al. 2014	model age
plagioclase-rich fraction A015_7 wash-1	Pb-Pb	4.5232	0.001		lizuka et al. 2014	model age
plagioclase-rich fraction A015_7 wash-2	Pb-Pb	4.6072	0.0072		lizuka et al. 2014	model age
plagioclase-rich fraction A015_8 residue	Pb-Pb	4.5139	0.0038		lizuka et al. 2014	model age
plagioclase-rich fraction A015_8 wash-1	Pb-Pb	4.5456	0.0008		lizuka et al. 2014	model age
plagioclase-rich fraction A015_8 wash-2	Pb-Pb	4.6352	0.0032		lizuka et al. 2014	model age
plagioclase-rich fraction A039_4 residue	Pb-Pb	4.5636	0.0135		lizuka et al. 2014	model age
plagioclase-rich fraction A039_4 wash-1	Pb-Pb	4.5515	0.0007		lizuka et al. 2014	model age
plagioclase-rich fraction A039_4 wash-2	Pb-Pb	4.6311	0.0058		lizuka et al. 2014	model age
plagioclase-rich fraction A047_4 residue	Pb-Pb	4.5595	0.0108		lizuka et al. 2014	model age
plagioclase-rich fraction A047_4 wash-1	Pb-Pb	4.5606	0.0006		lizuka et al. 2014	model age
plagioclase-rich fraction A047_4 wash-2	Pb-Pb	4.6722	0.0123		lizuka et al. 2014	model age

Sample	Method	Date	Error +/-	Note	Source	Type
plagioclase-rich fraction A047_5 residue	Pb-Pb	4.5528	0.0019		lizuka et al. 2014	model age
plagioclase-rich fraction A047_5 wash-1	Pb-Pb	4.5572	0.0005		lizuka et al. 2014	model age
plagioclase-rich fraction A047_5 wash-2	Pb-Pb	4.387	0.0275		lizuka et al. 2014	model age
weighted average of residues of 8 pyroxene-rich fractions and two whole-rock fractions and washes of two pyroxene-rich and one plagioclase-rich fractions (13 ages)	Pb-Pb	4.55635	0.00042		lizuka et al. 2014	model age
weighted average of residues of one whole-rock and six pyroxene-rich fractions (seven ages)	Pb-Pb	4.55631	0.00028		lizuka et al. 2014	model age
Ibitira WR-1	²⁰⁶ Pb- ²³⁸ U	4.629	0.03		Chen and Wasserburg 1985	model age
Ibitira WR-2	²⁰⁶ Pb- ²³⁸ U	4.567	0.013		Chen and Wasserburg 1985	model age
Ibitira WR-1	²⁰⁷ Pb- ²³⁵ U	4.577	0.007		Chen and Wasserburg 1985	model age
Ibitira WR-2	²⁰⁷ Pb- ²³⁵ U	4.559	0.005		Chen and Wasserburg 1985	model age
Ibitira WR-1	²⁰⁸ Pb- ²³² Th	4.972	0.036		Chen and Wasserburg 1985	model age
Ibitira WR-2	²⁰⁸ Pb- ²³² Th	4.658	0.022		Chen and Wasserburg 1985	model age
Single sample	Pu-Xe	4.581	0.025		Shukolyukov and Begemann 1996a	model age
Juvinas						
whole rock samples	K-Ar	3.98			Heymann, Mazor, and Anders 1968	model age
plagioclase sample	K-Ar	4.6			Hampel et al. 1980	model age
frB58	Pb-Pb	4.5676	0.0011		Manhès, Allègre, and Provost 1984	model age
frB60	Pb-Pb	4.5676	0.0034		Manhès, Allègre, and Provost 1984	model age
frB63	Pb-Pb	4.5648	0.001		Manhès, Allègre, and Provost 1984	model age
frC64	Pb-Pb	4.5646	0.0011		Manhès, Allègre, and Provost 1984	model age
frC65	Pb-Pb	4.5656	0.0008		Manhès, Allègre, and Provost 1984	model age
frC66	Pb-Pb	4.5658	0.0007		Manhès, Allègre, and Provost 1984	model age
frC67	Pb-Pb	4.5649	0.001		Manhès, Allègre, and Provost 1984	model age
frD70	Pb-Pb	4.5534	0.0006		Manhès, Allègre, and Provost 1984	model age
pla54	Pb-Pb	4.796	0.0075		Manhès, Allègre, and Provost 1984	model age
pla57	Pb-Pb	4.7278	0.0049		Manhès, Allègre, and Provost 1984	model age
pla62	Pb-Pb	4.821	0.0011		Manhès, Allègre, and Provost 1984	model age
pla70	Pb-Pb	4.7979	0.0044		Manhès, Allègre, and Provost 1984	model age
pyr62	Pb-Pb	4.5726	0.0038		Manhès, Allègre, and Provost 1984	model age
pyr70	Pb-Pb	4.5768	0.0017		Manhès, Allègre, and Provost 1984	model age
L1	Pb-Pb	4.634	0.003		Manhès, Allègre, and Provost 1984	model age
L2	Pb-Pb	4.8131	0.0097		Manhès, Allègre, and Provost 1984	model age
L3	Pb-Pb	4.8	0.0011		Manhès, Allègre, and Provost 1984	model age
Res	Pb-Pb	4.953	0.0015		Manhès, Allègre, and Provost 1984	model age
plaC	Pb-Pb	4.735			Manhès, Allègre, and Provost 1984	model age
average age	Pb-Pb	4.527	0.024	two zircons	Lee et al. 2009	model age
	²⁰⁷ Pb- ²⁰⁶ Pb	4.549	0.006	clast sample	Manhès and Allègre 1980	model age

Sample	Method	Date	Error +/-	Note	Source	Type
weighted average of 20 model ages determined on seven zircon grains	^{207}Pb - ^{206}Pb	4.545	0.015		Zhou et al. 2013	model age
Spot 1-1	^{207}Pb - ^{206}Pb	4.54	0.024		Zhou et al. 2013	model age
Spot 1-2	^{207}Pb - ^{206}Pb	4.493	0.022		Zhou et al. 2013	model age
Spot 1-3	^{207}Pb - ^{206}Pb	4.502	0.024		Zhou et al. 2013	model age
Spot 1-4	^{207}Pb - ^{206}Pb	4.54	0.024		Zhou et al. 2013	model age
Spot 1-5	^{207}Pb - ^{206}Pb	4.568	0.025		Zhou et al. 2013	model age
Spot 1-6	^{207}Pb - ^{206}Pb	4.52	0.024		Zhou et al. 2013	model age
Spot 1-7	^{207}Pb - ^{206}Pb	4.545	0.024		Zhou et al. 2013	model age
Spot 2-1	^{207}Pb - ^{206}Pb	4.557	0.025		Zhou et al. 2013	model age
Spot 2-2	^{207}Pb - ^{206}Pb	4.497	0.024		Zhou et al. 2013	model age
Spot 3-1	^{207}Pb - ^{206}Pb	4.563	0.016		Zhou et al. 2013	model age
Spot 3-2	^{207}Pb - ^{206}Pb	4.571	0.01		Zhou et al. 2013	model age
Spot 3-3	^{207}Pb - ^{206}Pb	4.559	0.011		Zhou et al. 2013	model age
Spot 4-1	^{207}Pb - ^{206}Pb	4.525	0.027		Zhou et al. 2013	model age
Spot 4-2	^{207}Pb - ^{206}Pb	4.576	0.015		Zhou et al. 2013	model age
Spot 4-3	^{207}Pb - ^{206}Pb	4.584	0.02		Zhou et al. 2013	model age
Spot 4-4	^{207}Pb - ^{206}Pb	4.523	0.021		Zhou et al. 2013	model age
Spot 5-1	^{207}Pb - ^{206}Pb	4.486	0.022		Zhou et al. 2013	model age
Spot 5-2	^{207}Pb - ^{206}Pb	4.511	0.019		Zhou et al. 2013	model age
Spot 6	^{207}Pb - ^{206}Pb	4.472	0.026		Zhou et al. 2013	model age
Spot 7	^{207}Pb - ^{206}Pb	4.516	0.041		Zhou et al. 2013	model age
weighted average of 20 model ages determined on seven zircon grains	^{207}Pb - ^{235}U	4.679	0.048		Zhou et al. 2013	model age
Spot 1-1	^{207}Pb - ^{235}U	4.581	0.036		Zhou et al. 2013	model age
Spot 1-2	^{207}Pb - ^{235}U	4.508	0.043		Zhou et al. 2013	model age
Spot 1-3	^{207}Pb - ^{235}U	4.546	0.038		Zhou et al. 2013	model age
Spot 1-4	^{207}Pb - ^{235}U	4.654	0.043		Zhou et al. 2013	model age
Spot 1-5	^{207}Pb - ^{235}U	4.613	0.052		Zhou et al. 2013	model age
Spot 1-6	^{207}Pb - ^{235}U	4.683	0.04		Zhou et al. 2013	model age
Spot 1-7	^{207}Pb - ^{235}U	4.703	0.048		Zhou et al. 2013	model age
Spot 2-1	^{207}Pb - ^{235}U	4.585	0.05		Zhou et al. 2013	model age
Spot 2-2	^{207}Pb - ^{235}U	4.657	0.041		Zhou et al. 2013	model age
Spot 3-1	^{207}Pb - ^{235}U	4.751	0.041		Zhou et al. 2013	model age
Spot 3-2	^{207}Pb - ^{235}U	4.716	0.03		Zhou et al. 2013	model age
Spot 3-3	^{207}Pb - ^{235}U	4.711	0.028		Zhou et al. 2013	model age
Spot 4-1	^{207}Pb - ^{235}U	4.561	0.046		Zhou et al. 2013	model age
Spot 4-2	^{207}Pb - ^{235}U	4.674	0.03		Zhou et al. 2013	model age
Spot 4-3	^{207}Pb - ^{235}U	4.837	0.032		Zhou et al. 2013	model age
Spot 4-4	^{207}Pb - ^{235}U	4.601	0.036		Zhou et al. 2013	model age
Spot 5-1	^{207}Pb - ^{235}U	4.552	0.037		Zhou et al. 2013	model age
Spot 5-2	^{207}Pb - ^{235}U	4.625	0.039		Zhou et al. 2013	model age
Spot 6	^{207}Pb - ^{235}U	4.851	0.024		Zhou et al. 2013	model age
Spot 7	^{207}Pb - ^{235}U	4.697	0.074		Zhou et al. 2013	model age
zircons	U-Pb	4.56			Bukovanska and Ireland 1993	model age
weighted average of 20 model ages determined on seven zircon grains	^{206}Pb - ^{238}U	4.915	0.1		Zhou et al. 2013	model age
Spot 1-1	^{206}Pb - ^{238}U	4.674	0.105		Zhou et al. 2013	model age

Sample	Method	Date	Error +/-	Note	Source	Type
Spot 1-2	²⁰⁶ Pb- ²³⁸ U	4.541	0.13		Zhou et al. 2013	model age
Spot 1-3	²⁰⁶ Pb- ²³⁸ U	4.645	0.113		Zhou et al. 2013	model age
Spot 1-4	²⁰⁶ Pb- ²³⁸ U	4.918	0.134		Zhou et al. 2013	model age
Spot 1-5	²⁰⁶ Pb- ²³⁸ U	4.715	0.161		Zhou et al. 2013	model age
Spot 1-6	²⁰⁶ Pb- ²³⁸ U	5.067	0.124		Zhou et al. 2013	model age
Spot 1-7	²⁰⁶ Pb- ²³⁸ U	5.079	0.155		Zhou et al. 2013	model age
Spot 2-1	²⁰⁶ Pb- ²³⁸ U	4.648	0.151		Zhou et al. 2013	model age
Spot 2-2	²⁰⁶ Pb- ²³⁸ U	5.035	0.129		Zhou et al. 2013	model age
Spot 3-1	²⁰⁶ Pb- ²³⁸ U	5.203	0.14		Zhou et al. 2013	model age
Spot 3-2	²⁰⁶ Pb- ²³⁸ U	5.06	0.101		Zhou et al. 2013	model age
Spot 3-3	²⁰⁶ Pb- ²³⁸ U	5.073	0.093		Zhou et al. 2013	model age
Spot 4-1	²⁰⁶ Pb- ²³⁸ U	4.643	0.138		Zhou et al. 2013	model age
Spot 4-2	²⁰⁶ Pb- ²³⁸ U	4.905	0.094		Zhou et al. 2013	model age
Spot 4-3	²⁰⁶ Pb- ²³⁸ U	5.461	0.105		Zhou et al. 2013	model age
Spot 4-4	²⁰⁶ Pb- ²³⁸ U	4.782	0.11		Zhou et al. 2013	model age
Spot 5-1	²⁰⁶ Pb- ²³⁸ U	4.701	0.111		Zhou et al. 2013	model age
Spot 5-2	²⁰⁶ Pb- ²³⁸ U	4.887	0.125		Zhou et al. 2013	model age
Spot 6	²⁰⁶ Pb- ²³⁸ U	5.8	0.352		Zhou et al. 2013	model age
Spot 7	²⁰⁶ Pb- ²³⁸ U	5.126	0.367		Zhou et al. 2013	model age
	Al-Mg	4.5645	0.0004		Schiller, Baker, and Bizzarro 2010	model age
	Pu-Xe	4.551	0.015	three samples	Shukolyukov and Begemann 1996a	model age
	Pu-Xe	4.548	0.023		Miura et al. 1998	model age
Moama						
average age of three extractions releasing 45–78% of ³⁹ Ar	Ar-Ar	4.48	0.007		Bogard and Garrison 2003	plateau age
sample at 350°C	Ar-Ar	0.866	0.07		Bogard and Garrison 2003	extraction age
sample at 400°C	Ar-Ar	1.441	0.073		Bogard and Garrison 2003	extraction age
sample at 500°C	Ar-Ar	1.439	0.052		Bogard and Garrison 2003	extraction age
sample at 600°C	Ar-Ar	2.213	0.015		Bogard and Garrison 2003	extraction age
sample at 675°C	Ar-Ar	2.865	0.017		Bogard and Garrison 2003	extraction age
sample at 725°C	Ar-Ar	3.743	0.01		Bogard and Garrison 2003	extraction age
sample at 775°C	Ar-Ar	4.167	0.01		Bogard and Garrison 2003	extraction age
sample at 810°C	Ar-Ar	4.345	0.011		Bogard and Garrison 2003	extraction age
sample at 847°C	Ar-Ar	4.396	0.012		Bogard and Garrison 2003	extraction age
sample at 880°C	Ar-Ar	4.426	0.012		Bogard and Garrison 2003	extraction age
sample at 900°C	Ar-Ar	4.473	0.012		Bogard and Garrison 2003	extraction age
sample at 915°C	Ar-Ar	4.484	0.012		Bogard and Garrison 2003	extraction age
sample at 925°C	Ar-Ar	4.483	0.011		Bogard and Garrison 2003	extraction age
sample at 940°C	Ar-Ar	4.447	0.009		Bogard and Garrison 2003	extraction age
sample at 975°C	Ar-Ar	4.363	0.011		Bogard and Garrison 2003	extraction age
sample at 1025°C	Ar-Ar	4.181	0.012		Bogard and Garrison 2003	extraction age
sample at 1100°C	Ar-Ar	4.217	0.018		Bogard and Garrison 2003	extraction age
sample at 1200°C	Ar-Ar	4.133	0.042		Bogard and Garrison 2003	extraction age
sample at 1350°C	Ar-Ar	4.294	0.107		Bogard and Garrison 2003	extraction age
sample at 1600°C	Ar-Ar	4.209	0.188		Bogard and Garrison 2003	extraction age
Moore County						
whole-rock samples	K-Ar	3.5			Heymann, Mazor, and Anders 1968	model age
	K-Ar	4.46			Shukolyukov and Begemann 1996b	model age
45–100% extractions	Ar-Ar	4.25	0.03		Bogard and Garrison 2003	plateau age
350°C	Ar-Ar	6.742	0.02		Bogard and Garrison 2003	step extraction age

Sample	Method	Date	Error +/-	Note	Source	Type
425°C	Ar-Ar	4.542	0.3		Bogard and Garrison 2003	step extraction age
500°C	Ar-Ar	2.102	0.315		Bogard and Garrison 2003	step extraction age
550°C	Ar-Ar	1.827	0.348		Bogard and Garrison 2003	step extraction age
625°C	Ar-Ar	3.21	0.074		Bogard and Garrison 2003	step extraction age
700°C	Ar-Ar	3.029	0.049		Bogard and Garrison 2003	step extraction age
750°C	Ar-Ar	4.083	0.03		Bogard and Garrison 2003	step extraction age
800°C	Ar-Ar	4.196	0.016		Bogard and Garrison 2003	step extraction age
830°C	Ar-Ar	4.23	0.015		Bogard and Garrison 2003	step extraction age
852°C	Ar-Ar	4.217	0.018		Bogard and Garrison 2003	step extraction age
875°C	Ar-Ar	4.223	0.014		Bogard and Garrison 2003	step extraction age
895°C	Ar-Ar	4.197	0.015		Bogard and Garrison 2003	step extraction age
920°C	Ar-Ar	4.215	0.014		Bogard and Garrison 2003	step extraction age
950°C	Ar-Ar	4.204	0.014		Bogard and Garrison 2003	step extraction age
975°C	Ar-Ar	4.231	0.008		Bogard and Garrison 2003	step extraction age
1000°C	Ar-Ar	4.25	0.008		Bogard and Garrison 2003	step extraction age
1025°C	Ar-Ar	4.245	0.007		Bogard and Garrison 2003	step extraction age
1050°C	Ar-Ar	4.218	0.008		Bogard and Garrison 2003	step extraction age
1100°C	Ar-Ar	4.22	0.009		Bogard and Garrison 2003	step extraction age
1150°C	Ar-Ar	4.189	0.01		Bogard and Garrison 2003	step extraction age
1155°C	Ar-Ar	4.157	0.04		Bogard and Garrison 2003	step extraction age
1225°C	Ar-Ar	4.117	0.03		Bogard and Garrison 2003	step extraction age
1325°C	Ar-Ar	4.229	0.017		Bogard and Garrison 2003	step extraction age
1425°C	Ar-Ar	4.267	0.008		Bogard and Garrison 2003	step extraction age
1500°C	Ar-Ar	4.255	0.018		Bogard and Garrison 2003	step extraction age
1600°C	Ar-Ar	4.272	0.61		Bogard and Garrison 2003	step extraction age
	Pu-Xe	4.548			Shukolyukov and Begemann 1996a	model age
Pasamonte						
whole rock samples	K-Ar	3.5			Heymann, Mazor, and Anders 1968	model age
high temperature, based on last fraction extracted	K-Ar	4.51	0.065		Podosek and Huneke 1973	model age
545°C extraction	K-Ar	3.595	0.062		Podosek and Huneke 1973	model age
630°C extraction	K-Ar	3.902	0.02		Podosek and Huneke 1973	model age
745°C extraction	K-Ar	4.066	0.005		Podosek and Huneke 1973	model age

Sample	Method	Date	Error +/-	Note	Source	Type
850°C extraction	K-Ar	4.069	0.004		Podosek and Huneke 1973	model age
935°C extraction	K-Ar	4.132	0.006		Podosek and Huneke 1973	model age
1040°C extraction	K-Ar	4.119	0.006		Podosek and Huneke 1973	model age
1195°C extraction	K-Ar	4.364	0.009		Podosek and Huneke 1973	model age
1515°C extraction	K-Ar	4.511	0.015		Podosek and Huneke 1973	model age
bulk plateau age, based on the first 80% Ar extracted	Ar-Ar	4.15	0.3		Podosek and Huneke 1973	plateau age
low temperature	Ar-Ar	4	0.05		Kunz et al. 1995	spectra model age
high temperature, 75% gas loss	Ar-Ar	4.4	0.1		Kunz et al. 1995	spectra model age
sample 1, low temperature	Ar-Ar	3.9	0.1		Kunz et al. 1995	spectrum model age
sample 1, high temperature, 90% gas loss	Ar-Ar	4.4	0.1		Kunz et al. 1995	spectrum model age
sample 5, low temperature	Ar-Ar	4.1	0.05		Kunz et al. 1995	spectrum model age
sample 5, high temperature, 70% gas loss	Ar-Ar	4.4	0.1		Kunz et al. 1995	spectrum model age
300°C	Ar-Ar	7.79	2.455		Kunz et al. 1995	extraction age
400°C	Ar-Ar	6.836	0.202		Kunz et al. 1995	extraction age
470°C	Ar-Ar	4.447	0.05		Kunz et al. 1995	extraction age
540°C	Ar-Ar	4.065	0.034		Kunz et al. 1995	extraction age
600°C	Ar-Ar	4.163	0.02		Kunz et al. 1995	extraction age
630°C	Ar-Ar	4.241	0.022		Kunz et al. 1995	extraction age
670°C	Ar-Ar	3.803	0.015		Kunz et al. 1995	extraction age
700°C	Ar-Ar	3.898	0.013		Kunz et al. 1995	extraction age
730°C	Ar-Ar	3.875	0.013		Kunz et al. 1995	extraction age
760°C	Ar-Ar	3.921	0.014		Kunz et al. 1995	extraction age
790°C	Ar-Ar	3.921	0.01		Kunz et al. 1995	extraction age
810°C	Ar-Ar	3.938	0.009		Kunz et al. 1995	extraction age
830°C	Ar-Ar	3.996	0.01		Kunz et al. 1995	extraction age
850°C	Ar-Ar	3.989	0.014		Kunz et al. 1995	extraction age
880°C	Ar-Ar	4.02	0.016		Kunz et al. 1995	extraction age
910°C	Ar-Ar	4.024	0.011		Kunz et al. 1995	extraction age
940°C	Ar-Ar	4.041	0.013		Kunz et al. 1995	extraction age
980°C	Ar-Ar	4.08	0.016		Kunz et al. 1995	extraction age
1020°C	Ar-Ar	4.162	0.026		Kunz et al. 1995	extraction age
1070°C	Ar-Ar	4.184	0.019		Kunz et al. 1995	extraction age
1120°C	Ar-Ar	4.21	0.027		Kunz et al. 1995	extraction age
1160°C	Ar-Ar	4.314	0.048		Kunz et al. 1995	extraction age
1200°C	Ar-Ar	4.325	0.041		Kunz et al. 1995	extraction age
1240°C	Ar-Ar	4.438	0.069		Kunz et al. 1995	extraction age
1340°C	Ar-Ar	4.348	0.029		Kunz et al. 1995	extraction age
1440°C	Ar-Ar	4.397	0.015		Kunz et al. 1995	extraction age
1580°C	Ar-Ar	4.443	0.072		Kunz et al. 1995	extraction age
300°C	Ar-Ar	6.458	0.655		Kunz et al. 1995	extraction age
350°C	Ar-Ar	5.442	0.189		Kunz et al. 1995	extraction age
400°C	Ar-Ar	4.402	0.073		Kunz et al. 1995	extraction age
450°C	Ar-Ar	4.189	0.032		Kunz et al. 1995	extraction age
500°C	Ar-Ar	4.331	0.019		Kunz et al. 1995	extraction age
550°C	Ar-Ar	4.487	0.013		Kunz et al. 1995	extraction age
600°C	Ar-Ar	4.209	0.005		Kunz et al. 1995	extraction age
640°C	Ar-Ar	4.1	0.004		Kunz et al. 1995	extraction age

Sample	Method	Date	Error +/-	Note	Source	Type
680°C	Ar-Ar	4.1	0.004		Kunz et al. 1995	extraction age
700°C	Ar-Ar	4.105	0.005		Kunz et al. 1995	extraction age
720°C	Ar-Ar	4.13	0.004		Kunz et al. 1995	extraction age
740°C	Ar-Ar	4.14	0.005		Kunz et al. 1995	extraction age
760°C	Ar-Ar	4.148	0.004		Kunz et al. 1995	extraction age
780°C	Ar-Ar	4.176	0.006		Kunz et al. 1995	extraction age
800°C	Ar-Ar	4.195	0.004		Kunz et al. 1995	extraction age
820°C	Ar-Ar	4.203	0.006		Kunz et al. 1995	extraction age
840°C	Ar-Ar	4.218	0.006		Kunz et al. 1995	extraction age
860°C	Ar-Ar	4.24	0.005		Kunz et al. 1995	extraction age
890°C	Ar-Ar	4.241	0.006		Kunz et al. 1995	extraction age
920°C	Ar-Ar	4.217	0.006		Kunz et al. 1995	extraction age
950°C	Ar-Ar	4.223	0.008		Kunz et al. 1995	extraction age
990°C	Ar-Ar	4.305	0.009		Kunz et al. 1995	extraction age
1030°C	Ar-Ar	4.357	0.011		Kunz et al. 1995	extraction age
1080°C	Ar-Ar	4.381	0.014		Kunz et al. 1995	extraction age
1150°C	Ar-Ar	4.436	0.006		Kunz et al. 1995	extraction age
1230°C	Ar-Ar	4.483	0.007		Kunz et al. 1995	extraction age
1270°C	Ar-Ar	4.567	0.066		Kunz et al. 1995	extraction age
1310°C	Ar-Ar	5.407	0.341		Kunz et al. 1995	extraction age
1380°C	Ar-Ar	4.666	0.222		Kunz et al. 1995	extraction age
300°C	Ar-Ar	6.191	0.948		Kunz et al. 1995	extraction age
450°C	Ar-Ar	6.099	0.169		Kunz et al. 1995	extraction age
530°C	Ar-Ar	4.637	0.121		Kunz et al. 1995	extraction age
600°C	Ar-Ar	4.477	0.077		Kunz et al. 1995	extraction age
670°C	Ar-Ar	4.698	0.031		Kunz et al. 1995	extraction age
730°C	Ar-Ar	4.007	0.027		Kunz et al. 1995	extraction age
790°C	Ar-Ar	3.997	0.022		Kunz et al. 1995	extraction age
830°C	Ar-Ar	4.076	0.021		Kunz et al. 1995	extraction age
880°C	Ar-Ar	4.23	0.021		Kunz et al. 1995	extraction age
940°C	Ar-Ar	4.267	0.022		Kunz et al. 1995	extraction age
1020°C	Ar-Ar	4.221	0.016		Kunz et al. 1995	extraction age
1120°C	Ar-Ar	4.255	0.023		Kunz et al. 1995	extraction age
1200°C	Ar-Ar	4.287	0.083		Kunz et al. 1995	extraction age
1320°C	Ar-Ar	4.437	0.033		Kunz et al. 1995	extraction age
1440°C	Ar-Ar	4.739	0.385		Kunz et al. 1995	extraction age
sample 7 plateau	Ar-Ar	4.245	0.024		Kunz et al. 1995	plateau age
sample 7, low temperature, 48% width	Ar-Ar	4	0.1		Kunz et al. 1995	spectrum model age
sample 7, high temperature, 35% gas loss	Ar-Ar	4.4	0.1		Kunz et al. 1995	spectrum model age
Revised Podosek and Huneke 1973 age	Ar-Ar	4.02			Quitté, Birck, and Allègre 2000	plateau age
	²⁰⁷ Pb- ²⁰⁶ Pb	4.573	0.006		Unruh, Nakamura, and Tatsumoto 1977	model age
	²⁰⁷ Pb- ²⁰⁶ Pb	4.572	0.005		Unruh, Nakamura, and Tatsumoto 1977	model age
	²⁰⁷ Pb- ²⁰⁶ Pb	4.484	0.004		Unruh, Nakamura, and Tatsumoto 1977	model age
	²⁰⁷ Pb- ²⁰⁶ Pb	4.454	0.01		Unruh, Nakamura, and Tatsumoto 1977	model age
	²⁰⁷ Pb- ²⁰⁶ Pb	4.963	0.03		Unruh, Nakamura, and Tatsumoto 1977	model age
	²⁰⁷ Pb- ²⁰⁶ Pb	4.912	0.01		Unruh, Nakamura, and Tatsumoto 1977	model age
	²⁰⁷ Pb- ²⁰⁶ Pb	4.709	0.008		Unruh, Nakamura, and Tatsumoto 1977	model age

Sample	Method	Date	Error +/-	Note	Source	Type
	²⁰⁷ Pb- ²⁰⁶ Pb	4.664	0.006		Unruh, Nakamura, and Tatsumoto 1977	model age
	²⁰⁷ Pb- ²⁰⁶ Pb	4.515	0.06		Unruh, Nakamura, and Tatsumoto 1977	model age
	²⁰⁷ Pb- ²⁰⁶ Pb	4.454	0.019		Unruh, Nakamura, and Tatsumoto 1977	model age
	²⁰⁷ Pb- ²⁰⁶ Pb	4.457	0.012		Unruh, Nakamura, and Tatsumoto 1977	model age
	²⁰⁷ Pb- ²⁰⁶ Pb	4.51	0.1		Unruh, Nakamura, and Tatsumoto 1977	model age
	²⁰⁷ Pb- ²⁰⁶ Pb	4.468	0.015		Unruh, Nakamura, and Tatsumoto 1977	model age
	²⁰⁷ Pb- ²⁰⁶ Pb	4.44	0.023		Unruh, Nakamura, and Tatsumoto 1977	model age
	²⁰⁷ Pb- ²⁰⁶ Pb	4.535	0.005		Unruh, Nakamura, and Tatsumoto 1977	model age
	²⁰⁷ Pb- ²⁰⁶ Pb	4.534	0.004		Unruh, Nakamura, and Tatsumoto 1977	model age
	²⁰⁷ Pb- ²⁰⁶ Pb	4.542	0.019		Unruh, Nakamura, and Tatsumoto 1977	model age
	²⁰⁷ Pb- ²⁰⁶ Pb	4.534	0.02		Unruh, Nakamura, and Tatsumoto 1977	model age
	²⁰⁷ Pb- ²⁰⁶ Pb	4.534	0.013		Unruh, Nakamura, and Tatsumoto 1977	model age
	²⁰⁷ Pb- ²⁰⁶ Pb	4.519	0.013		Unruh, Nakamura, and Tatsumoto 1977	model age
	²⁰⁷ Pb- ²⁰⁶ Pb	4.555	0.017		Unruh, Nakamura, and Tatsumoto 1977	model age
	²⁰⁷ Pb- ²⁰⁶ Pb	4.52	0.004		Unruh, Nakamura, and Tatsumoto 1977	model age
	²⁰⁶ Pb- ²³⁸ U	4.874	0.038		Unruh, Nakamura, and Tatsumoto 1977	model age
	²⁰⁶ Pb- ²³⁸ U	4.814	0.038		Unruh, Nakamura, and Tatsumoto 1977	model age
	²⁰⁶ Pb- ²³⁸ U	5.694	0.083		Unruh, Nakamura, and Tatsumoto 1977	model age
	²⁰⁶ Pb- ²³⁸ U	5.597	0.092		Unruh, Nakamura, and Tatsumoto 1977	model age
	²⁰⁶ Pb- ²³⁸ U	3.38	0.35		Unruh, Nakamura, and Tatsumoto 1977	model age
	²⁰⁶ Pb- ²³⁸ U	5.336	0.7		Unruh, Nakamura, and Tatsumoto 1977	model age
	²⁰⁶ Pb- ²³⁸ U	0.296	0.005		Unruh, Nakamura, and Tatsumoto 1977	model age
	²⁰⁶ Pb- ²³⁸ U	0.277	0.003		Unruh, Nakamura, and Tatsumoto 1977	model age
	²⁰⁶ Pb- ²³⁸ U	0.103	0.009		Unruh, Nakamura, and Tatsumoto 1977	model age
	²⁰⁶ Pb- ²³⁸ U	0.377	0.014		Unruh, Nakamura, and Tatsumoto 1977	model age
	²⁰⁶ Pb- ²³⁸ U	0.376	0.016		Unruh, Nakamura, and Tatsumoto 1977	model age
	²⁰⁶ Pb- ²³⁸ U	2.953	0.3		Unruh, Nakamura, and Tatsumoto 1977	model age
	²⁰⁶ Pb- ²³⁸ U	3.29	0.085		Unruh, Nakamura, and Tatsumoto 1977	model age
	²⁰⁶ Pb- ²³⁸ U	3.215	0.107		Unruh, Nakamura, and Tatsumoto 1977	model age
	²⁰⁶ Pb- ²³⁸ U	4.903	0.041		Unruh, Nakamura, and Tatsumoto 1977	model age
	²⁰⁶ Pb- ²³⁸ U	4.907	0.041		Unruh, Nakamura, and Tatsumoto 1977	model age

Sample	Method	Date	Error +/-	Note	Source	Type
	^{206}Pb - ^{238}U	4.522	0.14		Unruh, Nakamura, and Tatsumoto 1977	model age
	^{206}Pb - ^{238}U	4.5	0.15		Unruh, Nakamura, and Tatsumoto 1977	model age
	^{206}Pb - ^{238}U	1.851	0.031		Unruh, Nakamura, and Tatsumoto 1977	model age
	^{206}Pb - ^{238}U	1.477	0.03		Unruh, Nakamura, and Tatsumoto 1977	model age
	^{206}Pb - ^{238}U	1.798	0.043		Unruh, Nakamura, and Tatsumoto 1977	model age
	^{206}Pb - ^{238}U	3.39	0.027		Unruh, Nakamura, and Tatsumoto 1977	model age
	^{207}Pb - ^{235}U	4.663	0.015		Unruh, Nakamura, and Tatsumoto 1977	model age
	^{207}Pb - ^{235}U	4.645	0.015		Unruh, Nakamura, and Tatsumoto 1977	model age
	^{207}Pb - ^{235}U	4.806	0.031		Unruh, Nakamura, and Tatsumoto 1977	model age
	^{207}Pb - ^{235}U	4.784	0.044		Unruh, Nakamura, and Tatsumoto 1977	model age
	^{207}Pb - ^{235}U	4.421	0.175		Unruh, Nakamura, and Tatsumoto 1977	model age
	^{207}Pb - ^{235}U	5.032	0.23		Unruh, Nakamura, and Tatsumoto 1977	model age
	^{207}Pb - ^{235}U	1.724	0.015		Unruh, Nakamura, and Tatsumoto 1977	model age
	^{207}Pb - ^{235}U	1.644	0.011		Unruh, Nakamura, and Tatsumoto 1977	model age
	^{207}Pb - ^{235}U	0.865	0.085		Unruh, Nakamura, and Tatsumoto 1977	model age
	^{207}Pb - ^{235}U	1.786	0.053		Unruh, Nakamura, and Tatsumoto 1977	model age
	^{207}Pb - ^{235}U	1.784	0.072		Unruh, Nakamura, and Tatsumoto 1977	model age
	^{207}Pb - ^{235}U	3.955	0.195		Unruh, Nakamura, and Tatsumoto 1977	model age
	^{207}Pb - ^{235}U	4.061	0.06		Unruh, Nakamura, and Tatsumoto 1977	model age
	^{207}Pb - ^{235}U	4.014	0.08		Unruh, Nakamura, and Tatsumoto 1977	model age
	^{207}Pb - ^{235}U	4.645	0.014		Unruh, Nakamura, and Tatsumoto 1977	model age
	^{207}Pb - ^{235}U	4.646	0.016		Unruh, Nakamura, and Tatsumoto 1977	model age
	^{207}Pb - ^{235}U	4.536	0.06		Unruh, Nakamura, and Tatsumoto 1977	model age
	^{207}Pb - ^{235}U	4.523	0.068		Unruh, Nakamura, and Tatsumoto 1977	model age
	^{207}Pb - ^{235}U	3.419	0.027		Unruh, Nakamura, and Tatsumoto 1977	model age
	^{207}Pb - ^{235}U	3.161	0.036		Unruh, Nakamura, and Tatsumoto 1977	model age
	^{207}Pb - ^{235}U	3.396	0.036		Unruh, Nakamura, and Tatsumoto 1977	model age
	^{207}Pb - ^{235}U	4.136	0.015		Unruh, Nakamura, and Tatsumoto 1977	model age
	^{208}Pb - ^{232}Th	4.678	0.085		Unruh, Nakamura, and Tatsumoto 1977	model age
	^{208}Pb - ^{232}Th	14.8	0.6		Unruh, Nakamura, and Tatsumoto 1977	model age
	^{208}Pb - ^{232}Th	9.6			Unruh, Nakamura, and Tatsumoto 1977	model age

Sample	Method	Date	Error +/-	Note	Source	Type
	^{208}Pb - ^{232}Th	0.295	0.03		Unruh, Nakamura, and Tatsumoto 1977	model age
	^{208}Pb - ^{232}Th	0.57	0.2		Unruh, Nakamura, and Tatsumoto 1977	model age
	^{208}Pb - ^{232}Th	4.922	0.5		Unruh, Nakamura, and Tatsumoto 1977	model age
	^{208}Pb - ^{232}Th	4.16	0.25		Unruh, Nakamura, and Tatsumoto 1977	model age
	^{208}Pb - ^{232}Th	10.7			Unruh, Nakamura, and Tatsumoto 1977	model age
	^{208}Pb - ^{232}Th	3.597	0.099		Unruh, Nakamura, and Tatsumoto 1977	model age
	^{208}Pb - ^{232}Th	3.549	0.16		Unruh, Nakamura, and Tatsumoto 1977	model age
	^{208}Pb - ^{232}Th	8.627	0.35		Unruh, Nakamura, and Tatsumoto 1977	model age
two samples	Pu-Xe	4.576	0.019		Shukolyukov and Begemann 1996a	model age
Serra De Magé						
whole rock samples	K-Ar	2.7			Heymann, Mazor, and Anders 1968	model age
average of four extractions having the same age within uncertainties	Ar-Ar	3.386	0.007		Bogard and Garrison 2003	plateau age
350°C	Ar-Ar	6.1	0.114		Bogard and Garrison 2003	step extraction model age
450°C	Ar-Ar	2.548	0.191		Bogard and Garrison 2003	step extraction model age
525°C	Ar-Ar	1.231	0.25		Bogard and Garrison 2003	step extraction model age
600°C	Ar-Ar	1.77	0.122		Bogard and Garrison 2003	step extraction model age
650°C	Ar-Ar	0.499	0.199		Bogard and Garrison 2003	step extraction model age
700°C	Ar-Ar	2.779	0.18		Bogard and Garrison 2003	step extraction model age
775°C	Ar-Ar	3.112	0.093		Bogard and Garrison 2003	step extraction model age
825°C	Ar-Ar	3.316	0.033		Bogard and Garrison 2003	step extraction model age
875°C	Ar-Ar	3.387	0.037		Bogard and Garrison 2003	step extraction model age
925°C	Ar-Ar	3.372	0.045		Bogard and Garrison 2003	step extraction model age
975°C	Ar-Ar	3.388	0.06		Bogard and Garrison 2003	step extraction model age
1025°C	Ar-Ar	3.395	0.041		Bogard and Garrison 2003	step extraction model age
1075°C	Ar-Ar	3.461	0.045		Bogard and Garrison 2003	step extraction model age
1125°C	Ar-Ar	3.511	0.037		Bogard and Garrison 2003	step extraction model age
1175°C	Ar-Ar	3.619	0.048		Bogard and Garrison 2003	step extraction model age
1225°C	Ar-Ar	3.528	0.103		Bogard and Garrison 2003	step extraction model age
1275°C	Ar-Ar	3.585	0.158		Bogard and Garrison 2003	step extraction model age
1325°C	Ar-Ar	3.689	0.193		Bogard and Garrison 2003	step extraction model age
1400°C	Ar-Ar	3.783	0.053		Bogard and Garrison 2003	step extraction model age

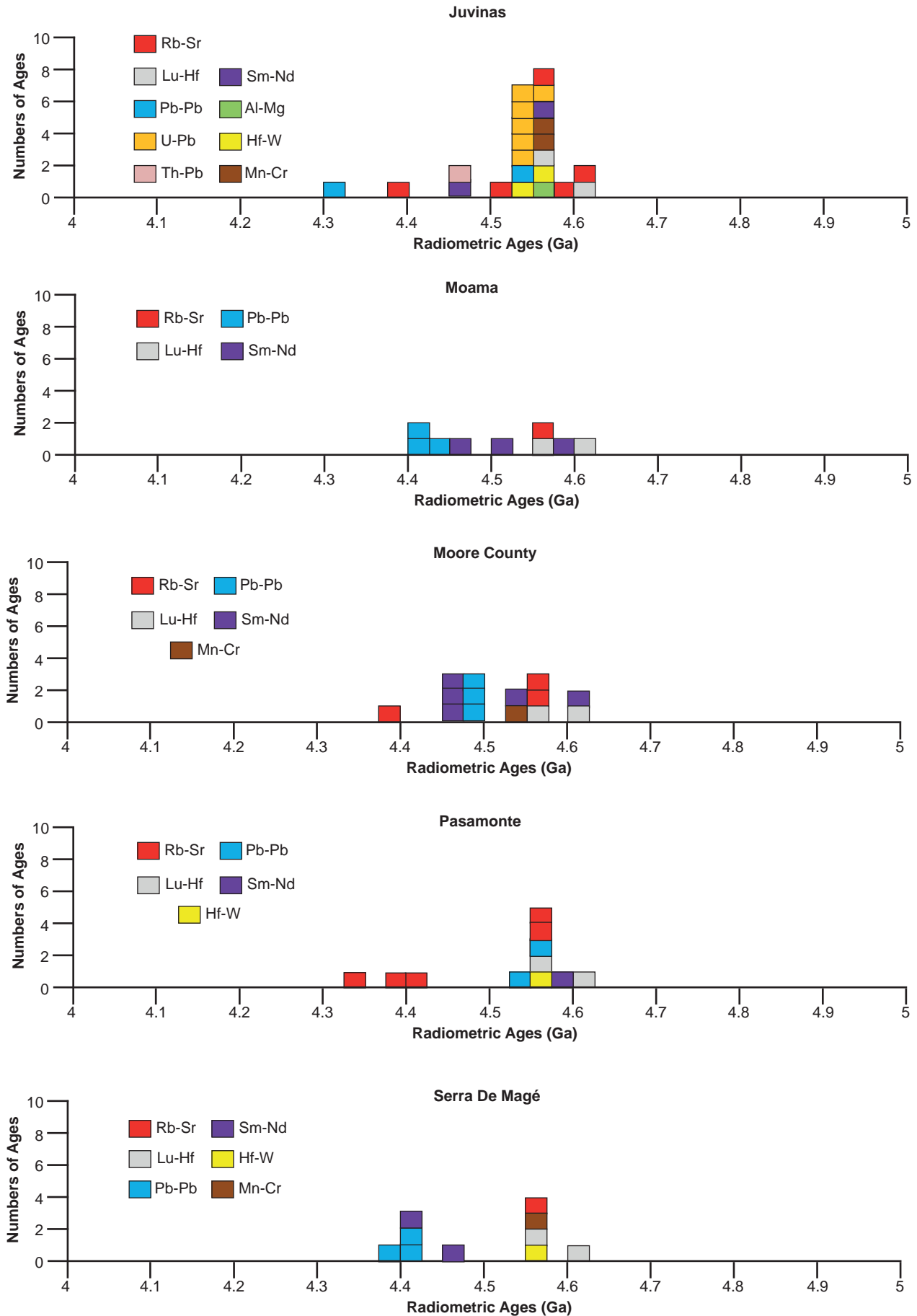
Sample	Method	Date	Error +/-	Note	Source	Type
1500°C	Ar-Ar	3.91	0.028		Bogard and Garrison 2003	step extraction model age
Stannern						
whole-rock samples	K-Ar	3.8			Heymann, Mazor, and Anders 1968	model age
545°C	K-Ar	3.86	0.028		Podosek and Huneke 1973	step model age
630°C	K-Ar	3.837	0.008		Podosek and Huneke 1973	step model age
745°C	K-Ar	3.704	0.003		Podosek and Huneke 1973	step model age
850°C	K-Ar	3.472	0.002		Podosek and Huneke 1973	step model age
935°C	K-Ar	3.514	0.007		Podosek and Huneke 1973	step model age
1040°C	K-Ar	3.64	0.003		Podosek and Huneke 1973	step model age
1195°C	K-Ar	3.591	0.003		Podosek and Huneke 1973	step model age
1515°C	K-Ar	3.923	0.006		Podosek and Huneke 1973	step model age
	K-Ar	3.57		mean of ages in literature	Shukolyukov and Begemann 1996a	model age
	Ar-Ar	3.7	0.2	based on nine extractions at stepped temperatures	Podosek and Huneke 1973	plateau age
three samples, low temperature	Ar-Ar	3.3	0.3		Kunz et al. 1995	plateau age
three samples, high temperature, 80% gas loss	Ar-Ar	4	0.2		Kunz et al. 1995	plateau age
drill core 1, basalt clast, 300°C	Ar-Ar	6.313	0.181		Kunz et al. 1995	step extraction age
350°C	Ar-Ar	3.632	0.028		Kunz et al. 1995	step extraction age
400°C	Ar-Ar	3.09	0.014		Kunz et al. 1995	step extraction age
450°C	Ar-Ar	3.564	0.008		Kunz et al. 1995	step extraction age
500°C	Ar-Ar	3.687	0.005		Kunz et al. 1995	step extraction age
550°C	Ar-Ar	3.679	0.005		Kunz et al. 1995	step extraction age
580°C	Ar-Ar	3.636	0.004		Kunz et al. 1995	step extraction age
600°C	Ar-Ar	3.523	0.005		Kunz et al. 1995	step extraction age
620°C	Ar-Ar	3.48	0.007		Kunz et al. 1995	step extraction age
640°C	Ar-Ar	3.392	0.005		Kunz et al. 1995	step extraction age
670°C	Ar-Ar	3.408	0.005		Kunz et al. 1995	step extraction age
690°C	Ar-Ar	3.471	0.006		Kunz et al. 1995	step extraction age
710°C	Ar-Ar	3.511	0.005		Kunz et al. 1995	step extraction age
740°C	Ar-Ar	3.543	0.005		Kunz et al. 1995	step extraction age
770°C	Ar-Ar	3.58	0.006		Kunz et al. 1995	step extraction age
810°C	Ar-Ar	3.597	0.006		Kunz et al. 1995	step extraction age
850°C	Ar-Ar	3.595	0.006		Kunz et al. 1995	step extraction age
890°C	Ar-Ar	3.57	0.006		Kunz et al. 1995	step extraction age

Sample	Method	Date	Error +/-	Note	Source	Type
930°C	Ar-Ar	3.537	0.006		Kunz et al. 1995	step extraction age
970°C	Ar-Ar	3.478	0.007		Kunz et al. 1995	step extraction age
1020°C	Ar-Ar	3.298	0.007		Kunz et al. 1995	step extraction age
1070°C	Ar-Ar	3.474	0.012		Kunz et al. 1995	step extraction age
1120°C	Ar-Ar	3.785	0.017		Kunz et al. 1995	step extraction age
1170°C	Ar-Ar	4.003	0.013		Kunz et al. 1995	step extraction age
1220°C	Ar-Ar	4.141	0.024		Kunz et al. 1995	step extraction age
1270°C	Ar-Ar	4.229	0.026		Kunz et al. 1995	step extraction age
1330°C	Ar-Ar	4.338	0.069		Kunz et al. 1995	step extraction age
1400°C	Ar-Ar	4.247	0.049		Kunz et al. 1995	step extraction age
drill core 2, recrystallized classic matrix 300°C	Ar-Ar	4.76	0.601		Kunz et al. 1995	step extraction age
350°C	Ar-Ar	3.672	0.069		Kunz et al. 1995	step extraction age
400°C	Ar-Ar	3.238	0.022		Kunz et al. 1995	step extraction age
450°C	Ar-Ar	3.588	0.011		Kunz et al. 1995	step extraction age
500°C	Ar-Ar	3.747	0.009		Kunz et al. 1995	step extraction age
540°C	Ar-Ar	3.715	0.008		Kunz et al. 1995	step extraction age
580°C	Ar-Ar	3.88	0.006		Kunz et al. 1995	step extraction age
600°C	Ar-Ar	3.596	0.01		Kunz et al. 1995	step extraction age
620°C	Ar-Ar	3.5	0.005		Kunz et al. 1995	step extraction age
640°C	Ar-Ar	3.405	0.007		Kunz et al. 1995	step extraction age
670°C	Ar-Ar	3.402	0.007		Kunz et al. 1995	step extraction age
690°C	Ar-Ar	3.448	0.007		Kunz et al. 1995	step extraction age
710°C	Ar-Ar	3.5	0.008		Kunz et al. 1995	step extraction age
740°C	Ar-Ar	3.543	0.009		Kunz et al. 1995	step extraction age
770°C	Ar-Ar	3.558	0.01		Kunz et al. 1995	step extraction age
810°C	Ar-Ar	3.545	0.01		Kunz et al. 1995	step extraction age
850°C	Ar-Ar	3.487	0.011		Kunz et al. 1995	step extraction age
890°C	Ar-Ar	3.432	0.013		Kunz et al. 1995	step extraction age
930°C	Ar-Ar	3.382	0.012		Kunz et al. 1995	step extraction age
970°C	Ar-Ar	3.282	0.014		Kunz et al. 1995	step extraction age

Sample	Method	Date	Error +/-	Note	Source	Type
1020°C	Ar-Ar	3.095	0.014		Kunz et al. 1995	step extraction age
1070°C	Ar-Ar	3.146	0.027		Kunz et al. 1995	step extraction age
1120°C	Ar-Ar	3.492	0.05		Kunz et al. 1995	step extraction age
1170°C	Ar-Ar	3.735	0.065		Kunz et al. 1995	step extraction age
1220°C	Ar-Ar	4.001	0.114		Kunz et al. 1995	step extraction age
1270°C	Ar-Ar	3.947	0.077		Kunz et al. 1995	step extraction age
1330°C	Ar-Ar	4.122	0.126		Kunz et al. 1995	step extraction age
1400°C	Ar-Ar	3.84	0.327		Kunz et al. 1995	step extraction age
	Pb-Pb	4.329			Manhès et al. 1975	model age
	Pb-Pb	4.13			Tera, Carlson, and Boctor 1987	model age
	Pu-Xe	4.46	0.028		Shukolyukov and Begemann 1996a	model age
	Pu-Xe	4.434	0.013		Miura et al. 1998	model age
Yamato 75011						
whole rock sample	K-Ar	4	0.5		Miura et al. 1993	model age
84 matrix, 11 extractions	Ar-Ar	3.94	0.04		Takeda, Mori, and Bogard 1994	plateau age
84 clast, 11 extractions	Ar-Ar	3.98	0.03		Takeda, Mori, and Bogard 1994	plateau age
84 matrix, temp. 300	Ar-Ar	3.76	0.05		Takeda, Mori, and Bogard 1994	degassing age
84 matrix, temp. 400	Ar-Ar	3.95	0.02		Takeda, Mori, and Bogard 1994	degassing age
84 matrix, temp. 500	Ar-Ar	4.01	0.02		Takeda, Mori, and Bogard 1994	degassing age
84 matrix, temp. 600	Ar-Ar	3.96	0.02		Takeda, Mori, and Bogard 1994	degassing age
84 matrix, temp. 700	Ar-Ar	3.97	0.02		Takeda, Mori, and Bogard 1994	degassing age
84 matrix, temp. 775	Ar-Ar	3.95	0.02		Takeda, Mori, and Bogard 1994	degassing age
84 matrix, temp. 850	Ar-Ar	3.88	0.04		Takeda, Mori, and Bogard 1994	degassing age
84 matrix, temp. 950	Ar-Ar	3.91	0.02		Takeda, Mori, and Bogard 1994	degassing age
84 matrix, temp. 1000	Ar-Ar	3.94	0.02		Takeda, Mori, and Bogard 1994	degassing age
84 matrix, temp. 1050	Ar-Ar	3.97	0.02		Takeda, Mori, and Bogard 1994	degassing age
84 matrix, temp. 1100	Ar-Ar	3.98	0.02		Takeda, Mori, and Bogard 1994	degassing age
84 matrix, temp. 1150	Ar-Ar	3.98	0.02		Takeda, Mori, and Bogard 1994	degassing age
84 matrix, temp. 1225	Ar-Ar	4.12	0.03		Takeda, Mori, and Bogard 1994	degassing age
84 matrix, temp. 1350	Ar-Ar	4.35	0.03		Takeda, Mori, and Bogard 1994	degassing age
84 matrix, temp. 1500	Ar-Ar	4.2	0.16		Takeda, Mori, and Bogard 1994	degassing age
84 clast, temp. 300	Ar-Ar	3.99	0.02		Takeda, Mori, and Bogard 1994	degassing age
84 clast, temp. 400	Ar-Ar	3.69	0.03		Takeda, Mori, and Bogard 1994	degassing age

Sample	Method	Date	Error +/-	Note	Source	Type
84 clast, temp. 500	Ar-Ar	4.05	0.02		Takeda, Mori, and Bogard 1994	degassing age
84 clast, temp. 575	Ar-Ar	3.83	0.06		Takeda, Mori, and Bogard 1994	degassing age
84 clast, temp. 650	Ar-Ar	3.99	0.03		Takeda, Mori, and Bogard 1994	degassing age
84 clast, temp. 725	Ar-Ar	4.03	0.02		Takeda, Mori, and Bogard 1994	degassing age
84 clast, temp. 800	Ar-Ar	3.97	0.02		Takeda, Mori, and Bogard 1994	degassing age
84 clast, temp. 850	Ar-Ar	3.98	0.02		Takeda, Mori, and Bogard 1994	degassing age
84 clast, temp. 900	Ar-Ar	3.96	0.02		Takeda, Mori, and Bogard 1994	degassing age
84 clast, temp. 950	Ar-Ar	3.96	0.02		Takeda, Mori, and Bogard 1994	degassing age
84 clast, temp. 1000	Ar-Ar	3.99	0.02		Takeda, Mori, and Bogard 1994	degassing age
84 clast, temp. 1050	Ar-Ar	4.08	0.02		Takeda, Mori, and Bogard 1994	degassing age
84 clast, temp. 1100	Ar-Ar	4.15	0.02		Takeda, Mori, and Bogard 1994	degassing age
84 clast, temp. 1150	Ar-Ar	4.23	0.02		Takeda, Mori, and Bogard 1994	degassing age
84 clast, temp. 1225	Ar-Ar	4.36	0.03		Takeda, Mori, and Bogard 1994	degassing age
84 clast, temp. 1300	Ar-Ar	4.48	0.03		Takeda, Mori, and Bogard 1994	degassing age
84 clast, temp. 1500	Ar-Ar	4.5	0.02		Takeda, Mori, and Bogard 1994	degassing age
matrix, low temperature	Ar-Ar	3.91	0.04		Kunz et al. 1995	spectrum model age
matrix, high temperature, 90% gas extraction	Ar-Ar	4.4	0.1		Kunz et al. 1995	spectrum model age
clast, low temperature	Ar-Ar	3.98	0.03		Kunz et al. 1995	spectrum model age
clast, high temperature, 90% gas extraction	Ar-Ar	4.5	0.1		Kunz et al. 1995	spectrum model age
73 matrix, whole rock, BABI	Rb-Sr	4.28	0.24		Nyquist et al. 1986	model age
73 matrix, <2.45 g/cu. cm., BABI	Rb-Sr	4.53	0.07		Nyquist et al. 1986	model age
73 matrix, 2.45–2.85 g/cu. cm., BABI	Rb-Sr	3.91	0.4		Nyquist et al. 1986	model age
73 matrix, 2.85–3.3 g/cu. cm., BABI	Rb-Sr	4.71	0.19		Nyquist et al. 1986	model age
73 matrix, 3.3 g/cu. cm., BABI	Rb-Sr	4.73	0.31		Nyquist et al. 1996	model age
84B clast, whole rock 1, BABI	Rb-Sr	4.34	0.89		Nyquist et al. 1986	model age
84B clast, whole rock 3, BABI	Rb-Sr	4.36	0.29		Nyquist et al. 1986	model age
84B clast, <2.45 g/cu. cm., BABI	Rb-Sr	4.57	0.05		Nyquist et al. 1986	model age
84B clast, 2.45–2.65 g/cu. cm., BABI	Rb-Sr	4.52	0.15		Nyquist et al. 1986	model age

Sample	Method	Date	Error +/-	Note	Source	Type
84B clast, 2.65–2.85 g/cu. cm., BABI	Rb-Sr	3.55	0.51		Nyquist et al. 1986	model age
84B clast, Plag, BABI	Rb-Sr	3.73	0.54		Nyquist et al. 1986	model age
84B clast, Lt. Px, BABI	Rb-Sr	4.11	0.11		Nyquist et al. 1986	model age
84B clast, Dk. Px, BABI	Rb-Sr	4.51	0.14		Nyquist et al. 1986	model age
84B clast, most Mag, BABI	Rb-Sr	4.66	0.12		Nyquist et al. 1986	model age
zircon 011-1a	²⁰⁷ Pb- ²⁰⁶ Pb	4.551	0.008		Misawa, Yamaguchi, and Kaiden 2005	model age
zircon 011-1b	²⁰⁷ Pb- ²⁰⁶ Pb	4.561	0.02		Misawa, Yamaguchi, and Kaiden 2005	model age
zircon 011-2a	²⁰⁷ Pb- ²⁰⁶ Pb	4.552	0.01		Misawa, Yamaguchi, and Kaiden 2005	model age
zircon 011-2b	²⁰⁷ Pb- ²⁰⁶ Pb	4.549	0.009		Misawa, Yamaguchi, and Kaiden 2005	model age
zircon 011-2c	²⁰⁷ Pb- ²⁰⁶ Pb	4.543	0.013		Misawa, Yamaguchi, and Kaiden 2005	model age
zircon 011-1a	²⁰⁶ Pb- ²³⁸ U	5.04	0.078		Misawa, Yamaguchi, and Kaiden 2005	model age
zircon 011-1b	²⁰⁶ Pb- ²³⁸ U	4.816	0.079		Misawa, Yamaguchi, and Kaiden 2005	model age
zircon 011-2a	²⁰⁶ Pb- ²³⁸ U	4.548	0.047		Misawa, Yamaguchi, and Kaiden 2005	model age
zircon 011-2b	²⁰⁶ Pb- ²³⁸ U	4.842	0.073		Misawa, Yamaguchi, and Kaiden 2005	model age
zircon 011-2c	²⁰⁶ Pb- ²³⁸ U	5.07	0.064		Misawa, Yamaguchi, and Kaiden 2005	model age
73 matrix, whole rock, chondrite	Sm-Nd	4.55	0.03		Nyquist et al. 1986	model age
73 matrix, 2.45–2.85 g/cu. cm., chondrite	Sm-Nd	4.52	0.03		Nyquist et al. 1986	model age
73 matrix, 2.85–3.3 g/cu. cm., chondrite	Sm-Nd	4.53	0.02		Nyquist et al. 1986	model age
73 matrix, 3.3 g/cu. cm., chondrite	Sm-Nd	4.51	0.02		Nyquist et al. 1996	model age
84B clast, whole rock 1, chondrite	Sm-Nd	4.55	0.02		Nyquist et al. 1986	model age
84B clast, whole rock 3, chondrite	Sm-Nd	4.54	0.02		Nyquist et al. 1986	model age
84B clast, <2.45 g/cu. cm., chondrite	Sm-Nd	4.51	0.04		Nyquist et al. 1986	model age
84B clast, Plag, chondrite	Sm-Nd	4.56	0.04		Nyquist et al. 1986	model age
84B clast, Lt. Px, chondrite	Sm-Nd	4.56	0.02		Nyquist et al. 1986	model age
84B clast, Dk. Px, chondrite	Sm-Nd	4.53	0.02		Nyquist et al. 1986	model age
84B clast, most Mag, chondrite	Sm-Nd	4.58	0.02		Nyquist et al. 1986	model age



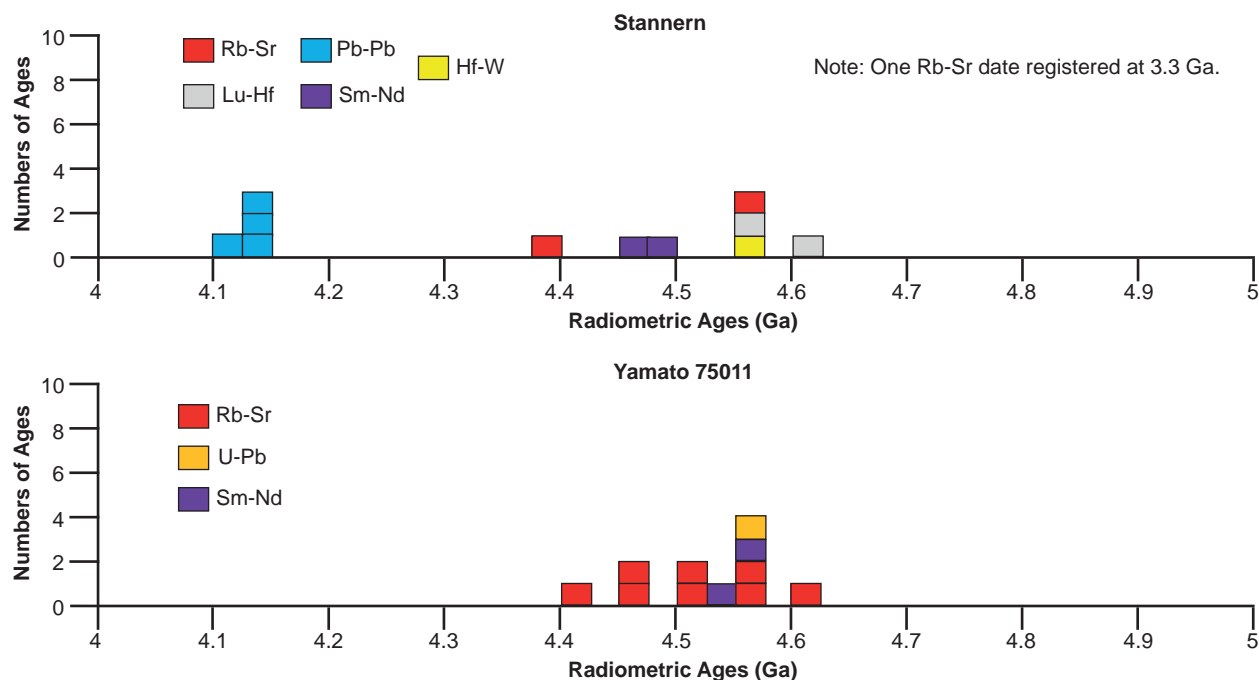


Fig. 6. Frequency versus radioisotope ages histogram diagram for the isochron ages for whole-rock samples and some or all components of 12 eucrite achondrites, with color coding being used to show the ages obtained by the different radioisotope dating methods.

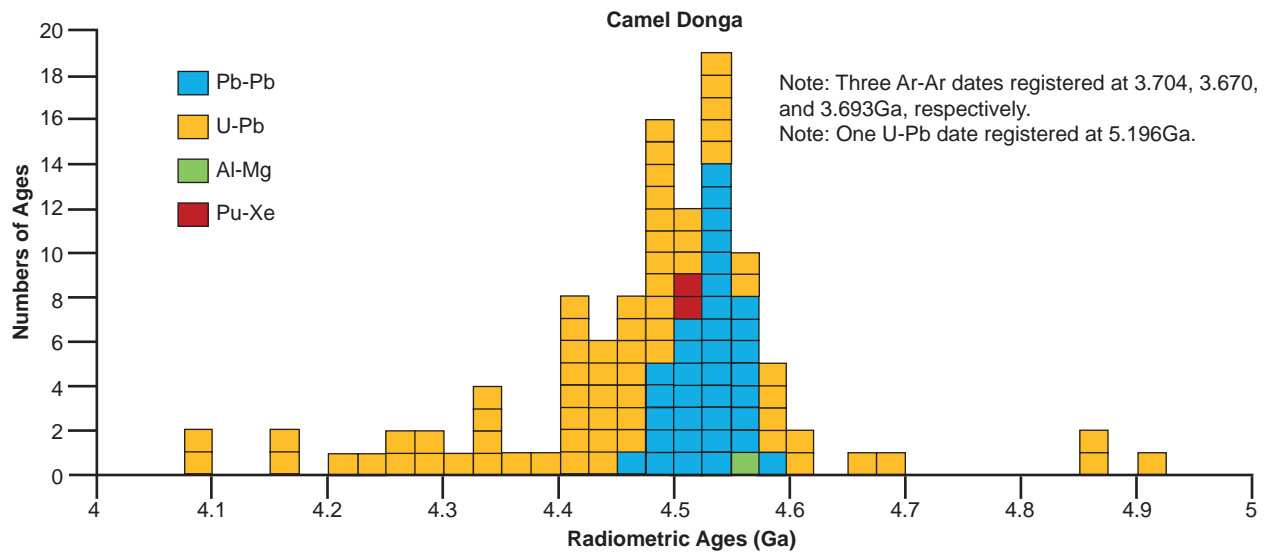
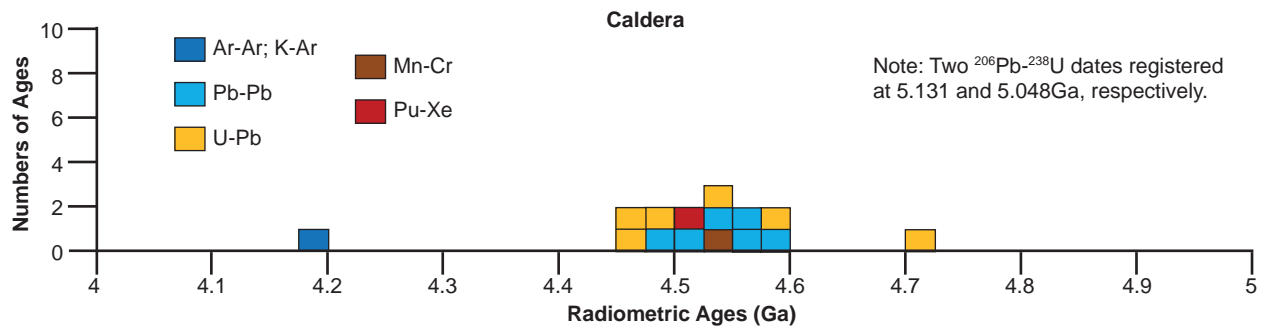
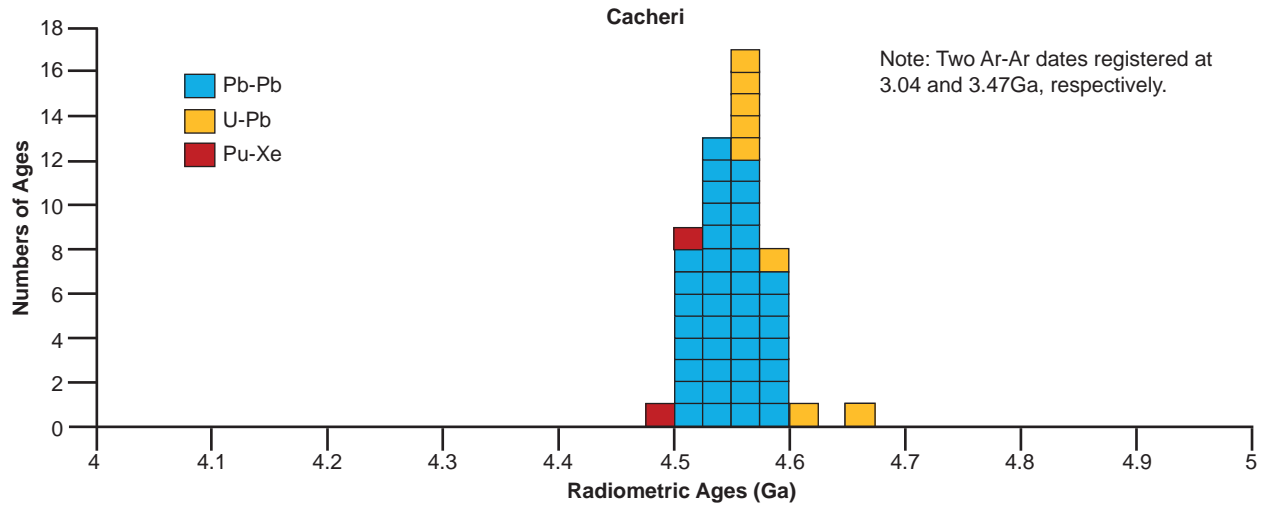
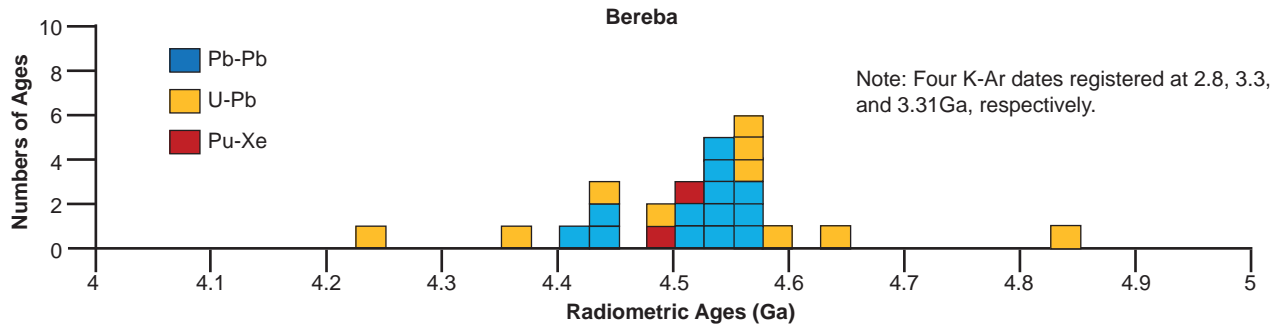
An explanation for the agreement of ages

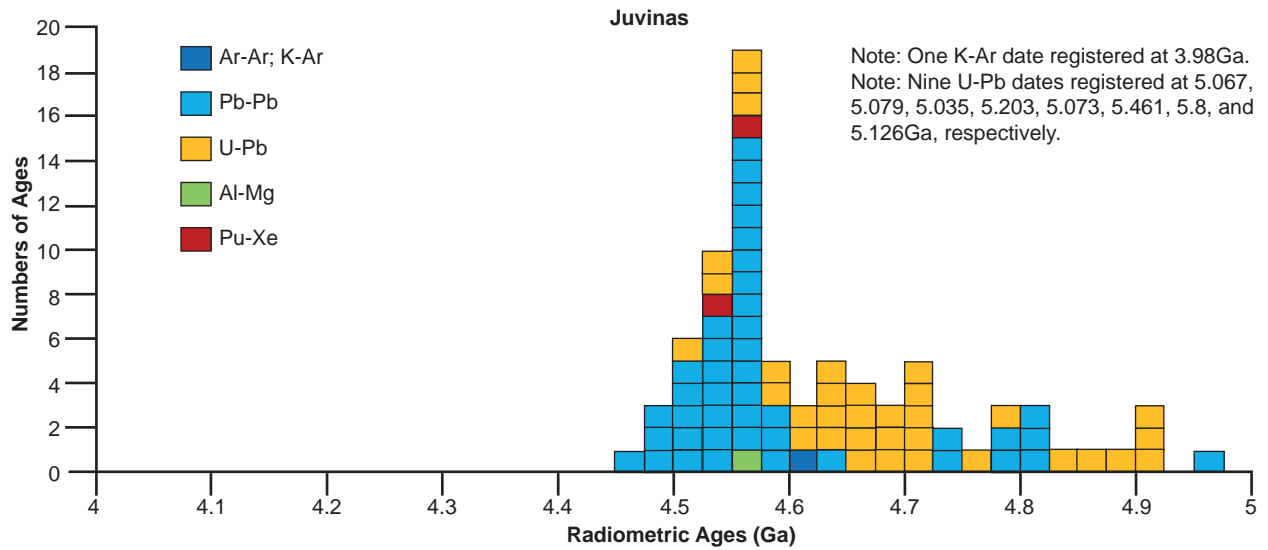
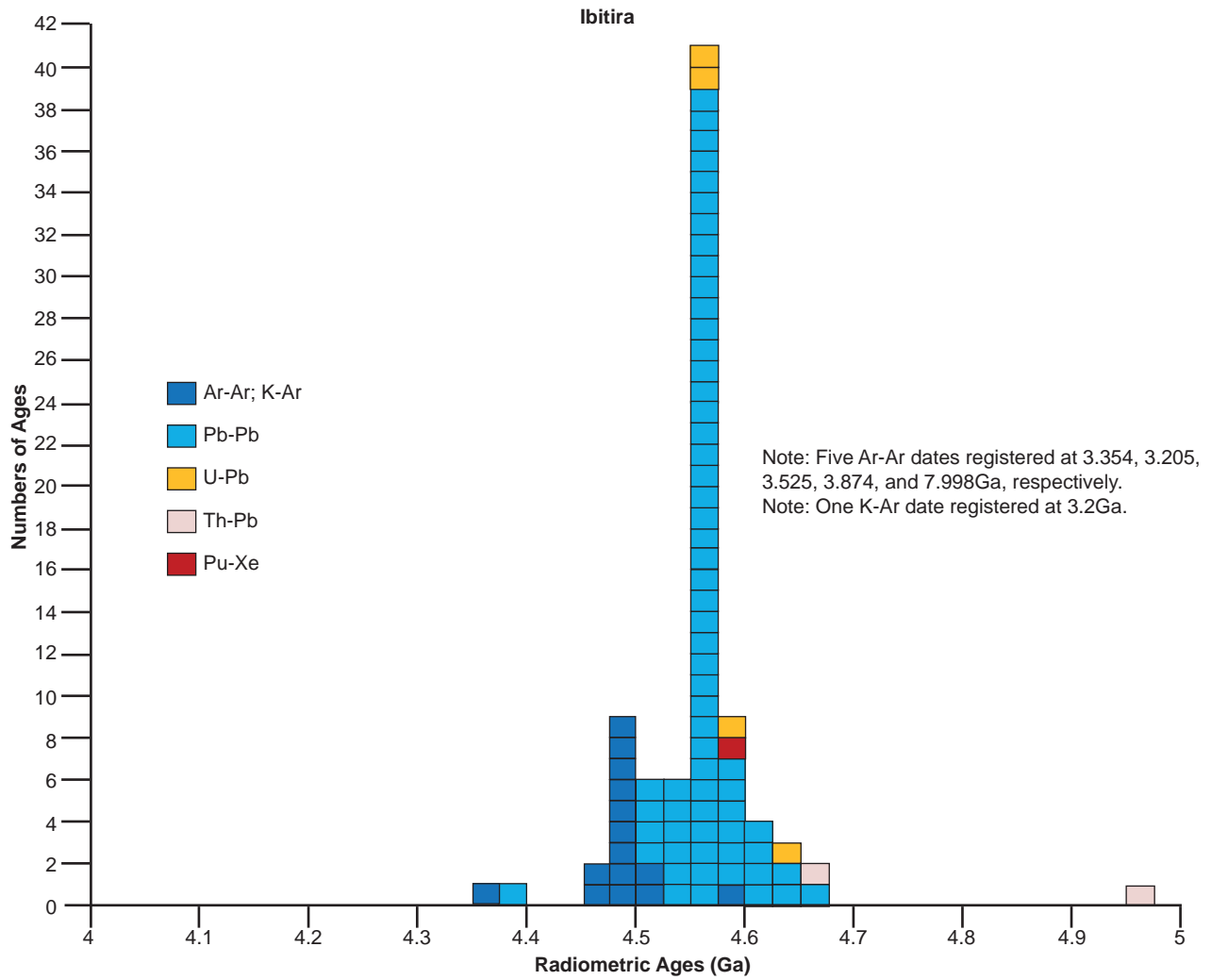
It has already been noted above that the Mn-Cr, Hf-W, Al-Mg, I-Xe, and Pu-Xe methods are calibrated directly or via intermediaries against the Pb-Pb ages yielded by other meteorites, which invariably guarantees the ages obtained by these methods will align with, or are adjusted to, the Pb-Pb ages that usually cluster around 4.55–4.57 Ga to date these eucrites. Indeed, as Snelling (2014a, b) found, the ages of most of the 28 meteorites investigated so far have been established directly by Pb-Pb ages or indirectly by Pb-Pb calibrated ages defining the clustering at 4.5–4.57 Ga.

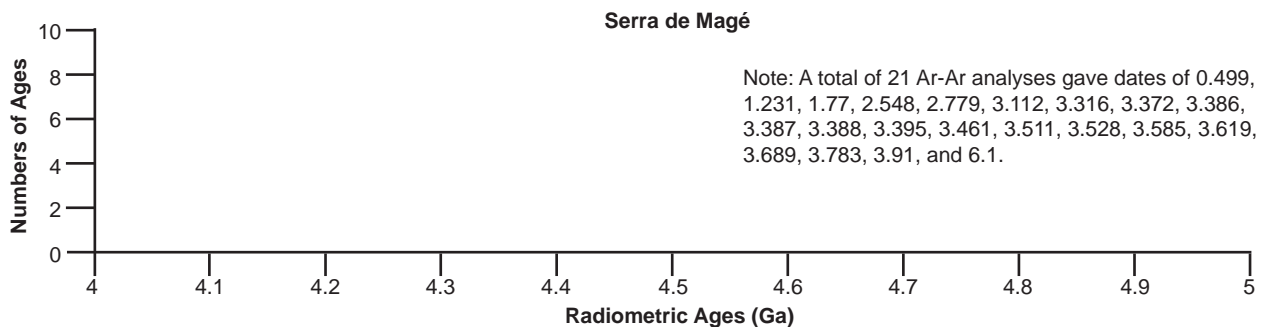
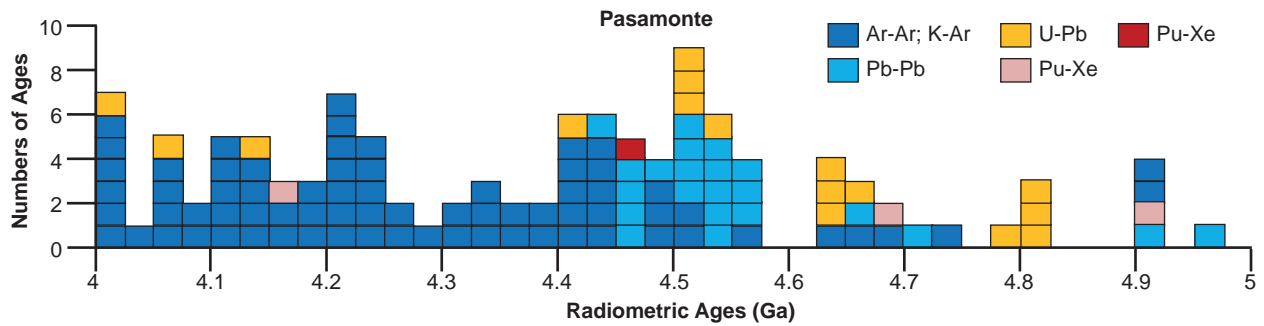
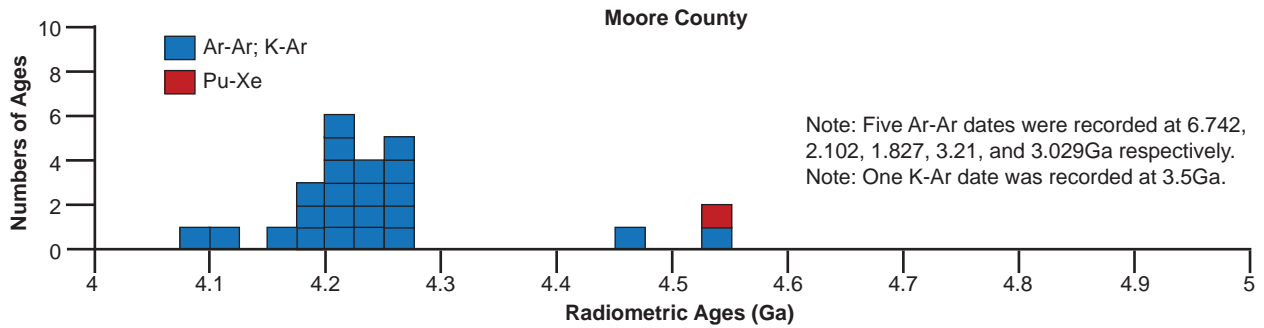
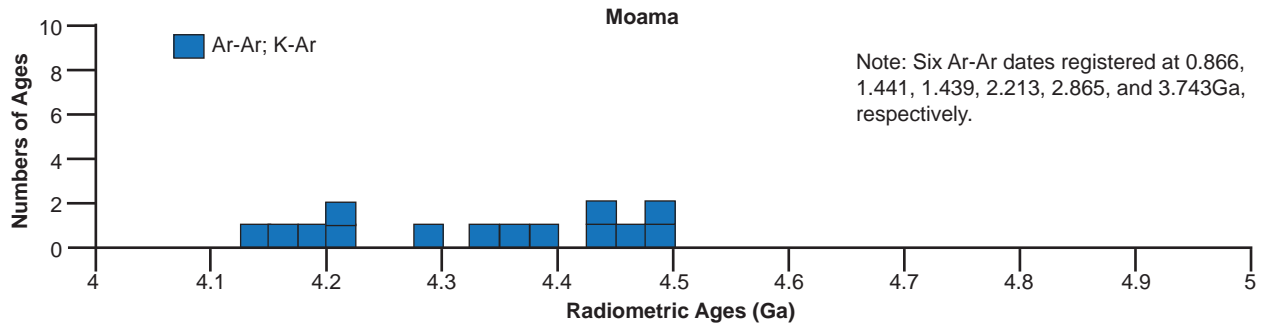
Examination of the relevant literature reveals that the ^{87}Rb decay rate has been determined by calibrating Rb-Sr dates against Pb-Pb dates on the same rock samples (Nebel, Scherer, and Mezger 2011; Snelling 2014c). Similarly, Snelling (2014d) has found that the ^{176}Lu decay rate has also been determined by calibrating Lu-Hf dates against Pb-Pb dates on the same mineral samples from the same rocks (Söderlund et al. 2004). In other words, the Rb-Sr and Lu-Hf dates were adjusted to agree with the Pb-Pb ages, so it is hardly surprising when the adjusted decay constants are used to calculate the Rb-Sr and Lu-Hf dates yielded by other rocks and minerals, and here by these meteorites, they often agree with the meteorites' 4.55–4.57 Ga Pb-Pb ages. It is also well known that the ^{40}K decay constant has been calibrated against standard samples of known Pb-Pb ages (Renne et al. 2010), so ultimately all K-Ar and Ar-Ar dates are adjusted accordingly. Even the ^{147}Sm decay constant has been calibrated against

Pb-Pb ages on the same samples (Dickin 2005, pp. 70–71; Lugmair 1974; Lugmair, Scheinin, and Marti 1975).

Therefore, ultimately *all* other radioisotopic dating methods have been effectively calibrated against Pb-Pb ages on the same rocks and minerals, and in some cases on the same meteorites. These calibrations are simply done by determining the Rb-Sr or Lu-Hf ages for specific rocks, meteorites, or minerals whose Pb-Pb ages have also been determined. Then it is assumed that the Pb-Pb ages are the most accurate and true ages for those rocks, meteorites, or minerals. So if the Rb-Sr or Lu-Hf ages disagree with the Pb-Pb ages, then the ^{87}Rb and ^{176}Lu half-life values are adjusted so that all the ages agree. It is thus hardly surprising that often there is agreement between all the radioisotope dates yielded on the same rocks, minerals and meteorites, except where it is interpreted that other factors have disturbed the radioisotope systems which thus have yielded a plethora of different dates (see below). This ultimately means that all meteorite ages are dependent on the reliability of determinations of the ^{238}U and ^{235}U decay constants, and the critical $^{238}\text{U}/^{235}\text{U}$ ratio. Yet discrepancies and variations have now been found between the $^{238}\text{U}/^{235}\text{U}$ ratio in U-bearing earth-based (terrestrial) minerals and rocks and the $^{238}\text{U}/^{235}\text{U}$ ratio in meteorites (Brennecka and Wadhwa 2012; Hiess et al 2012). It also may be significant that the estimated half-life of ^{238}U is 4.468 Ga, which is almost identical to the claimed 4.55–4.57 Ga age of the earth, the asteroids, and the meteorites derived from them.







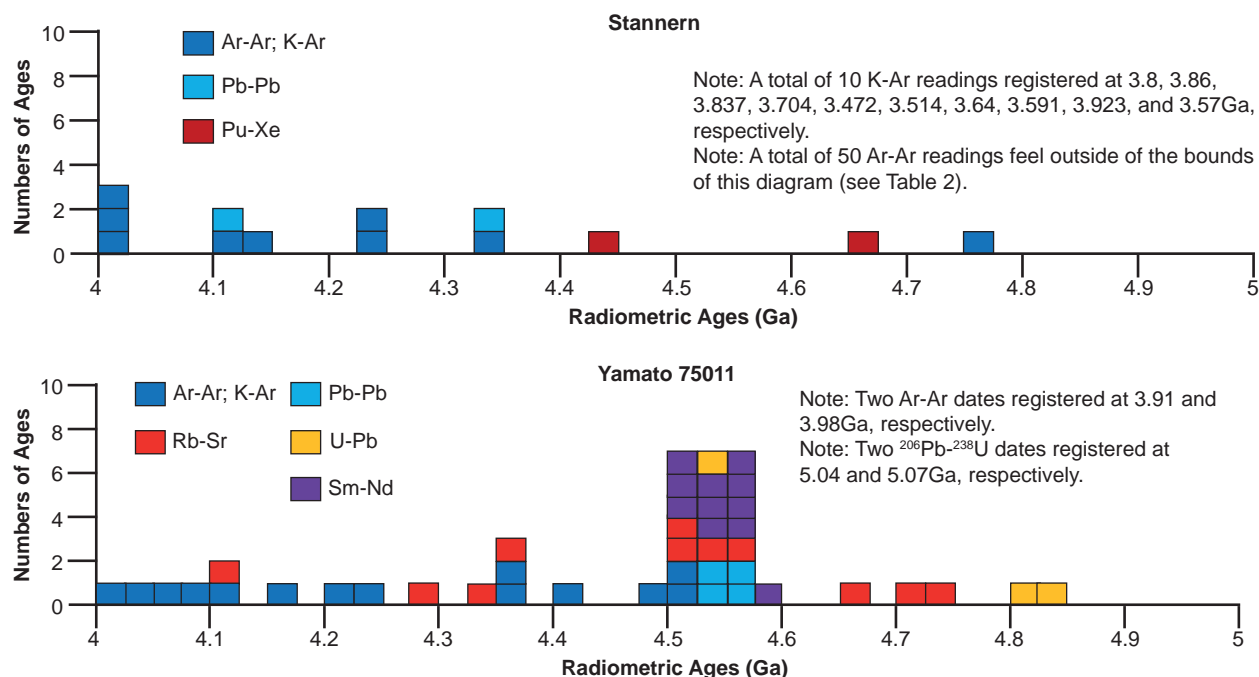


Fig. 7. Frequency versus radioisotope ages histogram diagram for the model ages for whole-rock samples and some or all components of 12 eucrite achondrites, with color coding being used to show the ages obtained by the different radioisotope dating methods.

Explanations for the scattering of ages

The usual explanation for such scattering of isochron and model ages is the thermal disturbance of the isotope systems subsequent to formation of the parent body from which the meteorites came, affecting either the parent body or subsequently the meteorites, or both (Bogard 2011; Lewis 1997; Trieloff et al. 2003). This must be especially the case where in this instance the scattering of ages is rife in the K-Ar, Ar-Ar, Rb-Sr, Sm-Nd, and U-Th-Pb systems. Confirmation of this explanation would seem to be provided by the fact that these eucrites (basaltic achondrites) are invariably metamorphosed, because it is well-documented that metamorphism resets these radioisotope systems (Faure and Mensing 2005; Snelling 2000).

However, not all these eucrites are metamorphosed, at least not to the same extent. Pasamonte (fig. 5a) and Serra de Magé (fig. 5c) are regarded as least metamorphosed or unmetamorphosed, though in the latter the original igneous pyroxenes have exsolved augite lamellae as a result of some metamorphism. Yet in both meteorites their radioisotope systems have been greatly disturbed. For Pasamonte the Rb-Sr isochron ages are younger than the 4.55–4.57 Ga clustering and the K-Ar, Ar-Ar, and U-Th-Pb model ages are widely scattered and are both younger and older. Similarly for Serra de Magé the Sm-Nd and Pb-Pb isochron ages are younger than the 4.55–4.57 Ga clustering, whereas the Ar-Ar model ages are widely scattered and invariably grossly younger.

McSween et al. (2011), based on the work of Bogard and Garrison (1995, 2003, 2009) and Bogard (2011), suggest another explanation for the lower Ar-Ar model ages for many eucrites, such as for Cacheri, Caldera, Camel Donga, Ibitira, Juvinas, Moama, Moore County, Pasamonte, Serra de Magé, Stannern, and Yamato 75011 in this study. Brecciated eucrites evidence significant Ar degassing, which reset their Ar-Ar ages to between 3.1–4.1 Ga. Since the timing of thermal and shock metamorphism is supposedly best determined from Ar-Ar ages, Bogard and Garrison (2009) argued that these young Ar-Ar ages represent impact cratering events on the surface of the parent asteroid 4-Vesta. They claimed that unbrecciated and unshocked eucrites have Ar-Ar ages near 4.5 Ga, whereas brecciated eucrites yield younger Ar-Ar ages that cluster on a probability plot in clusters at ~3.5, 3.8, 3.9, and 4.0 Ga (fig. 8). These they concluded were impact events that brecciated the eucrites and reset their Ar-Ar ages. However, in this study Ibitira, Moore County, Pasamonte, and Serra de Magé are all unbrecciated, as evidenced in thin sections (fig. 5), yet they yield many Ar-Ar ages younger than 4.5 Ga, some around 4.5 Ga, and quite a few well above 4.5 Ga.

Nevertheless, thermal disturbances tend to reset the radioisotope systems so that the resultant ages are lower than their original ages (Lewis 1997), whereas for all these eucrites the radioisotope ages are both younger and older than the believed formation age of the parent body, determined as 4.55–4.57 Ga from the

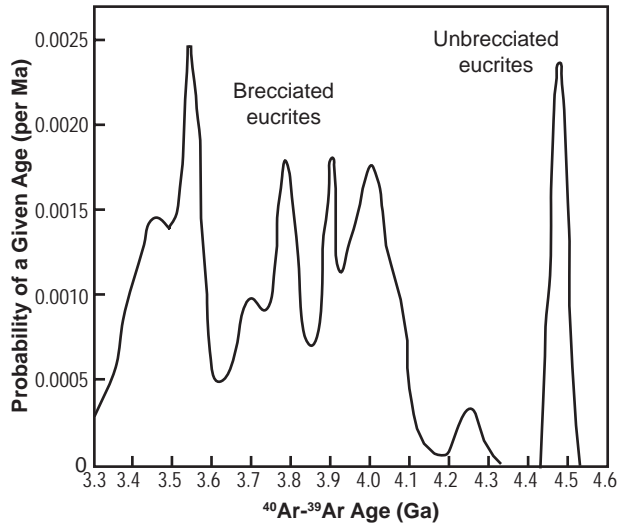


Fig. 8. Probability plot of ^{40}Ar - ^{39}Ar ages of unbrecciated and brecciated eucrites, based on the work of Bogard and Garrison (1995, 2003, 2009), after Bogard (2011) and McSween et al. (2011). The peaks are interpreted as representing major impact events on their parent asteroid 4-Vesta.

clustering of all the radioisotope systems at that age. So perhaps there might be an additional explanation for the scattering of both the isochron and model ages for all these eucrites (basaltic achondrites).

Internal layering in parent 4-Vesta

NASA's Dawn spacecraft mission to 4-Vesta investigated the asteroid's surface during 2011–2012 with a Visible and Infrared (VIR) Spectrometer for mineral identification and mapping, and a Gamma Ray and Neutron Detector (GRaND) for geochemical analysis and mapping (McSween et al. 2014). As a consequence new evidence was provided to strengthen considerably the connection of the HED meteorites to 4-Vesta (McSween et al. 2013, 2014). For example, high-resolution visible-near infrared spectra indicated pyroxene compositions and abundances like those of the HED meteorites, the mapped petrologic complexity (unlike the homogeneity of smaller asteroids) was consistent with the range of rock compositions among the HED meteorites, and geochemical measurements of the regolith were similar to the compositions of HED meteorites (and unlike those of other achondrite types). These results have further strengthened uniformitarians' attempts to explain the natural formation of 4-Vesta in the context of all other bodies in the solar system, and how it was shaped or modified by subsequent processes to produce its current internal structure and its surface features.

Regarded as a leftover planetary building block, with an average diameter of 510 km (317 mi) and a mean density of 3456 kg/m^3 (216 lbs/ft^3), 4-Vesta was once called the smallest terrestrial planet (McSween et al. 2014). It is believed by uniformitarians to

be an intact example of a large, differentiated protoplanet, like those claimed to be the building blocks of terrestrial planet accretion from the solar nebula, and based on analyses of the HED meteorites is postulated to have a basaltic upper crust (as represented by the noncumulate basaltic eucrites) that overlies a cumulate eucrite mid-crust layer and then a diogenite lower crust, with a depleted peridotitic (harzburgite) mantle beneath and then an iron core (Mandler and Elkins-Tanton 2013; Zuber et al. 2011). Petrological analyses of eucrites coupled with thermal evolution modeling has led to the proposal of two possible mechanisms of silicate-metal differentiation leading to the formation of the basaltic achondrites of Vesta's crust—the earlier model of equilibrium partial melting (Stolper 1977), or the later now popular model of crystallization of residual liquids (eucrites) and cumulates (diogenites) from a postulated cooling magma ocean (Mandler and Elkins-Tanton 2013; Righter and Drake 1997). For a body the size of 4-Vesta it is postulated that subsequent eruptions directly to the surface via dikes would be mechanically very difficult, so instead, large magma chambers would likely have formed in the subsurface and flows of basaltic eucrites could have erupted episodically from these chambers. Geochemical trends in basaltic eucrites (the main group trend and the Stannern trend) would seem to require multiple magmas and complex processes within this asteroid's crust (Barrat et al. 2007).

Thus a complex history for 4-Vesta has been elucidated by uniformitarians using the range of ages obtained for the HED meteorites yielded by the various radioisotope dating techniques. They even postulate that the differentiation of the crust and mantle occurred close to 4.56 Ga within 1–3 Myr of the formation of the solar system, as defined by the Pb-Pb isochron age of the CAIs in chondrites, along with core formation by silicate-metal fractionation at the same time or soon thereafter (McSween et al. 2011, 2014). The earliest magmatic activity supposedly occurred at ~5 Myr after formation of the solar system, and then persisted perhaps for as much as ~50–150 Myr. Then in common with other bodies in the solar system, in the period from 4.1 Ga to 3.5 Ga often called the “late heavy bombardment” 4-Vesta was evidently struck by careening, massive bolides, as deduced from the reset Ar-Ar ages (fig. 8).

A biblical perspective

Any such postulated history for the formation of the asteroid 4-Vesta, and of course for the solar system itself, is completely invalidated by the divinely provided biblical account of the six normal days of God creating during the Creation Week. On Day One God *ex nihilo* created the earth (Genesis 1:1),

and only on Day Four did He make the sun and the moon to provide light on the earth during the day and night respectively (Genesis 1:14–16). We are not specifically told that the rest of the solar system was also created on Day Four, but He did make the stars also on that day, and lights were placed in the expanse of the heavens to be for signs and seasons. From this description it is not unreasonable to conclude that the rest of the solar system was made on Day Four, including the asteroids. Furthermore, each entity God created and made during these six normal days of the Creation Week was formed exceedingly rapidly within the time and space of each normal day, so by the end of Day Four asteroid 4-Vesta was a completely formed entity, with an iron core, ultramafic mantle, and basaltic crust, all the necessary silicate-metal fractionation and crust-mantle differentiation happening exceedingly rapidly within hours, and thus not requiring the millions of years postulated by uniformitarians.

Given the general consensus that the asteroids consist of leftover material from the formation of the solar system, Snelling (2014a, b) proposed that the accepted coincident 4.55–4.57 Ga ages for the earth and many meteorites could be due to the earth and the parent asteroids having been created by God from the same primordial material, which He had created on Day One, as already proposed by Faulkner (1999, 2013). The simplest unifying assumption would therefore be that all such primordial material may have had the same created isotopic endowment. This assumption seems to be borne out by the earth apparently having the same time-integrated Pb isotopic endowment and thus being the same Pb-Pb “age” as the meteorites plotted on the geochron (Patterson 1956). The earth’s current Pb isotopic endowment was represented on that geochron by the Pb isotopic composition of a modern oceanic sediment sample, which would appear to contain the time-integrated Pb isotopic endowment from the earth’s beginning which was then processed through the earth’s subsequent rock cycle (Tyler 1990). However, while the possibility that the created initial ratios of parent to daughter elements were different for the earth compared to those created for other solar system objects could be considered, that possibility seems unwarranted if God made all the solar system objects (planets, moons, and asteroids) from the same primordial material He had created on Day One, which is consistent with them all having a common Designer. Nevertheless, if there were created differences in the initial Pb isotopic ratios, then it should not have been possible to plot the meteorites and the earth on the same Pb-Pb geochron, or meteorites on the same Pb-Pb, U-Pb, Rb-Sr, Sm-Nd, Lu-Hf, and Re-Os isochrons (Snelling in prep.).

It would also seem reasonable to propose that God created some of all the isotopes at the beginning in the primordial material, including isotopes that subsequently also formed by radioisotope decay as daughter isotopes from parent isotopes, regardless of when radioisotope decay started. In other words, when God made the primordial material He included in it ^{206}Pb , ^{207}Pb , and ^{208}Pb atoms along with ^{238}U , ^{235}U , and ^{232}Th atoms. It is reasonable to posit that He did, given that when created the “primordial material” likely had to have some initial isotopic ratios. Even the conventional scientific community has assumed the initial material of the solar system had the “primeval” Pb isotopic ratios as measured in the troilite (iron sulfide) in the Canyon Diablo iron meteorite (Faure and Mensing 2005). This is consistent with God creating a fully-functioning universe, as typified by Him creating fruit trees already bearing fruit in fully-functioning soil on land, all during Day Three, and the sun, moon, asteroids, and stars fully-functioning in their ordained positions and roles on Day Four. Thus when by the end of Day Four the asteroid 4-Vesta had been formed, all the necessary silicate-metal fractionation and crust-mantle differentiation of that primordial material to produce its internal layering had happened exceedingly rapidly within hours. That silicate-metal fractionation and crust-mantle differentiation may have also resulted in some redistribution or mixing of parent and daughter atoms, the latter having been originally created rather than derived via radioactive decay. These processes may explain some of the scattering in the radioisotope ages for these eucrite meteorites, especially those older than the 4.55–4.57 Ga clustering.

At what point in time radioactive decay began is unclear from Scripture, and is still a matter of debate among creationists. The RATE project considered the possibility of a large amount of accelerated decay occurring during the Creation Week, as radioisotope decay was not regarded as decay in the sense of deterioration of matter (Vardiman, Snelling, and Chaffin 2005). It is instead a transmutation process, by which one element is changed into another. The daughter element is certainly not inferior to the parent element. However, it is the radiation given off which is harmful that causes concern as to whether the radioisotope decay processes meet the standard of God’s declaration of His completed creation being “very good” (Genesis 1:31).

In the context of the decay evident today due to the operation of the second law of thermodynamics, Anderson (2103) contended that there is no real biblical evidence to suggest that the second law was inoperable prior to the curse, and so argued that rather the second law was in effect from the

beginning of creation. He thus also suggested that the tendency toward entropy implicit in the second law was never of a kind that conflicted with God's declaration that the creation was "very good," or that eventuated in the death of any sentient creature. On the other hand, it could be argued that radioisotope decay is more than the operation of the second law of thermodynamics; the additional outcome being the radiation produced which is harmful to life's biological and chemical makeup. Indeed, if billions of years of accelerated radioisotope decay had occurred mainly during the early part of the Creation Week, as considered a possibility by the RATE team (Vardiman, Snelling, and Chaffin 2005), the enormous burst of radiation would surely have been detrimental to all life on the earth, for example, the plants of Day Three. It is for this reason that many creationists are not comfortable with postulating that accelerated radioisotope decay happened during the Creation Week, so maybe there was no radioisotope decay at all until it was started as part of the curse.

The lack of any evidence of a pattern of isochron ages in these 12 basaltic achondrite meteorites (eucrites), as well as in the 16 chondrite meteorites previously studied (Snelling 2014a, b), that matches the pattern found during the RATE project (Snelling 2005c; Vardiman, Snelling, and Chaffin 2005) would therefore strongly suggest that all these meteorites and their parent asteroids have not experienced any episode of accelerated radioisotope decay, either at the time of the creation of the primordial material on Day One or of their formation on Day Four, or since. This could then be taken to infer that no accelerated radioisotope decay occurred anywhere in the solar system during the Creation Week, including on the earth during Days One–Three. Such a conclusion is based on the assumption that the mechanism of small changes to the binding forces in the nuclei of the parent radioisotopes proposed as the cause of a past episode of accelerated radioisotope decay (Vardiman, Snelling, and Chaffin 2005) would thus have affected every atom making up the earth, and by logical extension every atom of the universe at the same time, because God appears to have created the physical laws governing the universe to operate consistently through time and space.

On the other hand, if this assumption is true, and it is consistent with God's work of providentially maintaining the universe after He created it, then why is there evidence of an episode of accelerated radioisotope decay in the earth, but not in this asteroid and its meteorite fragments? The answer would seem to be that the accelerated radioisotope decay only occurred during the catastrophic global Flood event on the earth and that the asteroid 4-Vesta was not similarly affected. However, if the earth's

atoms were affected by accelerated radioisotope decay during the Flood, then surely every other atom in the universe would have been similarly affected. However, God is not bound by the physical laws He put in place at creation, as He can change them at any time anywhere or everywhere. After all, when Jesus Christ the Creator locally suspended the law of gravity as He walked on the stormy waters of the Sea of Galilee, the law of gravity was still operating at the same time to keep the disciples in their boat, their boat on the water and the earth in space in orbit around the sun. Thus God could have made small changes to the binding forces of the nuclei of only the earth's atoms during the Flood to cause accelerated radioisotope decay only on the earth, while leaving the atoms making up the rest of the solar system and universe untouched. Perhaps the reason God initiated accelerated radioisotope decay only on the earth was to generate the heat necessary to initiate and drive the catastrophic plate tectonics which reshaped the earth's surface during the Flood.

Another reason for arguing that accelerated radioisotope decay occurred in earth's rocks only during the Flood is that the earth's rocks contain the physical evidence of only 500–600 million years' worth of radioisotope decay (as calculated using today's measured decay rates), which equates to the same time period postulated by uniformitarians during which the geologic record of the Flood accumulated (Snelling 2009). This physical evidence of radioisotope decay in earth's rocks is provided by radiohalos and fission tracks (Snelling 2005a, b). Each fully-formed U radiohalo, no matter where in the geologic record it occurs or the supposed age of its host rock, only represents up to 100 million years' worth of U decay, so even if it is in a Precambrian (pre-Flood or Creation Week) granite it still only records up to 100 million or so years' worth of U decay that occurred during the Flood, at the same time as new granites containing U radiohalos were forming in plutons which had intruded into fossil-bearing (and therefore Flood-deposited) sedimentary strata. On the other hand, up to 600 or so million years' worth of fission tracks are found in zircon grains matching the radioisotope ages of those same zircon grains at the base of the strata record of the Flood (Snelling 2005b).

This still does not fully explain why there is such a spread of radioisotope "ages" from 4.03Ga to the present in the earth's rocks, or why the radioisotope "ages" of the oldest earth rock (the Acasta Gneiss, Canada) and the oldest mineral in an earth rock (a zircon grain in the Jack Hills sandstone, Western Australia) are 4.03Ga and 4.4Ga respectively rather than 4.56Ga, the supposed age of the earth. The answer might be that the earth's rocks, subsequent

to their creation on Day One, first suffered from the processes of mixing of isotopes and re-setting of radioisotope “clocks” in the mantle and crust during the Day Three “Great Upheaval” when God formed the dry land, and then further suffered from mixing of isotopes and resetting of radioisotope “clocks” in the mantle and crust as a consequence of the catastrophic plate tectonics during the Flood, as well as the concurrent accelerated radioisotope decay.

By comparison, the Day Three “Great Upheaval” which the Scriptures describe as occurring on the earth could not have affected other bodies in the solar system, including the asteroid 4-Vesta which is the likely source of the meteorites in this study, because these other bodies were not created until Day Four. Thus we can be dogmatic that this event was earth-specific, as it was designed to produce the continental crust and the dry land on the earth in readiness for the subsequent creation of plants, birds, animals, and man. In any case, so far our observations of the surfaces of asteroids do not indicate any continental crust on them akin to that which formed on the earth on Day Three. However, when they were formed on Day Four their formation could have included incredibly rapid silicate-metal fractionation and mantle-crust differentiation with accompanying redistribution of the previously created parent and (what uniformitarians now interpret as) daughter isotopes.

The scatter in the radioisotope ages of the 28 meteorites studied thus far would then be due to processes subsequent to the initial creation of the parent asteroids from the primordial material on Day Four of the Creation Week that have reset the radioisotope “clocks” at various times, such as the initial fractionation and differentiation, heating due to impact cratering, impact disintegration and re-coalescing of the asteroids, space weathering, and heating on passage of the meteorites through the earth’s atmosphere (Bogard and Garrison 2009; Cloutis, Binzel and Gaffey 2014; Michel 2014; Norton 2002).

Where to from here?

As concluded by Snelling (2014a, b) from his studies of 16 chondrite meteorites, based on the assumptions made the 4.55–4.57 Ga radioisotope “ages” for the Bereba, Cacheri, Camel Donga, Ibitira, Juvinas, Pasamonte, Serra de Magé, and Yamato 75011 basaltic achondrite meteorites (eucrites) obtained primarily by Pb-Pb radioisotope isochron and model age dating of various constituent minerals and fractions (for example, Iizuka et al. 2014; Manhès, Allègre, and Provost 1984; Misawa, Yamaguchi, and Kaiden 2005; Tera, Carlson, and Boctor 1997; Zhou et al. 2013) are likely not their true real-time ages.

The assumptions on which the radioisotope dating methods are based are simply unprovable, and in the light of the possibility of an inherited primordial geochemical signature, subsequent resetting of radioisotope “clocks” due to impact cratering of asteroids, and the evidence in earth rocks for past accelerated radioisotope decay, mixing of isotopes and resetting of radioisotope “clocks,” these assumptions are unreasonable.

However, we still need to develop a coherent and comprehensive explanation of what these radioisotope compositions in both meteorites and earth rocks really represent and mean within our biblical young-age creation-Flood framework for earth and universe history. We have some possible clues already, as discussed here, and a clearer picture may yet emerge from continued investigations now in progress. Examination of the radioisotope dating data for the remaining groups of achondrite meteorites is necessary to complete our understanding of what the meteorite radioisotope “ages” might mean. If only the earth was affected by accelerated radioisotope decay during the Flood, then it is also necessary to examine the radioisotope dating data for lunar rocks to determine whether the moon was affected by that aspect of the Flood catastrophe or not. Additionally, the radioisotope dating data for many more earth rocks from all levels of the geologic record need to be collated and examined. If accelerated radioisotope decay only occurred during the Flood, then it might be expected that the radioisotope “ages” of pre-Flood (mostly Precambrian) strata determined by the different methods would be noticeably discordant (Snelling 2005c), whereas the radioisotope “ages” of the strata formed during the Flood (mostly Phanerozoic) would be mostly concordant. This difference might be expected due to the pre-Flood rocks having already been formed and their radioisotope “clocks” started before the onset of the accelerated radioisotope decay during the Flood, when their radioisotope “clocks” would have been speeded up by different amounts according to the atomic weights of the parent radioisotopes. In contrast, the Flood rocks would have had their radioisotopes reset when those rocks formed and so their radioisotope “clocks” started only during the accelerated radioisotope decay of the Flood event. It may take the collation and examination of the huge radioisotope dating data sets of as many different earth rocks as possible from all levels of the geologic record to enable any firm conclusions to be made.

Whatever the radioisotope dating data for the earth’s rocks may reveal, it is already well-established that there are so many problems with the radioisotope dating methods which render them totally unreliable in providing time markers for the different stages

in the earth's history. Indeed, the investigations of determinations of the decay constants of each of the parent radioisotopes needs to be completed to provide further documentation of the uncertainties in that key time assumption. Therefore, even though most of these eucrites (basaltic achondrite meteorites) yield a consistent Pb-Pb isochron and model age of 4.55–4.57 Ga that cannot be their true real-time age, which according to the biblical paradigm is only about 6000 real-time years.

Conclusions

After decades of numerous careful radioisotope dating investigations of basaltic achondrite meteorites (eucrites) their Pb-Pb isochron and model age of 4.55–4.57 Ga has been well established. This date for these eucrites is supported for many of them by a strong clustering of their Pb-Pb isochron and model ages in the 4.55–4.57 Ga range, as well as being confirmed by both isochron and model age results via the U-Pb method, and to a lesser extent, by the Rb-Sr, Lu-Hf, and Sm-Nd methods. The Hf-W, Mn-Cr, Al-Mg, I-Xe, and Pu-Xe methods are all calibrated against the Pb-Pb isochron method, so their results are not objectively independent. Thus the Pb-Pb isochron dating method stands supreme in the conventional evolutionary uniformitarian community as the ultimate, most precise tool for determining the ages of the basaltic achondrite meteorites.

There are no discernible patterns in the isochron and model ages for these eucrites, apart from considerable scatter of the Rb-Sr, Sm-Nd, and some Pb-Pb isochron ages, and the considerable scatter of the K-Ar, Ar-Ar, Rb-Sr, U-Pb, Th-Pb, and even some Pb-Pb model ages. These basaltic achondrite ages do not follow the systematic pattern found in Precambrian rock units during the RATE project. The α -decay isochron ages are not always older than the β -decay isochron ages for particular eucrites, and among the β -decayers the isochron ages are not always older according to the increasing heaviness of the atomic weights of the parent radioisotopes, or the increasing lengths of their half-lives. Thus there appears to be no consistent evidence in these basaltic achondrite meteorites similar to the evidence found in earth rocks of past accelerated radioisotope decay.

Any explanation for the 4.55–4.57 Ga age for these basaltic achondrite meteorites needs to consider their origin. These meteorites are regarded as fragments of the asteroid 4-Vesta, debris derived from impact cratering of its surface and collisions with other asteroids. Even in the naturalistic paradigm the asteroids, and thus the meteorites, are regarded as “primordial material” left over from the formation of the solar system. Similarly, it has been

suggested the Hebrew of the Genesis text allows for God to have made “primordial material” on Day One of the Creation Week from which He made the earth on Day One and the non-earth portion of the solar system on Day Four. Thus today's measured radioisotope compositions of these eucrites may reflect a geochemical signature of that “primordial material,” which included atoms of all elemental isotopes created by God. Therefore if some, or perhaps most, of the daughter isotopes were thus “inherited” by these basaltic achondrite meteorites when they were formed from that “primordial material,” and the parent isotopes in the meteorites have only been subjected to some subsequent radioisotope decay (and none at accelerated rates), then the 4.55–4.57 Ga Pb-Pb isochron “age” for these eucrites cannot be their true real-time age, which according to the biblical paradigm is only about 6000 real-time years.

However, these conclusions and suggested explanations as discussed are still only tentative, their confirmation or adjustment awaiting the examination of more radioisotope dating data from meteorites in remaining groups. Furthermore, further extensive studies of the radioisotope dating of lunar rocks and rocks from all levels of the earth's geologic record are required to attempt to systematize what proportions of the isotopes in each radioisotope dating system measured today are due to inheritance from the “primordial material,” past accelerated radioisotope decay, and mixing, additions, and subtractions in the earth's mantle and crust through earth history, particularly during the Day Three Upheaval and then subsequently during the Flood.

Acknowledgments

The invaluable help of my research assistant Lee Anderson Jr. in compiling these radioisotope dating data into the tables and then plotting the data in the color coded age versus frequency histogram diagrams is acknowledged. Also, our production assistant Laurel Hemmings is especially thanked for her painstaking work in preparing these papers for publication.

References

- Allègre, C.J., J.-L. Birck, S. Fourcade, and M.P. Semet. 1975. Rubidium-87/strontium-87 age of Juvinas basaltic achondrite and early igneous activity in the solar system. *Science* 187, no. 4175:436–438.
- Amelin, Y., A.N. Krot, I.D. Hutcheon, and A.A. Ulyanov. 2002. Lead isotopic ages of chondrules and calcium-aluminum-rich inclusions. *Science* 297, no. 5587:1678–1683.
- Amelin, Y., M. Wadhwa, and G.W. Lugmair. 2006. Pb-isotopic dating of meteorites using ^{202}Pb - ^{205}Pb double spike: Comparison with other high-resolution chronometers. *Lunar and Planetary Science Conference* 37: #1970.

- Amelin, Y.A., A. Kaltenbach, T. Iizuka, C.H. Stirling, T.R. Ireland, M. Petaev, and S.B. Jacobsen. 2010. U-Pb chronology of the Solar System's oldest solids with variable $^{238}\text{U}/^{235}\text{U}$. *Earth and Planetary Science Letters* 300, no. 3–4:343–350.
- Anderson, L.A. Jr. 2013. Thoughts on the goodness of creation: In what sense was creation “perfect”? *Answers Research Journal* 6:391–397. <https://answersingenesis.org/physics/thoughts-on-the-goodness-of-creation-in-what-sense-was-creation-perfect/>.
- Bansal, B.M., C.-Y. Shih, and H. Wiesmann. 1985. Rb-Sr internal isochron age of a subophitic basalt clast from the Y75011 eucrite. *Lunar and Planetary Science Conference* 16:25–26.
- Barrat, J.A., A. Yamaguchi, R.C. Greenwood, M. Bohn, J. Cotten, M. Benoit, and I.A. Franchi. 2007. The Stannern trend eucrites: Contamination of main group eucritic magmas by crustal partial melts. *Geochimica et Cosmochimica Acta* 71, no. 16:4108–4124.
- Basaltic Volcanism Study Project. 1981. *Basaltic volcanism on the terrestrial planets*. New York, New York: Pergamon Press, Inc.
- Binzel, R.P., and S. Xu. 1993. Chips off of asteroid Vesta: Evidence for the parent body of basaltic achondrite meteorites. *Science* 260, no. 5105:186–191.
- Birck, J.-L., and C.J. Allègre. 1978. Chronology and chemical history of the parent body of basaltic achondrites studied by the ^{87}Rb - ^{87}Sr method. *Earth and Planetary Science Letters* 39, no. 1:37–51.
- Blichort-Toft, J., M. Boyet, P. Télouk, and F. Albarède. 2002. ^{147}Sm - ^{143}Nd and ^{176}Lu - ^{176}Hf in eucrites and the differentiation of the HED parent body. *Earth and Planetary Science Letters* 204, no. 1–2:167–181.
- Bogard, D.D., G.J. Taylor, K. Keil, M.R. Smith, and R.A. Schmitt. 1985. Impact melting of the Cachari eucrite 3.0 Gy ago. *Geochimica et Cosmochimica Acta* 49, no. 4:941–946.
- Bogard, D.D., and D.H. Garrison. 1995. ^{39}Ar - ^{40}Ar age of the Ibitira eucrite and constraints on the time of pyroxene equilibration. *Geochimica et Cosmochimica Acta* 59, no. 20:4317–4322.
- Bogard, D.D., and D.H. Garrison. 2003. ^{39}Ar - ^{40}Ar ages of eucrites and thermal history of asteroid 4 Vesta. *Meteoritics and Planetary Science* 38, no. 5:669–710.
- Bogard, D.D., and D.H. Garrison. 2009. Ar-Ar impact heating ages of eucrites and timing of the LHB. *Lunar and Planetary Science Conference* 40: #1131.
- Bogard, D.D. 2011. K-Ar ages of meteorites: Clues to parent-body thermal histories. *Chemie der Erde* 71, no. 3:207–226.
- Boyet, M., R.W. Carlson, and M. Horan. 2010. Old Sm-Nd ages for cumulate eucrites and redetermination of the solar system initial $^{146}\text{Sm}/^{144}\text{Sm}$ ratio. *Earth and Planetary Science Letters* 291, no. 1–4:173–181.
- Brazzle, R.H., O.V. Pravdivtseva, A.P. Meshik, and C.M. Hohenberg. 1999. Verification and interpretation of the I-Xe chronometer. *Geochimica et Cosmochimica Acta* 63, no. 5:739–760.
- Brennecke, G.A., and M. Wadhwa. 2012. Uranium isotope compositions of the basaltic angrite meteorites and the chronological implications for the early Solar System. *Proceedings of the National Academy of Sciences USA* 109, no. 24:9299–9303.
- Bukovanska, M., and T.R. Ireland. 1993. Zircons in eucrites: Pristine and disturbed U-Pb systematics. *Meteoritics* 28, no. 3:333.
- Carlson, R.W., F. Tera, and N.Z. Boctor. 1988. Radiometric geochronology of the eucrites Nuevo Laredo and Bereba. *Lunar and Planetary Science Conference* 19:166–167.
- Chen, J.H., and G.J. Wasserburg. 1985. U-Th-Pb isotopic studies of meteorite ALHA 81005 and Ibitira. *Lunar and Planetary Science Conference* 16:119–120.
- Claydon, J.L., S.A. Crowther, and J.D. Gilmour. 2012. Xenon in the anomalous eucrites Bunburra Rockhole and Ibitira. *Lunar and Planetary Science Conference* 43:#1884.
- Claydon, J.L., S.A. Crowther, and J.D. Gilmour. 2013. The I-Pu-Xe system in anomalous and Vestian eucrites: Was Vesta unusually large? *Lunar and Planetary Science Conference* 44:#2173.
- Clayton, R.N., and T.K. Mayeda. 1996. Oxygen-isotope studies of achondrites. *Geochimica et Cosmochimica Acta* 60, no. 11:1999–2018.
- Cloutis, E.A., R.P. Binzel, and M.J. Gaffey. 2014. Establishing asteroid-meteorite links. *Elements* 10, no. 1:25–30.
- Consolmagno, G.J., and M.J. Drake. 1977. Composition and evolution of the eucrite parent body: Evidence from rare earth elements. *Geochimica et Cosmochimica Acta* 41, no. 9:1271–1282.
- Cumming, G.L. 1969. A recalculation of the age of the solar system. *Canadian Journal of Earth Sciences* 6, no. 4:719–735.
- Dalrymple, G.B. 1991. *The age of the earth*. Stanford, California: Stanford University Press.
- Dalrymple, G.B. 2004. *Ancient earth, ancient skies*. Stanford, California: Stanford University Press.
- Dickin, A.P. 2005. *Radiogenic isotope geology*. 2nd ed. Cambridge, United Kingdom: Cambridge University Press.
- Drake, M.J. 2001. The eucrite/Vesta story. *Meteoritics and Planetary Science* 36, no. 4:501–513.
- Faulkner, D.R. 1999. A biblically-based cratering theory. *Creation Ex Nihilo Technical Journal* 13, no. 1:100–104.
- Faulkner, D.R. 2013. A proposal for a new solution to the light travel time problem. *Answers Research Journal* 6:295–300. <https://answersingenesis.org/astronomy/starlight/a-proposal-for-a-new-solution-to-the-light-travel-time-problem/>
- Faure, G., and T.M. Mensing. 2005. *Isotopes: Principles and applications*. 3rd ed. Hoboken, New Jersey: John Wiley & Sons.
- Galer, S.J.G., and G.W. Lugmair. 1996. Lead isotope systematics of noncumulate eucrites. *Meteoritics and Planetary Science* 31:A47–A48.
- Garrison, D.H., and D.D. Bogard. 1995. ^{39}Ar - ^{40}Ar age of Ibitira: Dating the time of chemical equilibration of eucritic pyroxenes? *Lunar and Planetary Science Conference* 26:443–444.
- Göpel, C., G. Manhès, and C.-J. Allègre. 1992. U-Pb study of the Acapulco meteorite. *Meteoritics* 27, no. 3:226.
- Göpel, C., G. Manhès, and C.-J. Allègre. 1994. U-Pb systematics of phosphates from equilibrated ordinary chondrites. *Earth and Planetary Science Letters* 121, no. 1–2:153–171.
- Hamet, J., N. Nakamura, D.M. Unruh, and M. Tatsumoto. 1978. Origin and history of the cumulate eucrite Moama as inferred from REE abundances, Sm-Nd and U-Pb systematics. *Proceedings of the Lunar and Planetary Science Conference* 9:1115–1136.

- Hampel, W., H. Wänke, H. Hofmeister, B. Spettel, and G.F. Herzog. 1980. ^{26}Al and rare gases in Allende, Bereba and Juvinas: Implications for production rates. *Geochimica et Cosmochimica Acta* 44, no. 3:539–547.
- Hans, U., T. Kleine, and B. Bourdon. 2013. Rb-Sr chronology of volatile depletion in differentiated protoplanets: BABI, ADOR and ALL revisited. *Earth and Planetary Science Letters* 374:204–214.
- Hiess, J., D.J. Condon, N. McLean, and S.R. Noble. 2012. $^{238}\text{U}/^{235}\text{U}$ systematics in terrestrial uranium-bearing minerals. *Science* 335, no. 6076:1610–1614.
- Heymann, D., E. Mazor, and E. Anders. 1968. Ages of calcium-rich achondrites – I. Eucrites. *Geochimica et Cosmochimica Acta* 32, no. 12:1241–1268.
- Iizuka, T., A. Kaltenbach, Y. Amelin, C.H. Stirling, and A. Yamaguchi. 2013. U-Pb isotope systematics of eucrites in relation to their thermal history. *Lunar and Planetary Science Conference* 44:#1907.
- Iizuka, T., Y. Amelin, A. Kaltenbach, P. Koefoed, and C.H. Stirling. 2014. U-Pb systematics of the unique achondrite Ibitira: Precise age determination and petrogenetic implications. *Geochimica et Cosmochimica Acta* 132:259–273.
- Jacobsen, S.B. and G.J. Wasserburg. 1984. Sm-Nd isotopic evolution of chondrites and achondrites, II. *Earth and Planetary Science Letters* 67, no. 2:137–150.
- Jacobsen, B., Q.-Z. Yin, F. Moynier, Y. Amelin, A.N. Krot, K. Nagashima, I.D. Hutcheon, and H. Palme. 2008. ^{26}Al - ^{26}Mg and ^{207}Pb - ^{206}Pb systematics of Allende CAIs: Canonical solar initial $^{26}\text{Al}/^{27}\text{Al}$ ratio reinstated. *Earth and Planetary Science Letters* 272, no. 1–2:353–364.
- Kennedy, T., F. Jourdan, A.W.R. Bevan, M.A.M. Gee, and A. Frew. 2013. Impact history of the HED parent body(ies) clarified by new $^{40}\text{Ar}/^{39}\text{Ar}$ analyses of four HED meteorites and one anomalous basaltic achondrite. *Geochimica et Cosmochimica Acta* 115:162–182.
- Kleine, T., C. Münker, K. Mezger, and H. Palme. 2002. Rapid accretion and early core formation on asteroids and the terrestrial planets from Hf-W chronometry. *Nature* 418:952–955.
- Kleine, T., K. Mezger, C. Münker, H. Palme, and A. Bischoff. 2004. ^{182}Hf - ^{182}W isotope systematics of chondrites, eucrites, and martian meteorites: Chronology of core formation and early mantle differentiation in Vesta and Mars. *Geochimica et Cosmochimica Acta* 68, no. 1:2935–2946.
- Kleine, T., K. Mezger, H. Palme, E. Scherer, and C. Münker. 2005. The W isotope composition of eucrite metals: constraints on the timing and cause of the thermal metamorphism of basaltic eucrites. *Earth and Planetary Science Letters* 231, no. 1–2:41–52.
- Krot, A.N., K. Keil, C.A. Goodrich, E.R.D. Scott, and M.K. Weisberg. 2005. Classification of meteorites. In *Meteorites, Comets, and Planets*, ed. A.M. Davis, *Treatise on Geochemistry*, vol. 1, 83–128. Amsterdam, Netherlands: Elsevier.
- Kunz, J., M. Trierloff, K.D. Bobe, K. Metzler, D. Stöffler, and E.K. Jessberger. 1995. The collisional history of the HED parent body inferred from ^{40}Ar - ^{39}Ar ages of eucrites. *Planetary and Space Science* 43, no. 3:527–543.
- Lee, S.R., H. Kim, D.-L. Cho, H. Kenji, and H. Hidaka. 2009. U-Pb dating of zircons from eucrites: A preliminary report. *Geochimica et Cosmochimica Acta* 73:A737.
- Lewis, J.S. 1997. *Physics and chemistry of the solar system*. Rev. ed. London, England: Academic Press.
- Lugmair, G.W. 1974. Sm-Nd ages: A new dating method. *Meteoritics* 9, no. 4:369.
- Lugmair, G.W., and N.B. Scheinin. 1975. Sm-Nd systematics of the Stannern meteorite. *Meteoritics* 10, no. 4:447–448.
- Lugmair, G.W., N.B. Scheinin, and K. Marti. 1975. Search of extinct ^{146}Sm , 1. The isotopic abundance of ^{142}Nd in the Juvinas meteorite. *Earth and Planetary Science Letters* 27, no. 1:79–84.
- Lugmair, G.W., and K. Marti. 1977. Sm-Nd-Pu timepieces in the Angra dos Reis meteorite. *Earth and Planetary Science Letters* 35, no. 2:273–284.
- Lugmair, G.W., N.B. Scheinin, and R.W. Carlson. 1977. Sm-Nd systematics of the Serra de Mage eucrite. *Meteoritics* 12, no. 3:300–301.
- Lugmair, G.W., and S.J.G. Galer. 1992. Age and isotopic relationships among the angrites Lewis Cliff 86010 and Angra dos Reis. *Geochimica et Cosmochimica Acta* 56, no. 4:1673–1694.
- Lugmair, G.W., and A. Shukolyukov. 1998. Early solar system timescales according to ^{53}Mn - ^{53}Cr systematics. *Geochimica et Cosmochimica Acta* 62, no. 16:2863–2886.
- Mandler, B.E., and L.T. Elkins-Tanton. 2013. The origin of eucrites, diogenites, and olivine diogenites: Magma ocean crystallization and shallow magma chamber processes on Vesta. *Meteoritics and Planetary Science* 48, no. 11:2333–2349.
- Manhès, G., and C.J. Allègre 1980. U-Th-Pb systematics of the Juvinas achondrite. *Meteoritics* 15, no. 4:329.
- Manhès, G., C.J. Allègre, and A. Provost. 1984. U-Th-Pb systematics of the eucrite “Juvinas”: Precise age determination and evidence for exotic lead. *Geochimica et Cosmochimica Acta* 48, no. 11:2247–2264.
- Manhès, G., M. Tatsumoto, D.M. Unruh, J.-L. Birck, and C.J. Allègre. 1975. Comparative ^{238}U - ^{206}Pb , ^{235}U - ^{207}Pb , ^{232}Th - ^{208}Pb , ^{206}Pb - ^{207}Pb and ^{87}Rb - ^{87}Sr ages of basaltic achondrites and early evolution of the solar system. *Lunar Science* VI:546–547.
- Manhès, G., C. Göpel, and C.J. Allègre. 1987. High resolution chronology of the early solar system based on lead isotopes. *Meteoritics* 22:453–454.
- McCord, T.B., J.B. Adams, and T.V. Johnson. 1970. Asteroid Vesta: Spectral reflectivity and compositional implications. *Science* 168, no. 3938:1445–1447.
- McSween, H.Y. Jr., D.W. Mittlefehldt, A.W. Beck, R.G. Mayne, and T.J. McCoy. 2011. HED meteorites and their relationship to the geology of Vesta and the Dawn mission. *Space Science Reviews* 163, no. 1–4:141–174.
- McSween, H.Y. Jr., R.P. Binzel, M.C. De Sanctis, E. Ammannito, T.H. Prettyman, A.W. Beck, V. Reddy et al. 2013. Dawn; the Vesta-HED connection; and the geologic context for eucrites, diogenites, and howardites. *Meteoritics and Planetary Science* 48, no. 11:2090–2104.
- McSween, H.Y. Jr., M.C. De Sanctis, T.H. Prettyman, and the Dawn Science Team. 2014. Unique, antique Vesta. *Elements* 10, no. 1:39–44.
- Michel, P. 2014. Formation and physical properties of asteroids. *Elements* 10, no. 1:19–24.
- Misawa, K., A. Yamaguchi, and H. Kaiden. 2005. U-Pb and ^{207}Pb - ^{206}Pb ages of zircons from basaltic eucrites: Implications for early basaltic volcanism on the eucrite parent body. *Geochimica et Cosmochimica Acta* 69, no. 24:5847–5861.

- Mittlefehldt, D.W. 2005. Achondrites. In *Meteorites, comets, and planets*, ed. A.M. Davis, *Treatise on geochemistry*, vol. 1, 291–324. Amsterdam, The Netherlands: Elsevier.
- Mittlefehldt, D.W., T.J. McCoy, C.A. Goodrich, and A. Kracher. 1998. Non-chondritic meteorites from asteroidal bodies. In *Planetary materials*, ed. J.J. Papike, *Reviews in mineralogy*, vol. 36, 4-1–4-195. Washington, DC: Mineralogical Society of America.
- Miura, Y.N., K. Nagao, and T. Fujitani. 1993. ^{81}Kr terrestrial ages and grouping of Yamato eucrites based on noble gas and chemical compositions. *Geochimica et Cosmochimica Acta* 57, no. 8:1857–1866.
- Miura, Y.N., K. Nagao, N. Sugiura, T. Fujitani, and P.H. Warren. 1998. Noble gases, ^{81}Kr -Kr exposure ages and ^{244}Pu -Xe ages of six eucrites, Bereba, Binda, Camel Donga, Juvinas, Millbillillie, and Stannern. *Geochimica et Cosmochimica Acta* 62, no. 13:2369–2387.
- Morris, J.D. 2007. *The young earth*. Rev. ed., pp. 59–61. Green Forest, Arkansas: Master Books.
- Nebel, O., E.E. Scherer, and K. Mezger. 2011. Evaluation of the ^{87}Rb decay constant by age comparison against the U-Pb system. *Earth and Planetary Science Letters* 301, no. 1–2:1–8.
- Nichols R.H., C.M. Hohenberg, K. Kehm, Y. Kim, and K. Marti. 1994. I-Xe studies of the Acapulco meteorite: Absolute I-Xe ages of individual phosphate grains and the Bjurböle standard. *Geochimica et Cosmochimica Acta* 58, no. 11:2553–2561.
- Norton, O.R. 2002. *The cambridge encyclopedia of meteorites*. Cambridge, United Kingdom: Cambridge University Press.
- Nyquist, L.E., H. Takeda, B.M. Bansal, C.-Y. Shih, H. Wiesmann, and J.L. Wooden. 1986. Rb-Sr and Sm-Nd internal isochron ages of a subophitic basalt clast and a matrix sample from the Y75011 eucrite. *Journal of Geophysical Research* 91, no. B8:8137–8150.
- Nyquist, L.E., Y.D. Reese, H. Wiesmann, and C.-Y. Shih. 1999. Two ages for Ibitira: A record of crystallization and recrystallization? *Meteoritics and Planetary Science* 34:A87–A88.
- Papanastassiou, D.A., and G.J. Wasserburg. 1969. Initial strontium isotopic abundances and the resolution of small time differences in the formation of planetary objects. *Earth and Planetary Science Letters* 5:361–376.
- Patchett, P.J., and M. Tatsumoto. 1980. Lu-Hf total-rock isochron for the eucrite meteorites. *Nature* 288:571–574.
- Patterson, C. 1956. Age of meteorites and the earth. *Geochimica et Cosmochimica Acta* 10, no. 4:230–237.
- Podosek, F.A., and J.C. Huneke. 1973. Argon 40-argon 39 chronology of four calcium-rich achondrites. *Geochimica et Cosmochimica Acta* 37, no. 3:667–684.
- Prinzhofer, A., D.A. Papanastassiou, and G.J. Wasserburg. 1992. Samarium-neodymium evolution of meteorites. *Geochimica et Cosmochimica Acta* 56, no. 2:797–815.
- Quitté, G., J.-L. Birck, and C.J. Allègre. 2000. ^{182}Hf - ^{182}W systematics in eucrites: The puzzle of iron segregation in the early solar system. *Earth and Planetary Science Letters* 184, no. 1:83–94.
- Renne, P.R., R. Mundil, G. Balco, K. Min, and K.R. Ludwig. 2010. Joint determination of ^{40}K decay constants and $^{40}\text{Ar}^*/^{40}\text{K}$ for the Fish Canyon sanidine standard, and improved accuracy for $^{40}\text{Ar}/^{39}\text{Ar}$ geochronology. *Geochimica et Cosmochimica Acta* 74, no. 18:5349–5367.
- Righter, K., and M.J. Drake. 1997. A magma ocean on Vesta: Core formation and petrogenesis of eucrites and diogenites. *Meteoritics and Planetary Science* 32, no. 6:929–944.
- Schiller, M., J.A. Baker, and M. Bizzarro. 2010. ^{26}Al - ^{26}Mg dating of asteroidal magmatism in the young solar system. *Geochimica et Cosmochimica Acta* 74, no. 16:4844–4864.
- Shields, R.M., W.H. Pinson, and P.M. Hurley. 1965. The Rb 87 -Sr 87 age of stony meteorites. *Massachusetts Institute of Technology 13th Annual Program Report*, pp. 121–144.
- Shukolyukov, A., and F. Begemann. 1996a. Pu-Xe dating of eucrites. *Geochimica et Cosmochimica Acta* 60, no. 13:2453–2471.
- Shukolyukov, A., and F. Begemann. 1996b. Cosmogenic and fissionogenic noble gases and ^{81}Kr -Kr exposure age clusters of eucrites. *Meteoritics and Planetary Science* 31, no. 1:61–72.
- Snelling, A.A. 2000. Geochemical processes in the mantle and crust. In *Radioisotopes and the age of the earth: A young-earth creationist research initiative*, ed. L. Vardiman, A.A. Snelling, and E.F. Chaffin, 123–304. El Cajon, California: Institute for Creation Research, and St. Joseph, Missouri: Creation Research Society. <http://www.icr.org/rate/>.
- Snelling, A.A. 2005a. Radiohalos in granites: Evidence of accelerated nuclear decay. In *Radioisotopes and the age of the earth: Results of a young-earth creationist research initiative*, ed. L. Vardiman, A.A. Snelling, and E.F. Chaffin, 101–207. El Cajon, California: Institute for Creation Research, and Chino Valley, Arizona: Creation Research Society. <http://www.icr.org/article/radiohalos-granites-evidence-for-accelerated/>.
- Snelling, A.A. 2005b. Fission tracks in zircons: Evidence for abundant nuclear decay. In *Radioisotopes and the age of the earth: Results of a young-earth creationist research initiative*, ed. L. Vardiman, A.A. Snelling, and E.F. Chaffin, 209–324. El Cajon, California: Institute for Creation Research, and Chino Valley, Arizona: Creation Research Society. <http://www.icr.org/article/fission-tracks-zircons-evidence-for/>.
- Snelling, A.A. 2005c. Isochron discordances and the role of inheritance and mixing of radioisotopes in the mantle and crust. In *Radioisotopes and the age of the earth: Results of a young-earth creationist research initiative*, ed. L. Vardiman, A.A. Snelling, and E.F. Chaffin, 393–524. El Cajon, California: Institute for Creation Research, and Chino Valley, Arizona: Creation Research Society. <http://www.icr.org/article/isochron-discordances-role-inheritance/>.
- Snelling, A.A. 2009. *Earth's catastrophic past: Geology, creation and the Flood*. Dallas, Texas: Institute for Creation Research.
- Snelling, A.A. 2014a. Radioisotope dating of meteorites: I. The Allende CV3 carbonaceous chondrite. *Answers Research Journal* 7:103–145. <https://answersingenesis.org/astronomy/age-of-the-universe/radioisotope-dating-meteorites-i-allende-cv3-carbonaceous-chondrite/>.
- Snelling, A.A. 2014b. Radioisotope dating of meteorites: II. The ordinary and enstatite chondrites. *Answers Research Journal* 7:239–296. <https://answersingenesis.org/astronomy/age-of-the-universe/radioisotope-dating-meteorites-i-allende-cv3-carbonaceous-chondrite/>.
- Snelling, A.A. 2014c. Determination of the radioisotope decay constants and half-lives: Rubidium-87 (^{87}Rb). *Answers Research Journal* 7:311–322. <https://answersingenesis.org/geology/radiometric-dating/determination-radioisotope-decay-constants-and-half-lives-rubidium-87-87rb/>.

- Snelling, A.A. 2014d. Determination of the radioisotope decay constants and half-lives: Lutetium-176 (^{176}Lu). *Answers Research Journal* 7:483–497. <https://answersingenesis.org/geology/radiometric-dating/determination-radioisotope-decay-constants-and-half-lives-lutetium-176/>.
- Snelling, A.A. n.d. Radioisotope dating of meteorites. V: Isochron ages of groups of meteorites. *Answers Research Journal* (in preparation).
- Söderlund, U., P.J. Patchett, J.D. Vervoort, and C.E. Isachsen. 2004. The ^{176}Lu decay constant determined by Lu-Hf and U-Pb isotope systematics of Precambrian mafic intrusions. *Earth and Planetary Science Letters* 219, no. 3–4:311–324.
- Stolper, E.M. 1977. Experimental petrology of eucritic meteorites. *Geochimica et Cosmochimica Acta* 41:587–681.
- Takeda, H. 1997. Mineralogical records of early planetary processes on the howardite, eucrite, diogenite parent body with reference to Vesta. *Meteoritics and Planetary Science* 32:841–853.
- Takeda, H., H. Mori, and D.D. Bogard. 1994. Mineralogy and ^{39}Ar - ^{40}Ar age of an old pristine basalt: Thermal history of the HED parent body. *Earth and Planetary Science Letters* 122, no. 1–2:183–194.
- Tatsumoto, M., and D.M. Unruh. 1975. Formation and early brecciation of the Juvinas achondrite inferred from U-Th-Pb systematics. *Meteoritics* 10:500–501.
- Tatsumoto, M., D.M. Unruh, and G.A. Desborough. 1976. U-Th-Pb and Rb-Sr systematics of Allende and U-Th-Pb of Orgueil. *Geochimica et Cosmochimica Acta* 40:617–634.
- Tera, F., R.W. Carlson, and N.Z. Boctor. 1987. Isotopic and petrologic investigation of the eucrites Cacheri, Moore County and Stannern. *Lunar and Planetary Science Conference* 18:1004–1005.
- Tera, F., R.W. Carlson, and N.Z. Boctor. 1997. Radiometric ages of basaltic achondrites and their relation to the early history of the solar system. *Geochimica et Cosmochimica Acta* 61, no. 8:1713–1731.
- Trieloff, M., E.K. Jessberger, I. Herrwerth, J. Hopp, C. Fléniel, M. Ghélls, M. Bourot-Denise, and P. Pellas. 2003. Structure and thermal history of the H-chondrite parent asteroid revealed by thermochronometry. *Nature* 422:502–506.
- Tyler, D.J. 1990. The tectonically-controlled rock cycle. In *Proceedings of the Second International Conference on Creationism*, ed. R.E. Walsh and C.L. Brooks, Vol. 2, 293–301. Pittsburgh, Pennsylvania: Creation Science Fellowship.
- Unruh, D.M., N. Nakamura, and M. Tatsumoto. 1977. History of the Pasamonte achondrite: Relative susceptibility of the Sm-Nd, Rb-Sr, and U-Pb systems to metamorphic events. *Earth and Planetary Science Letters* 37, no. 1:1–12.
- Vardiman, L., A.A. Snelling, and E.F. Chaffin, eds. 2005. *Radioisotopes and the age of the earth: Results of a young-earth creationist research initiative*. El Cajon, California: Institute for Creation Research, and Chino Valley, Arizona: Creation Research Society. <http://www.icr.org/rate2/>.
- Wadhwa, M., and G.W. Lugmair. 1996. Age of the eucrite “Caldera” from convergence of long-lived and short-lived chronometers. *Geochimica et Cosmochimica Acta* 60, no. 23:4889–4893.
- Wadhwa, M., C.N. Foley, P.E. Janney, and L. Spivak-Birndorf. 2004. Mg isotope systematics in eucrites: Implications for the ^{26}Al - ^{26}Mg chronometer. *Lunar and Planetary Science Conference* 35:#1843.
- Wasserburg, G.J., F. Tera, D.A. Papanastassiou, and J.C. Huneke. 1977. Isotopic and chemical investigations on Angra dos Reis. *Earth and Planetary Science Letters* 35, no. 2:294–316.
- Weisberg, M.K., T.J. McCoy, and A.N. Krot. 2006. Systematics and evaluation of meteorite classification. In *Meteorites and the early solar system II*, ed. D.S. Lauretta and H.Y. McSween Jr., 19–52. Tucson, Arizona: University of Arizona Press.
- Yamaguchi, A., G.J. Geoffrey, K. Keil, C. Floss, G. Crozaz, L.E. Nyquist, D.D. Bogard et al. 2001. Post-crystallization reheating and partial melting of eucrite EET90020 by impact into the hot crust of asteroid 4Vesta ~4.50Ga ago. *Geochimica et Cosmochimica Acta* 65, no. 20:3577–3599.
- Zhou, Q., Q.-Z. Yin, B. Bottke, P. Claeys, X.-H. Li, F.-Y. Wu, Q.-L. Li, Y. Liu, and G.-Q. Tang. 2011. Early basaltic volcanism and late heavy bombardment on Vesta: U-Pb ages of small zircons and phosphates in eucrites. *Lunar and Planetary Science Conference* 42:#2575.
- Zhou, Q., Q.-Z. Yin, E.D. Young, X.-H. Li, F.-Y. Wu, Q.-L. Li, Y. Liu, and G.-Q. Tang. 2013. SIMS Pb-Pb and U-Pb age determination of eucrite zircons at $5\mu\text{m}$ scale and the first 50Ma of the thermal history of Vesta. *Geochimica et Cosmochimica Acta* 110:152–175.
- Zuber, M.T., H.Y. McSween Jr., R.P. Binzel, L.T. Elkins-Tanton, A.S. Konopliv, C.M. Pieters, and D.E. Smith. 2011. Origin, internal structure and evolution of 4 Vesta. *Space Science Reviews* 163:77–93.

